

Understanding the role of ERK signaling pathway and mechanotransduction in breast cancer

*A thesis submitted in partial fulfilment of the requirement for the degree
of*

Doctor of Philosophy

by

Sreeja Dattachoudhury

Roll No: 156106022



Supervisor

Prof. Bithiah Grace Jaganathan

**Department of Biosciences and Bioengineering
Indian Institute of Technology
Guwahati Guwahati-781 039, Assam, India**



INDIAN INSTITUTE OF TECHNOLOGY GUWAHATI
DEPARTMENT OF BIOSCIENCES AND BIOENGINEERING
GUWAHATI-781039

DECLARATION

I do hereby declare that the research findings of this thesis entitled “**Understanding the role of ERK signaling pathway and mechanotransduction in breast cancer**” is the result of research work carried out by me in the Department of Biosciences and Bioengineering, Indian Institute of Technology Guwahati, Guwahati, Assam, India under the supervision of **Prof. Bithiah Grace Jaganathan**.

Date: 28.06.2023

Sreeja Dattachoudhury

(Candidate)

Roll No: 156106022



INDIAN INSTITUTE OF TECHNOLOGY GUWAHATI
DEPARTMENT OF BIOSCIENCES AND BIOENGINEERING
GUWAHATI-781039

CERTIFICATE

It is certified that the work described in this thesis entitled “**Understanding the role of ERK signaling pathway and mechanotransduction in breast cancer**” by Ms. Sreeja Dattachoudhury (Roll No: 156106022) for the award of degree of Doctor of Philosophy is an authentic record of the results obtained from the research work carried out under my supervision in the Department of Biosciences and Bioengineering, Indian Institute of Technology Guwahati, Guwahati, Assam, India, and this work has not been submitted elsewhere for the award of any other degree.

Date:28.06.2023

Prof. Bithiah Grace Jaganathan

(Thesis Supervisor)

INDEX.....	Page No
List of figures.....	7-9
Abbreviations.....	10-12
Synopsis.....	13-17
1.0 Scientific Background	18-46
1.1 Cancer – Initiation, Progression, Therapy and Resistance.....	18-21
1.2 Breast cancer.....	21-23
1.3 Metastatic cancer progression.....	23-23
1.4 Signaling pathway dysregulated in cancer.....	23-24
1.5 ERK signaling pathway.....	24-27
1.6 Sorafenib.....	27-28
1.7 BVD-523.....	28-30
1.8 Breast cancer markers.....	30-32
1.9 Mechanotransduction in cancer.....	32-33
1.10 ECM and its interaction with breast cancer cells.....	33-36
1.11 Role of PIEZO1 in regulating cancer cell behavior.....	37-38
1.12 Yoda1.....	38-40
1.13 PIEZO1 in mediating mechanotransduction.....	40-46
2.0 Aims and Objectives.....	47
3.0 Materials and methods.....	48-59
3.1 Materials.....	48
3.1.1 Chemicals and reagents.....	48
3.1.1.1 Stains and dyes	
3.1.1.2 Inhibitors and activators	
3.1.1.3 Antibodies	
3.1.2 Cell lines.....	49
3.1.3 Cell culture media and reagents.....	49
3.1.4 Solutions and buffers.....	49
3.1.4.1 Buffers and solutions for cell culture	
3.1.4.2 Buffers and solutions for Immunocytochemistry	
3.1.4.3 Buffers for SDS-PAGE and Immunoblotting	

3.2 Methods	50-59
3.2.1 Cell culture	
3.2.2 Cell counting	
3.2.3 Apoptosis analysis	
3.2.4 Ki67 staining and cell cycle analysis	
3.2.5 Phenotyping	
3.2.6 Phospho flow cytometry	
3.2.7 ROS analysis	
3.2.8 Colony formation assay	
3.2.9 Spheroid formation assay	
3.2.10 Wound healing assay	
3.2.11 Spheroid migration assay	
3.2.12 SDS-PAGE and Immunoblotting	
3.2.13 Immunocytochemistry	
3.2.14 Gene silencing	
3.2.15 Calcium flux analysis	
3.2.16 Shear stress experiment	
3.2.17 Anoikis culture	
3.2.18 Gene expression analysis	
3.2.19 Data analysis	
4.0 Results	60-112
4.1 Effect of ERK1/2 inhibition in breast cancer cells by multikinase RAF inhibitor Sorafenib.....	60-72
4.2 Effect of ERK1/2 inhibition in breast cancer cells by ERK1/2 specific inhibitor BVD-523.....	73-79
4.3 Effect of PIEZO1 activation by chemical agonist Yoda1 in breast cancer cells.....	80-94
4.4 Effect of PIEZO1 inhibition through PIEZO1 silencing in breast cancer cells.....	95-112
5.0 Discussion	113-122
5.1 ERK pathway inhibition diminishes breast cancer cell proliferation and metastatic	

properties	113-116
5.2 Role of PIEZO1 in breast cancer cells.....	116-123
6.0 Conclusion.....	124-125
7.0 References.....	126-136
Acknowledgement.....	137
List of Publications and Conferences.....	138



List of figures

Figure No.	List of figures	Page No.
Fig.1.1	Crosstalk between different signaling molecules of the ERK signaling pathways involved in breast cancer development and progression.	27
Fig.1.2	Mechanical forces in modulating ERK signaling in cancer cells.	36
Fig.1.3	PIEZO1 in mediating mechanotransduction in various stages of breast cancer	40
Fig.4.1.1	Effect of Sorafenib on proliferation and survival of breast cancer cells.	60
Fig.4.1.2	Gene expression and signaling pathway changes due to sorafenib treatment	61
Fig.4.1.3	Effect of Sorafenib on proliferation and survival	62
Fig.4.1.4	Effect of Sorafenib treatment on spheroid growth	63
Fig.4.1.5	Effect of Sorafenib treatment on breast cancer stem cells	64-65
Fig.4.1.6	Effect of Sorafenib treatment on cytoskeleton of breast cancer stem cells	66-67
Fig.4.1.7	Effect of Sorafenib treatment on migration and invasion of breast cancer stem cells	68-70
Fig.4.1.8	Gene expression and signaling pathway changes due to sorafenib treatment	71
Fig.4.2.1	Effect of ERK1/2 inhibition on cell proliferation, survival and morphology	73-74
Fig.4.2.2	Effect of ERK1/2 inhibition on spheroid growth	75

List of figures

Fig.4.2.3	Effect of ERK1/2 inhibition on cell cycle	75
Fig.4.2.4	Effect of ERK1/2 inhibition on self-renewal ability	76-77
Fig.4.2.5	Effect of ERK1/2 inhibition on migration	78
Fig.4.3.1	Effect of PIEZO1 activation on proliferation of breast cancer cells	81
Fig.4.3.2	Effect of PIEZO1 activation on proliferation and self-renewal in breast cancer	82-83
Fig.4.3.3	Effect of PIEZO1 activation on migration and invasion in breast cancer	84-85
Fig.4.3.4	Effect of PIEZO1 activation on cell cycle and expression of proliferation genes in breast cancer	87
Fig.4.3.5	Effect of PIEZO1 activation on stemness in breast cancer	88-89
Fig.4.3.6	Effect of PIEZO1 activation on mitochondrial ROS generation in breast cancer	90
Fig.4.3.7	Effect of PIEZO1 activation on signaling pathways in breast cancer	91
Fig.4.3.8	Effect of PIEZO1 activation on cellular self-renewal ability and growth progression in breast cancer	92-93
Fig.4.4.1	Lentiviral mediated gene silencing of PIEZO1 gene of breast cancer cells determined by real time PCR and flow cytometry	95
Fig.4.4.2	Effect of PIEZO1 silencing on intracellular Ca ²⁺ influx of breast cancer cells.	96
Fig.4.4.3	Effect of PIEZO1 silencing on cellular morphology and F-actin arrangement of breast cancer cells	97

List of figures

Fig.4.4.4	Effect of PIEZO1 silencing on proliferation of breast cancer cells	98-99
Fig.4.4.5	Effect of PIEZO1 silencing on self-renewal ability of breast cancer cells.	99-100
Fig.4.4.6	Effect of PIEZO1 silencing on migration of breast cancer cells	101
Fig.4.4.7	Effect of PIEZO1 silencing on gene expression changes in proliferation and migration related genes of breast cancer cells.	103
Fig.4.4.8	Effect of PIEZO1 silencing on modulation of genes involved in key signaling pathways	104-105
Fig.4.4.9	Effect of Yoda1 induced PIEZO1 activation on the self-renewal ability of breast cancer cells.	106-107
Fig.4.4.10	Effect of Yoda1 induced PIEZO1 activation on the self-renewal ability and survival of breast cancer cells under anoikis condition	108-109
Fig.4.4.11	Effect of PIEZO1 regulation on the self-renewal ability and survival of breast cancer cells under shear stress/anoikis condition.	111-112

ABBREVIATIONS

AD: Adherent culture

B-cat: Beta Catenin

Bcl-2: B-cell lymphoma-2

BM: bone Marrow

BVD: BVD-523(Ulixertinib)

CASR: Ca²⁺-sensing receptor

CD: Cluster of differentiation

cDNA: complementary DNA **CON:** control

DAPI: 4',6-diamidino-2-phenylindole

Dooku1: 2-[(2,6-Dichlorobenzyl)thio]-5-(1*H*-pyrrol-2-yl)-1,3,4-oxadiazole

DOX: Doxorubicin

HG - DMEM: Dulbecco's modified Eagles medium-high

DMSO: Dimethyl Sulphoxide

DNA: Deoxyribonucleic acid

dNTP: deoxy nitro triphosphates

dT: deoxy thymidines

ECM: Extra cellular matrix

EMT: Epithelial to mesenchymal transition

EGF: Epidermal growth factor

ERK: extracellular signal regulated kinase

EtBr: ethidium Bromide

F-actin: Filamentous-actin

ABBREVIATIONS

FAK: focal adhesion kinases

FBN: fibronectin

FBS: foetal bovine serum

FDA: food and drug administration

FITC: fluorescence iso thiocyanate

GAP: GTPase activating protein

GAPDH: glyceroldehyde-3-phosphate de hydrogenase

GDI: guanine nucleotide dissociation inhibitors

GDP: guanine nucleoside di phosphate

GTP: guanine nucleoside tri phosphate

GTPases: guanosine triphosphatases

HEK 293FT: human epithelial kidney 293FT

MCF7: Michigan cancer foundation 7

MDA-MB-231: MD Anderson metastatic breast 231

m-ROS: mitochondrial reactive oxygen species

PBS: phosphate buffered saline

PE: phycoerythrin

PEI: Poly Ethylene Imine

PI: propidium iodide

PLL: poly-l-lysine

Rac1: ras-related C3 botulinum toxin substrate 1

RBC: red blood cell

RHO: Ras homolog gene family

ABBREVIATIONS

RNA: ribonucleic acid

ROS: reactive oxygen species

RT: reverse transcriptase

SOC: super optimal broth with catabolite repression

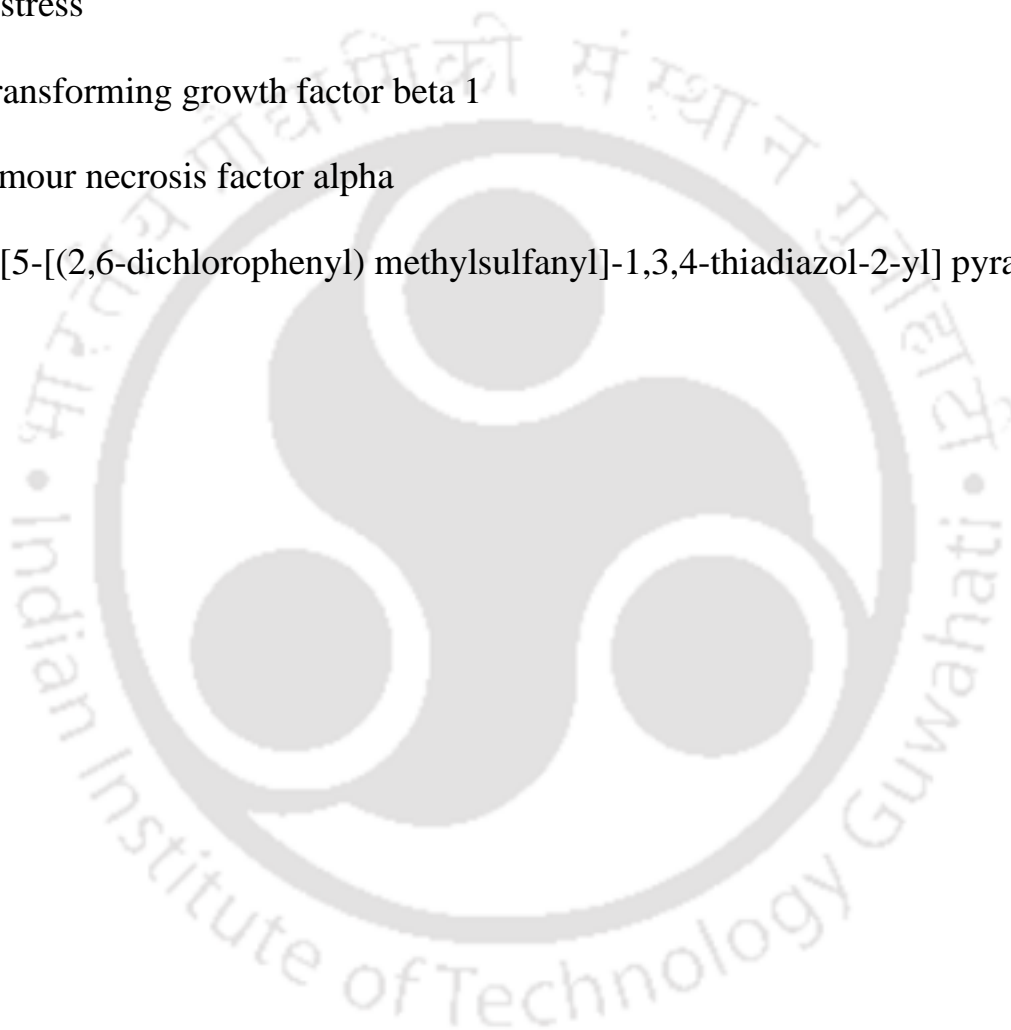
Sora: Sorafenib

SS: Shear stress

TGFβ1: transforming growth factor beta 1

TNFα: tumour necrosis factor alpha

Yoda1: 2-[5-[(2,6-dichlorophenyl) methylsulfanyl]-1,3,4-thiadiazol-2-yl] pyrazine



Synopsis

Synopsis:

Breast cancer, the leading cause of death among women worldwide, is characterized by uncontrolled cell proliferation, migration, invasion and metastasis. Several signaling pathways have been found to regulate breast cancer cell proliferation, migration, metastasis and angiogenesis. One such pathway which plays a crucial role in breast cancer cell growth, division and invasion is the ERK signaling pathway. Aberrant activity of its downstream signaling kinases is the forerunners of malignancy. Thus, targeting the ERK signaling pathway at different levels provided insights into the mechanism by which oncogenic properties like stemness, chemoresistance, anoikis resistance, epithelial to mesenchymal transitions (EMT) are inhibited by and large.

The present study focuses on understanding ERK signaling pathway in breast cancer progression as the first objective using a pan-ERK inhibitor, sorafenib and ERK1/2 specific inhibitor BVD-523 (BVD). Sorafenib is an FDA-approved multi-kinase inhibitor commonly used to treat patients with renal and hepatocellular cancer. The current study aims to understand the role of sorafenib treatment in regulating breast cancer migration, metastasis, and modulating intracellular signaling cascade.

Sorafenib treatment significantly inhibited cell survival and induced the accumulation of cells in the G1 phase of the cell cycle. Sorafenib treatment modified the metastatic feature of breast cancer cells by significantly inhibiting the invasion of breast cancer cells into the collagen matrix. The reduction in migration was accompanied by upregulation of EpCAM expression, E-cadherin (CDH1) and TIMPs expression but a downregulation of MMPs, MMP1 and MMP9. Breast cancer stem cells, responsible for cancer initiation, progression, chemoresistance and recurrence were identified as CD44 +/CD24-/lo along with other markers such as ALDH and CD49F. CD24 expression, which inhibits stemness in breast cancer cells, was upregulated, whereas CD44, which promotes stemness, was downregulated upon sorafenib treatment. However, sorafenib did not affect the expression of ALDH1A3, a marker that in combination with CD44 and CD24 expression identifies breast cancer stem cells. Also, CD49F, a breast cancer stem cell marker and an indicator of metastasis, was downregulated on sorafenib treatment, suggesting its anti-metastatic effect. Furthermore, sorafenib treatment drastically reduced phospho-ERK1/2 levels, thereby abrogating the ERK signaling. Sorafenib downregulated phosphorylated levels of p38MAPK and STAT5 in MDA-MB-231 cells. Thus, sorafenib treatment effectively inhibited proliferation, migration, invasion of breast cancer cells, modified gene expression, signaling and could be used in combination with other drugs to inhibit metastasis in breast cancer patients.

In continuation to the study with sorafenib treatment and to understand the specific role of ERK

Synopsis

signaling in breast cancer, the study was carried out with ERK1/2 specific inhibitor BVD-523 and its role in regulating breast cancer proliferation, survival, migration and stem-cell-ness were elucidated. BVD has shown promising effects in preliminary clinical trials, with high potency and selectivity, when used in combination with other B-RAF/RAS targets both *in vitro* and *in vivo*. When treated with BVD, breast cancer cell lines MCF7 and MDA-MB-231 showed a significant dose-dependent decrease in cell number and BVD treatment resulted in significant reduction in cell viability. In addition, cell cycle showed accumulation of cells in G1 phase followed by a simultaneous reduction in the S- phase and G2/Mphase, suggesting cell cycle arrest and growth inhibition. Treatment with BVD significantly reduced the rate of cell migration in both MCF7 and MDA-MB-231 cells. In line with these data, marked inhibition of spheroid growth rate upon BVD treatment was observed. BVD treatment of either cell type for 48 hours or continuous treatment for a period of twelve days, showed a significant reduction the colony formation ability of both MCF7 and MDA-MB-231 cells. BVD-treated MDA-MB-231 cells showed significant downregulation in the expression of CD44 and CD49F and increased expression of CD24 and EpCAM. MCF7 cells with BVD showed a marked decrease in CD24 and EpCAM. These differences indicate a differential role of ERK signaling in different subtypes of breast cancer. Immunoblotting of BVD- treated breast cancer cells showed a dose dependent increase in the levels of pERK1/2, accompanied with decrease in the expression of its downstream anti-apoptotic protein, Bcl2, in MDA-MB-231 treated with $>1 \mu\text{M}$ BVD. Both MCF7 and MDA-MB-231 cells showed a downregulation of β - catenin expression upon treatment with BVD, which possibly mediates the anti-proliferative effects observed with BVD treatment.

ERK signaling also regulates how the cells respond to external stimuli such as the mechanical stress. Thus, in the next objective, the thesis focused on the mechanotransduction aspects of breast cancer, as there are numerous studies that suggest that mechanostimulus induces cellular changes in cancer cells driving their metastatic phenotype. Matrix stiffness has been identified as a critical factor in the progression of cancer. Studies have found that the Raf kinase inhibitor, Sorafenib showed reduced efficacy on stiffer microenvironments, rich in collagen. Hence further studies on the matrix stiffness may provide better screening of advanced chemotherapeutic options [1] PIEZO ion channels function as biological pressure sensors in both vertebrates and invertebrates. During tumour progression in a confined tissue space, the growing tumour mass experiences alterations in the mechanical cues in the form of increased tissue stiffness. PIEZO1 is activated by various types of mechanical stimuli as well as by some chemically synthesized small molecules. One such compound named Yoda1 has been identified as an agonist for both mice and human PIEZO1. PIEZO1 has been found to be activated by Yoda1 even in the absence of other cellular components. Thus Yoda1 can provide detailed insight to the study PIEZO1 regulation and function. [2]

Synopsis

The effect of PIEZO1 activation on the proliferation of breast cancer cells was assessed by treating MCF7 and MDA-MB-231 cells with its chemical agonist Yoda1 and Dooku1, an allosteric antagonist of Yoda1 to ascertain the specificity of Yoda1-induced activation of PIEZO1. Treatment with either Yoda1 or Dooku1 did not significantly affect the cell viability or proliferation, although Yoda-treated MCF7 cells showed a reduction in CCND1 expression. However, Yoda1-treated MCF7 and MDA-MB-231 cells had reduced colony-forming abilities, with the cells forming fewer and smaller colonies than the non-treated conditions. Yoda-treated MCF7 cells showed a significant upregulation of NANOG and OCT4 indicating that Yoda1 and Dooku1 can act synergistically to affect gene expression. Yoda1 treatment lowered the migration rate of MDA-MB-231 and MCF7 cells. Further, Yoda1-treated MCF7 cells showed significant downregulation in the expression of EMT-associated gene SNAI2. The expression of stemness markers CD24, CD44 and EPCAM was altered upon Yoda1 and Dooku1 treatment. Both MCF7 and MDA-MB-231 cells treated with Yoda1 for 48 hours showed a significant upregulation of p-ERK1/2 levels compared to control cells. Yoda1 treatment significantly reduced the expression of RHOA in both MCF7 and MDA-MB-231 cells, which could not be rescued by Dooku1. Treatment of MDA-MB-231 cells either with Yoda1 or Dooku1 showed a significant reduction in the expression of β -catenin, and their combination showed additive effect.

Considering the effect of Yoda-induced PIEZO1 activation on the ERK-phosphorylation in breast cancer cells, the role of PIEZO1 activation in mediating the sorafenib-sensitivity of MCF7 and MDA-MB-231 cells was assessed. MCF7 and MDA-MB-231 cells were subjected to colony formation assay under treatment with Yoda1/Sorafenib or their combination. In MDA-MB-231 cells, there was a similar reduction of colony size in sorafenib and Yoda1+sorafenib combination treatment compared to control cells. Whereas, MCF7 cells treated with the combination of Yoda1 and sorafenib produced significantly larger colonies than sorafenib only treated condition. Thus, the studies with PIEZO1 activator Yoda1 showed that PIEZO1 activation leads to reduction in migration and proliferation of breast cancer cells. Although Dooku1 was reported as PIEZO1 inhibitor, according to the results obtained, Dooku1 failed to reverse the effects of Yoda1. So, a different strategy was followed to downregulate PIEZO1 expression. For this, lentiviral mediated gene silencing method was utilized to modulate PIEZO1 expression.

PIEZO1 was silenced by lentiviral-mediated method to understand the role of PIEZO1 in breast cancer progression. PIEZO1 silencing significantly downregulated PIEZO1 activity and its expression at mRNA and protein levels. Although PIEZO1 downregulation did not impact the proliferation, it plays a role in modulating the self-renewal ability of MDA-MB-231 cells. PIEZO1 silencing significantly inhibited the migration potential of both MCF7 and MDA-MB-231 cells. A

Synopsis

significant downregulation was observed in NOTCH2, β -CATENIN (B-Cat) and FZD2 (Frizzled-2) genes in MDA-MB-231^{shPIEZO1} (PIEZO1 silenced MDA-MB-231) cells indicating suppression of Wnt signaling pathway. Further, genes that determine cancer stem cells and their self-renewal include OCT4, NANOG, SOX2, ALDH1-A3 were significantly downregulated, which correlates with the reduced colony-forming ability observed in PIEZO1 silenced cells. To understand the role of PIEZO1 further, PIEZO1 silenced MCF7 cells were treated with Yoda1 to check how the silenced cells respond to the PIEZO1 activation stimuli. Yoda1 treatment significantly reduced the colony formation ability in both control and MCF7^{shPIEZO1} cells.

Similarly, the 3D growth of cells as spheroid was significantly reduced in the presence of Yoda1, however, the growth inhibitory effect of Yoda1 was less pronounced in MCF7^{shPIEZO1} (PIEZO1 silenced MCF7) cells compared to the control cells. In contrast, no significant changes in the spheroid growth were observed in Yoda1 treated control and MDA-MB-231^{shPIEZO1} cells. As the ERK1/2 pathway is one of the key signaling pathways modulated by PIEZO1 modification, the effect of ERK1/2 inhibitor BVD523 on the growth of MCF7 and MDA-MB-231 as 3D spheroid was determined. BVD523 treatment significantly reduced the growth of MCF7 cells regardless of PIEZO1 expression levels; however, MCF7^{shPIEZO1} cells were less sensitive to BVD523 treatment, and the growth inhibition was not as pronounced as seen in the control cells. MDA-MB-231 cells, on the other hand, exhibited larger spheroid size on BVD523 treatment; however, PIEZO1 silencing significantly inhibited the spheroid growth, suggesting a context-dependent role of PIEZO1 in breast cancer cells of different subtypes.

Cancer cells acquire anoikis resistance to survive during metastasis to distant organs. Moreover, during dissemination to the distant organs through the circulatory system, they undergo shear stress and activate mechanosensing-related signaling pathways for survival and invasion into the tissue at the secondary site. PIEZO1 silencing significantly inhibited the self-renewal and survival of MCF7^{shPIEZO1} cells, and treatment with doxorubicin (Dox) completely abrogated the cell survival in both control and PIEZO1 silenced MCF7 cells. However, PIEZO1 silencing did not impact the colony-forming ability of MDA-MB-231 cells when Dox was added to the anoikis culture.

PIEZO1 silencing reduced the mechanosensing ability and enhanced the survival of the cells under stress conditions, specifically, the highly metastatic MDA-MB-231 breast cancer cells compared to MCF7 cells. In agreement with the increased survival and colony-forming ability observed in PIEZO1 silenced MDA-MB-231 cells, MDA-MB-231^{shPIEZO1} cells had significantly higher expression of survival factors BCL2, RHOA and phosphoERK1/2. Thus, PIEZO1 silencing differentially modulates the breast cancer cells with reduced PIEZO1 favoring the survival and self-renewal of metastatic breast cancer cells MDA-MB-231 by enhancing the expression of survival genes BCL2 and pERK1/2.

Synopsis

Thus, ERK signaling plays a major role in breast cancer progression and inhibition of ERK with sorafenib or BVD-523 as a combinatorial therapy can inhibit metastatic breast cancer progression. Furthermore, mechanostimulus plays an important role in breast cancer metastasis and modifying the expression of mechanosensor protein PIEZO1 can impact the breast cancer progression in a context-dependent manner.



INTRODUCTION

1.1 Cancer – Initiation, Progression, Therapy and Resistance

Cancer, in simple terms is defined as the uncontrollable cell growth and replicative potential that occurs due to the dysregulation of various cell signaling pathways accumulating a range of mutations and can invade distant tissue from the site of origin. Both genetic and epigenetic mechanisms have been known to be the causative agents. Cancer cells can traverse through blood vessel and lymphatic system between two different sites. Cancer, in fact is the second leading and the most alarming cause of death affecting a large number of people worldwide. Salient characteristic features of cancer include - limitless replicative growth potential, evasion of apoptosis, dysregulation in cell cycle regulatory check points, improper differentiation, abnormality in cell membrane, mutation in cell signaling molecules, change in cell morphology and cytoskeletal protein orientation. The process of malignant transformation occurs eventually starting from a healthy cell, accumulating mutations and undergoing a vast range of changes in several cellular properties. This later gives rise to a localized bunch of tumorigenic cells (benign tumor) which in turn via angiogenesis, degrade the basal membrane to invade neighboring tissue sites and ultimately metastasize to colonize distant organs. The delay in diagnosis, due to lack of awareness can lead to poor prognosis in patients including resistance to chemotherapy and promoting stemness behavior. Development of cancer begins upon the advent of mutations in a cell, directed to proliferate continuously. This in turn is followed by the selection of rapidly proliferating and growing cells in the population which leads to enhanced tumor growth and malignancy.

To argue with the fact regarding the origin, progression and sustenance of cancer, it can be said that cancer is a three-way interacting system which arises and interacts based on cellular (molecular level), interacting neighboring cells with the tumorigenic stroma and interplay between different levels involving the entire organism. All the genes, metabolites, miRNA, signaling molecules followed by different interaction at the cell surface level with the surrounding stroma and the immune or endocrine systems influence each other. [3]

The three-stage theory of carcinogenesis is one of the most widely accepted theories in the field for the development of cancer. This theory categorizes cancer development into three stages: initiation, promotion, and progression.

Initiation marks the point of initial cell mutation, which engages one or more than one cellular change. These changes or mutations, can be either spontaneous or can start upon exposure to a carcinogen. These

cells, then upon further divisions, give rise to cancerous daughter cells.

Definite regions of DNA are involved with maintaining normal cell growth and repair – these genes upon activation give rise to oncogenes. Oncogenes upon aberrant activation leads to the disruption of cell development cycle. Another well-known set of genes known as the tumor suppressor genes are the components of DNA which suppress or inhibit cell division; mutations in these tumor suppressor genes and oncogenes therefore, give rise to new clone of cells, arising from the cellular changes that have a selective and replicative advantages over normal parent cells. The new cells develop the ability to evade apoptosis and proliferate in an uncontrolled manner.

Promotion is the second stage of cancer development and progression where the transformed cells are instructed to divide. Both the intracellular and extracellular environment influence the development of cancer. Transformation of a cell to its malignant stage requires repeated exposure to oncogenic agents which drive the growth of the mutated cell.

During **progression**, the third stage of cancer development, the tumor cells keep accumulating further mutations in order to compete with each other, eventually making them more aggressive and heterogeneous in nature. Heterogeneity is referred to the multiple genetic variants of a transformed cell that has undergone mutation. Increased heterogeneity corresponds to harder to diagnose and treat cancer since cancer cells found in one lump or mass act and look differently from other mass.

Metastasis is the salient characteristic feature of malignant tumor. It arises as a result of loss of adhesion molecules which help bind the cells together with each other as well as with the extracellular matrix. This loss of adhesion aids the cancer cells to break away from the neighboring cells and invade other tissues, by passing through the basal membrane and entering the blood and lymphatic system to be transported to distant sites of the body. [4] [5]

Several treatment options are available for cancer patients – surgery, **chemotherapy**, radiotherapy, immunotherapy, hormone therapy, bone marrow transplant. Among all the options available, one of the most widely prescribed mode of therapy depending on the cancer type, is chemotherapy. It uses anti-cancer drugs which can be provided either orally or intravenously. These drugs then travel via bloodstream to reach targeted cancer cells in most parts of the body.

Based on the time period of administration of chemo drugs, the chemotherapeutic treatment is primarily of two kinds- adjuvant and neo-adjuvant therapy. Especially in breast cancer, patients are provided with chemo drugs – once before the surgical procedure of tumour tissue removal, called the neo-adjuvant therapy. This helps shrink the size of tumours which are larger in size upon initial diagnosis and hence

difficult to surgically remove. Adjuvant therapy is provided post-surgery to completely eradicate any remaining cancer cells that might be present but difficult to identify. On a broader scale, chemotherapeutic drugs are anti-metabolites that interfere with the ability of cancer cells to divide and grow. [6] Interestingly, neoadjuvant type of chemotherapy has recently been recognized as a better option for downstaging primary tumour in the breast and axillary lymph node, that has not spread to distant organs from the site of origin. Further evaluations of the neoadjuvant chemotherapy can provide a validated prognostic factor in both basic research and clinical trials. [7] Identification of different types of cancer-specific biomarkers are progressively being carried out which mark the way for the advancement of cancer therapeutics. Systemic and targeted approaches are considered to be the future of cancer medicine but it still cannot be denied that chemotherapy remains a widely accepted therapeutic option currently, despite having side effects on the patients' physical and psychological health. Chemotherapeutic pharmaceuticals are still the frontline choice for advanced stage malignancies in which surgery or radiation therapy are generally not prescribed for certain reasons. [8]

Since cancer cells grow and divide at a faster rate than normal cells, they are generally under higher endogenous stress, which in turn offers a favourable situation for the anti-cancer drugs to effectively destroy them in comparison to the surrounding cells. In order to treat solid cancers, some of the inhibitor therapies are used which include PARP inhibitors, p-53 or MDM2 inhibitors, tyrosine kinase inhibitors, hedgehog pathway blockers, proteasome inhibitors. Based on the type and stage of cancer, the chemotherapeutic drugs are prescribed to neutralise the effect of cancer cells and amend the stress caused by tumour growth. The dosage and timespan are two important parameters for the treatment. Despite all the factors being taken into consideration, the cons of chemotherapy cannot be avoided. The primary hindrance in the way of chemotherapy is the relapse of the disease. During this stage, cancer cells have been found to undergo resistant to a broad range of chemotherapeutic drugs. [9] [10]

Prolonged exposure to drugs makes the cancer cells resistant to the treatment and thus specialized planning is required and carried out before administering the chemo drugs to the patients which collectively determine the drug combination, dosages, duration of cycles and additional supplements.

Although overall incidences of cancer are on the rise, the risk of mortality from cancer has reportedly decreased continuously since 1991, resulting in a general decline of 32% in cancer death rate as of 2019. The success of longer life span after treatment, accounts to the improvement in lifestyle changes and in implementing better habits, as seen in patients with lung cancer. In case of colon and breast cancer, combination chemotherapeutic treatments or adjuvant therapies based on prolonged research, have paved way for the betterment of patient survival in clinical trials. Treatment targeted against various types of

cancer, progressed in the past decade owing to early detection, targeted therapies, and development of advanced surgical techniques. Along with lung cancer and melanoma, liver cancer occurrence and treatment showed considerable improvement, whereas in case of prostate and breast cancer, higher incidence rate among patients despite the ability of both the types of cancers being amenable to early detection, is a matter of concern. It can be said that increase in investment in existing cancer control interventions and basic clinical research can be beneficial to gain detailed knowledge on advanced therapeutic strategies and henceforth promote the awareness among socioeconomic inequalities. [11]

1.2 Breast cancer

Breast cancer, currently is the most prevalent cancer affecting a large population of women worldwide. It is a heterogeneous disease at the molecular level. Mutations arise that include activation of hormone receptors, growth factor receptors or genetic mutations like BRCA. Several treatment options are available, notably radiation therapy, surgery, systemic therapies that include hormone therapy, chemotherapy, using bone stabilizing agents, poly (ADP-ribose) and immunotherapy. [12] The accumulation of different genetic and epigenetic changes in breast cancer cells over a period of time leads to malignancy at a fatal level if not diagnosed and treated on time. Age, unhealthy body weight, overexposure to hormones like oestrogen, genetic factors (hereditary causes) can contribute to the cancerous phenotype. [13]

Breast cancer types have been classified into the following subtypes for example a) Infiltrating (invasive) ductal carcinoma b) Ductal carcinoma in situ c) Infiltrating (invasive) lobular carcinoma. d) Lobular carcinoma in situ e) Triple negative breast cancer (TNBC) f) Inflammatory breast cancer g) Rare and aggressive h) Paget's disease of the breast. The lobules which are the milk producing

glands; the ducts which carry the milk from lobule to the nipple and connective tissue consisting of fibrous and adipose tissue which connects, protects and supports them together. Invasive ductal and invasive lobular carcinoma have been the most common type of breast cancer among all the other types. Invasive ductal carcinoma being the type where the cancer cells grow out of the ducts to other parts of the breast tissue and invasive lobular carcinoma involves the cells migrating out of the lobules to the nearby sites.

Based on histopathological types, breast cancer can be further subdivided into ER, PR, HER2/ERBB2 (hormone receptor status). At the molecular level, the classification is based on gene expression patterns later to be modified and finally distributed into the following categories - luminal A (ER⁺/PR⁺/HER2⁻), comprising about 70% of all the breast cancers, luminal B – about 12% of all cases, HER2-enriched (ER⁻/PR⁻/HER2⁺) – 5% of all the types and basal-like or triple negative (ER⁻/PR⁻/HER2⁻) constitute another 12% of total number of cases. The triple negative ones are more proliferating and aggressive by

nature, than the other subtypes. Treatment of patients with TNBC poses a problem since no target endocrine or HER2 therapies are applicable, that eventually relies on chemotherapy which is non-specific as well as cytotoxic. This necessitates the development of a more specific drug targets for these higher-grade carcinomas. The highly invasive claudin low subgroup exhibited heterogeneity and six molecular subtypes. These are also characterised by poor five-year prognosis. [14]

Presence of stem cell like behaviour in breast cancer cells imparts to the development of chemo resistant phenotype. It has been found from some literature review that the interaction between the cancer stem cells and their microenvironment affects cell remodelling by undergoing epithelial to mesenchymal transformation, increased signaling for self-renewal capacity as well as over expression of ATP-binding cassette transporter proteins or the drug efflux proteins [15]. Thus, it is very crucial to evaluate the mechanisms of signaling pathways involved in chemoresistance in breast cancer cells which may help to understand the current treatment conditions thoroughly to achieve a higher success rate. [16]

The event where cancer cells proliferate vigorously and migrate vehemently, breaking away from the initial site of origin to a distant site or organ is the rate limiting step which is known as metastasis which is instrumental to the different forms of cancer. [16]

In breast cancer, patients suffer from extreme pain and suffering while undergoing therapeutic treatments to combat the morbid effects of metastasis. Newer blood vessels form at the site surrounding the tumour cells, also known as angiogenesis which facilitate widespread distribution of tumour cells gaining potential to become cancerous. [17] [18]. Breast cancer is one of the major types of cancer among women worldwide. Two major reasons which cause menace to the patients are metastasis and chemoresistance. Metastasis is the spread of tumor to distant sites of the body from the point of origin whereas chemoresistance is defined as hindrance to the chemotherapeutic procedures occurring due to the failure of chemo drugs to have a considerable effect on the targeted cells either due to evacuation of the drugs by the cells via pumping mechanism or relapse of cancer after a certain period of time once the effect of the drug gets evaded. [19-21] Breast cancer stem cells, are identified as CD44⁺/CD24⁻/lo along with other markers like ALDH and CD49F. These are responsible for cancer initiation, progression, chemoresistance and recurrence. CD44⁺/CD24⁻/lo phenotype is enriched in basal like breast cancer like that of MDA-MB-231 cells which show CD44⁺/CD24⁻/lo phenotype.

Improper regulation of cell adhesion molecules and integrins along with overexpression of matrix metalloproteinases (MMPs) and epithelial-to-mesenchymal transition (EMT) induce invasive behaviour of metastatic breast cancer cells. In addition to the mentioned causes, metastatic development is further contributed by the breast cancer stem cells due to their inherent resistance to chemotherapeutic drugs. ERK1/2 and p38 MAPK signaling pathway are important regulators of several cancer pathways.

Constitutive activation of these pathways can also add to the metastatic and chemo-resistant behaviour of the tumour cells. [22]

1.3 Metastatic cancer progression

In majority of cancers, especially in breast cancer, both neoplastic cells and the stromal cells around them undergo progressive alteration at the time of transformation of normal tissue into higher grade malignant tissue. This is a multistep process reflect changes in heterotypic signaling between stroma and tumour parenchyma. The entire progression depends on reciprocal interactions between supporting stromal cell and neoplastic cells. Incipient neoplasia initiates recruiting and activating stromal cell types that gather into a preliminary pre neoplastic stroma. This in turn reciprocally responds by augmenting the neoplastic phenotypes of the nearby cancer cells. The reprogramming of normal stromal cells continues to serve the budding neoplasm. Thus, signal originating in the tumour stroma induce the cancer cells to invade adjacent tissue and disseminate to other sites. This stage of tumour progression known as the reciprocal heterotypic signaling give rise to metastasis.

The circulating cancer cells, released from primary tumours, leave a microenvironment created by supportive tumour stroma and enter into a normal tissue microenvironment in a distant organ. This can explain the reason of absence of many heterotypic signals in the site of dissemination, that shaped their phenotype previously in the primary tumour site. The succession of reciprocal cancer cell to stromal cell interactions are repeated in the distant site where the disseminated cancer cells proceed to colonize new organs. [23] [24] Surprisingly, in some of the disseminated metastatic sites, the tumour micro environment is already favourable for the newly arrived cancer cells and thus are called “metastatic niches”. Major components of induced premetastatic niches include tumour promoting inflammatory cells. The signaling interaction between the tumour stroma and cancer cells prove to play important roles in different stages of progression of metastatic cancer and hence needs proper understanding of dynamic variations to help develop novel therapeutic targets for both primary and secondary tumours.

1.4 Signaling pathways dysregulated in cancer

Hormones, growth factors, cytokines in circulation, regulate cell proliferation, differentiation, angiogenesis, apoptosis and senescence. The extracellular chemical signals received by the cells, are then propagated to intracellular processes through kinase signaling in a sequential manner. The signal transduction system with growth factors, transmembrane receptor proteins and secondary cytoplasmic messengers represent attractive targets for chemotherapy. [25] In cancer cells, signal transduction is a highly

orchestrated process that involves receptor tyrosine kinases (RTKs) which induce multiple cytoplasmic kinases, often serine/threonine kinases. Within the cell, there exist more than one signaling pathways which either work independently, in parallel or in cross talks and interconnections. Dysregulation of these intracellular signaling pathway molecules are responsible for cancer development. The three major signaling pathways, involved in cancer signaling are - Phosphatidyl inositol-3-kinase (PI3K)/AKT, protein kinase C (PKC) family, and mitogen-activated protein kinase (MAPK)/Ras signaling cascades. Specific blocking of only one of the kinases, have been, reportedly, able to limit the oncogenic activity in clinical trials. Detailed evaluation of the signal transduction pathways has helped to develop several kinase inhibitors in the past few decades which target kinases at the level of receptors (upstream) or downstream serine/ threonine kinases. [26]

Anticancer treatment employs the inhibition of multiple molecular targets by single drugs or selective target specificity involving multiple drugs in appropriate combination, as reported in preclinical and clinical studies. Molecules involved with vascular endothelial cells and pericytes are also recruited as important targets for anticancer therapies. Therefore, optimal therapeutic efficacy may be obtained involving multiple molecules in both tumour and supportive tissues. [26]

mTOR is an intracellular serine/threonine kinase that is a central to the regulation of cell growth and proliferation, angiogenesis, nutrient uptake, utilisation and metabolism. The well-known ligands which bind to and activate cell surface receptors are growth factors such as epidermal growth factor (EGF), insulin growth factor, platelet-derived growth factor and vascular endothelial growth factor. Activation of the intracellular phosphatidylinositol 3 kinase-serine- threonine kinase-mTOR (PI3K-AKT-mTOR) pathway leads to enhanced protein synthesis. Deregulation in m-TOR linked pathways have been identified and studied as an increased risk in many cancers. The deregulations include mutation or overexpression of growth factor receptors, loss of function of tumour suppressor genes or gain of function mutations in m-TOR linked pathways. Targeting these mutations can be successful in strategic development of anti-cancer drugs since the dysregulated pathways promote overgrowth, survival, proliferation migration and angiogenesis of tumour cells. [27]

1.5 ERK signaling pathway

ERK signaling was selected for this study based on its importance in cancer metastatic signaling. High ERK levels correlate with poor prognosis in triple-negative breast cancer patients. It has been known from several literature reviews that protein kinase dysregulation plays crucial role in cancer specially breast cancer progression and hence it becomes increasingly difficult to treat patients with metastatic breast cancer due to poor prognosis.

Mitogen-activated protein kinase (MAPK) cascades are major signaling pathways responsible for the regulation of different cellular processes which include proliferation, differentiation, apoptosis and stress responses. The MAPK pathway has been categorized into three main kinases, MAPK kinase kinase, MAPK kinase and MAPK, which in turn activate and phosphorylate the subsequent downstream proteins. The extracellular signal-regulated kinases ERK1 and ERK2 are evolutionarily conserved, ubiquitous serine-threonine kinases, known to regulate both normal and pathological cell signaling. ERK expression is critical for cancer development and progression. The Ras/Raf/MAPK (MEK)/ERK pathway is one of the most vastly studied pathways, playing a central role in the development and survival of cancer cells.

[28] [29]

ERK cascades are extremely regulated cascades, responsible for performing basic cellular processes, like proliferation and differentiation. All these regulatory factors affect bispecific phosphatases, scaffold proteins, signal duration/intensity and the dynamic subcellular localization of cascade components. The importance of the ERK cascade amplifies with the fact that ERK disorders are harmful to the normal functioning of the cells and ultimately to the entire physiology. Aberrant activation of upstream proteins and kinases in the ERK pathway has been reported to induce various diseases, inflammation, developmental disorders, neurological disorders and especially cancer [30].

Epithelial to mesenchymal transition, a hallmark feature of metastatic cancer, is characterised by dysregulation of cell adhesion molecules, integrins and overexpression of matrix metallo- proteinases (MMPs) [31],[32]. Intracellular signaling pathways such as ERK1/2 and p38 MAPK are known to be activated in advanced stage of tumour progression [33, 34]ERK signaling was found to have an important role in metastatic signaling where elevated ERK levels correlate with poor prognosis in triple-negative breast cancer patients [35].

The four crucial MAPK cascades that have been identified in eukaryotic cells responsible for maintaining cellular homeostasis are ERK, JNK/stress-activated protein kinase, p38 MAPK and ERK5 signal transduction pathways. Each MAPK signaling cascade comprise of three tiers: MAP3K, MAPKK and MAPK. Previous studies have elucidated that the JNK and p38 MAPK pathways are mainly related to stress and apoptosis of cells; whereas the ERK/MAPK signaling pathway, is closely related to cell proliferation and differentiation in the cell signal transduction network. [36] [37]. ERK pathway gets activated by multiple ligands like cytokines, growth factors, viruses, G- protein coupled receptor ligands as well as oncogenes. The small G proteins Ras, an upstreamprotein of the Raf-MEK-ERK pathway and downstream Raf kinase, MEK1/2 and ERK1/2 arethe key molecules. Ras has an active GTP-binding conformation and an inactive GDP-bindingconformation by which it can alternate between the two states to regulate signal transduction. Ras has been known to be activated by many factors, such as epidermal growth factor (EGF), tumour necrosis factor (TNF), activators of protein kinase C (PKC) and Src family

members. Upon binding of an extracellular signal to its specific receptor, growth factor receptor-binding protein 2 (Grb2) comes and binds to the activated receptor. It then interacts with the proline-rich sequence at the C-terminus of son of sevenless (SOS) to form the receptor-Grb2-SOS complex. Binding of SOS to the Tyr phosphorylation site on the receptor eventually leads to the translocation of cytoplasmic SOS to the membrane. SOS along with Ras-GDP induce the replacement of GDP with GTP in Ras, thereby activating Ras to initiate the Ras pathway. The Raf protein kinase is a protein encoded by the *raf* gene. Upon binding to Ras, Raf exhibits serine/threonine protein kinase activity and gets activated. Its C-terminal catalytic domain can then interact with MEK, and its catalytic subregion is phosphorylated at the serine residue, activating MEK. The two MEK subtypes, MEK1 and MEK2, have molecular weights of 44 and 45 kDa, respectively. MEK is a dual-specificity kinase which by phosphorylating the Tyr and Thr regulatory sites, activates ERK. This activation confers double specificity and improves the accuracy of signal transduction. MAPK/ERK is a Ser/Thr protein kinase. MEK anchors ERK in the cytoplasm. When the signaling pathway is inactive, ERK is localized to the cytoplasm. Once a signal stimulates the phosphorylation and dimerization of ERK, activated ERKs are translocated to the nucleus, where they promote cytoplasmic target protein phosphorylation or regulate the activity of other protein kinases, followed by further phosphorylation of downstream substrates. [38] The process of ERK2 phosphorylation and translocation into the nucleus has been studied and it was found that both phosphorylated and unphosphorylated ERK2 form a homologous dimer before translocating to the nucleus which is necessary for its action. [39]

ERK/MAPK signaling pathway can also be activated via the following ways: i) Ca^{2+} activation; ii) receptor tyrosine kinase Ras activation; iii) PKC-mediated activation; and iv) G protein-coupled receptor activation [40] As by now it is known that unstimulated cells host ERK1/2 in the cytoplasm, but once activated, ERK1/2 is translocated to the nucleus where it regulates the activity of various transcription factors through phosphorylation. This leads to the eventual regulation of cell metabolism. Cytoskeletal components such as microtubule-associated protein (MAP) 1, MAP2 and MAP4 are phosphorylated in the cytoplasm to regulate cell morphology and cytoskeletal redistribution [41]. Cytoplasmic ERK1/2 can phosphorylate a series of other protein kinases which are upstream of the ERK pathway, such as SOS, Raf-1 and MEK in a negative feedback regulatory manner. Activation of ERK/MAPK signaling pathways leads to the activation of other extracellular signaling pathways. ERK upon activation enters the nucleus to bind to the transcription factors which in turn triggers gene expression in response to external stimuli and regulate cell proliferation, differentiation, apoptosis and transcription.

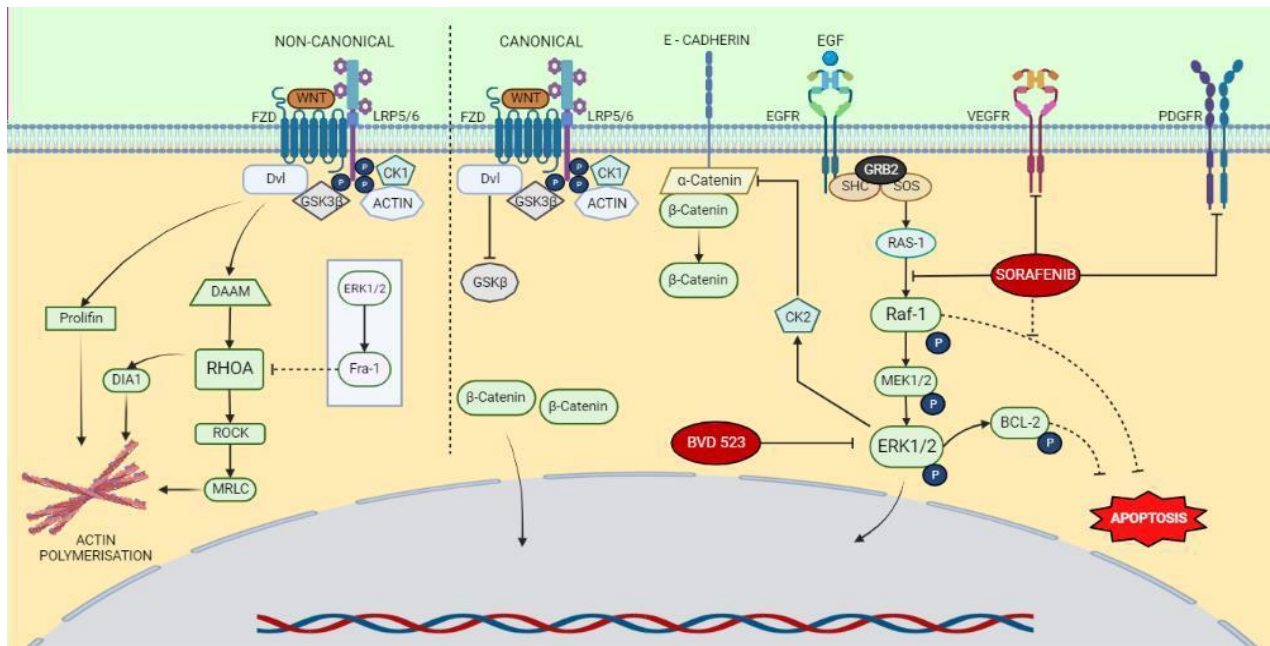


Fig 1.1 Crosstalk between different signaling molecules of the ERK signaling pathways involved in breast cancer development and progression.

1.6 Sorafenib

Sorafenib is a multi-kinase inhibitor targeting receptor tyrosine kinases and is an FDA approved anticancer drug used for hepatocellular and renal carcinoma. It is highly effective against hepatocellular carcinoma where it has been shown to inhibit metastatic migration. In addition to the functional effects, Sorafenib is a potent inhibitor of cell surface receptor tyrosine kinases such as VEGF and PDGF receptor kinases, Flt-3, and c-kit. In addition, Sorafenib also inhibits intracellular serine/threonine kinases such as Raf-1. As per earlier reports it has been observed that in other cell types, Sorafenib downregulated phosphorylated levels of p38MAPK and STAT5. p38MAPK activation transduces metastatic signaling and proliferation, while STAT5 signaling promotes tumour growth and metastasis in breast cancer cells [42] [43].

However, its role in breast cancer migration, metastasis and intracellular signaling is unknown and hence for this study Sorafenib is used in targeting breast cancer cell proliferation, migration and metastasis.

In hepatocellular carcinoma, Sorafenib treatment led to the inhibition of cell cycle, cell adhesion and proliferation-related genes followed by overexpression of apoptosis-related genes [44]. Moreover, it caused inhibition of angiogenesis and downregulation of RAF/MEK/ERK pathway in hepatocellular carcinoma implying its anti-tumorigenic activity [45]. In one of the studies carrying out clinical trials, Sorafenib has been used in breast cancer patients as a mono-therapeutic agent, in endocrine therapy as well as in combination with other cytotoxic drugs like taxanes, capecitabine, bevacizumab, gemcitabine. Its combination with gemcitabine, capecitabine and tamoxifen were found to be more promising than others [46].

However, molecular effects of Sorafenib on breast cancer cells were not studied and needs to be evaluated. Hence, important inhibitory effects of Sorafenib treatment on the invasive and metastatic potential of breast cancer cells requires further exploration.

1.7 BVD-523

In case of Pancreatic ductal adenocarcinoma (PDAC), effective therapeutic treatment is still an unmet medical requirement. Even though KRAS oncogene which is present in more than 95% of PDAC, could be a strategic target but it had shown unsuccessful attempts clinically. Hence, targeting mitogenic RAF-MEK-ERK pathway, the key effector cascades of KRAS oncoprotein, can be a potential strategic target. Nevertheless, RAF / MEK inhibitors did not succeed at clinical trials due to reactivation of ERK signaling via multiple mechanisms. Thus, requirement of ERK-specific inhibitors came to light to effectively inhibit the pathway.

Ulixertinib or BVD-523 is known as a first-in-class ERK-specific inhibitor. It showed promising antitumor activity in a phase I clinical trial for advanced solid tumours having BRAF and NRAS mutations. Ulixertinib therefore inhibits *in-vitro* growth of multiple PDAC lines effectively and potentially uplifts the cytotoxic effect of gemcitabine. It also helps in upregulating the PI3K-AKT pathway through activating the HER/ErbB family proteins. Simultaneous inhibition of PI3K or HER proteins in association with Ulixertinib, synergistically acted in suppressing PDAC cell growth both *in vitro* and *in vivo*. [47]

In case of chronic lymphocytic leukemia, genetic mutations of the RAS-BRAF-MAPK-ERK pathway are yet to be thoroughly studied in patients. Upon clinical and biological analysis of the concerned patients with mutations in this pathway, the *in vitro* response of primary cells to BRAF and ERK inhibitors showed putative damaging mutations 5.5% of patients. BRAF was mutated in 2% of patients and genes upstream of B-RAFTs were mutated in 2.6% of patients whereas genes downstream of BRAF like MAPK2K1, MAPK2K2 and MAPK1 were mutated in 1.1% of patients. Majority of the mutations were sub-clonal and missense where patients had higher lactate dehydrogenase levels along with ZAP-70, CD49d, CD38, trisomy 12 and unmutated immunoglobulin heavy-chain variable region genes and a worse 5-year time to first treatment. Gene expression analysis revealed that there is an upregulation of genes of the MAPK pathway in the group carrying RAS-BRAF-MAPK-ERK pathway mutations, implying this pathway to be the foremost cellular process to be affected by novel mutations.

In conclusion, although larger cohort of patients are required to study the RAS-BRAF-MAPK-ERK pathway in details, it is one of the core cellular processes affected by novel mutations in chronic lymphocytic leukemia. Due to its association with unfavourable clinical features, it could be pharmacologically targeted and inhibited. [48]

As reported from earlier works, elevated MAPK signaling is a characteristic feature of cancer. Direct ERK1/2 inhibition may be a more promising approach to bypass ERK1/2 reactivation caused by upstream kinases like BRAF, MEK1/2. The selectivity and dynamics of ERK1/2 inhibitors are much less studied compared with BRAF or MEK inhibitors.

Some of the inhibitors like PD0325901, LY3214996, and Ulixertinib have been prone to ERK1/2 reactivation over the course of time. Mainly two kinds of ERK1/2 reactivation have been observed, the first is reversed by adding a fresh dose of inhibitors while the second continues despite adding more treatments to it. The cells became resistant to MEK1/2 inhibitor PD0325901 because of ERK1/2 reactivation but remained sensitive to Ulixertinib. This suggested that ERK inhibition correlated with drug induced toxicity in multiple cell lines. [49]

Concurrent inhibition of both MAPK and PI3K signaling pathways showed effective response in cancer therapy by overcoming drug resistance of MAPK signaling pathway inhibitors. The drugs developed against the target signaling pathways showed promising effect against proliferative and tumorigenic profiles in colon cancer cell lines. Drug combination of BVD- 523 with GDDC-0980 in HCT-116 xenograft model showed drastic reduction in tumour growth sans toxic effects. [50]

RAS–RAF–MEK–ERK (MAPK) pathway is a feasible therapeutic target due to its aberrant activation across various cancers. But there lies a disadvantage with BRAF and MEK-targeted combination therapy since most of the treated patients develop chemoresistance after few months or about a year; which may be due to reactivation of ERK signaling. [51]

The downstream signaling regulators of the RAS-RAF-MEK, - ERKs are crucial regulators of the MAP-K pathway. There are a broad range of clinically trialled RAF and MEK inhibitors or the upstream MAPK inhibitors which show resistance and hence necessitates the availability of drug targets that are specific like targeting ERK (ERK1 and ERK2 isoforms). To assess the activity of ERK isoform inhibitors, analyses of recombinant proteins are carried out. Independent and direct profiling of native ERK1 and ERK2 activity poses to be a strategically better complementary system to probe and target ERK function. [52]

A quantitative chemo-proteomic strategy uses the active site targeted probes to quantify native ERK function in a manner that is isoform specific. A single isoleucine or leucine difference in the substrate binding sites of ERK makes it feasible to profile ERK1 and ERK2 separately and vividly across a wide range of cell or tissue types. This helps to determine the efficacy of academic (VX-11e) and clinical (Ulixertinib) ERK inhibitors, which revealed that more than ninety percent of inactivation is required for both native ERK1 and ERK2, in order to properly exert cellular anti-proliferative activity. [52]

In case of KRAS dependent cancer, RAF-MEK-ERK cascade kinase is a key regulator. Even then pharmacological inhibitors directed against RAF and MEK did not show considerable effect in inhibiting KRAS mutant cancers. This may be due to reactivation of ERK probably occurring as a result of

reprogrammed dynamic signaling. ERK inhibition leads to MYC oncoprotein degradation associated with senescence like phenotype. This helps arrest cell growth and identify PI3K-AKT-mTOR signaling as a crucial modulator of ERK inhibitorsensitivity. This validates the development of a greater number of cancer chemotherapeutics targeting specifically ERK. [53]

1.8 Breast cancer markers

Expression of CD44 is found to be associated with enhanced self-renewal, proliferation and metastasis. Particularly, in breast cancers the percentage expression of CD44⁺/CD24⁻/CK⁺/CD45⁻ was more in malignant lesions than non-malignant ones. [54]. In support of this statement, research from other findings claimed significant reduction of proliferation and migration upon knockdown of CD44 in breast cancer cells.[55]

CD44, the well-known cell adhesion protein and a key regulator in cellular migration, has been found to contain cholesterol enriched membrane microdomains or the lipid rafts. Raftaffiliation of CD44 has been found to be negatively correlated with migration of highly invasivebreast cancer cell lines, unlike the non-invasive cell lines where raft affiliation of CD44 gotincreased. CD44 palmitoylation levels were lesser in primary cultures from invasive ductalcarcinomas as compared to non-tumorigenic ones. Co-localisation of CD44 with ezrin, a lipidraft marker was also found to be lesser in invasive ductal carcinoma rather than in-situ ductalcarcinoma cultures. [56] Highly metastatic cancer cell line is characterised byEpithelial to mesenchymal transition and CD44⁺/CD24⁻ (marker of stem cell phenotype).MCF7 breast cancer cell line however lacks CD44⁺/CD24⁻ subpopulation of cells and has rarepopulation exhibiting greater Matrigel invasive ability. To obtain cells of opposite migratoryand invasive potential, via sequential selection process using Matrigel, MCF7-14 was analysed comparatively with parental MCF7 and aggressive mesenchymal MDA-MB-231 cells usingmicroarray expression profiles of epithelial and mesenchymal markers. MCF7-14 cellsexpressed E cadherin but neither vimentin or fibronectin. Beta catenin levels were also foundin nucleus apart from membrane localisation; which helps in imparting enhanced migratory and invasive capability in MCF7-14 cells as compared to MCF7 parental cells. This is coupled with enhanced CD44 expression and inhibited CD24 expression. [57] Cancer stem cell phenotype in breast cancer cells is characterised by the presence of EpCAMexpression which helps in promoting metastasis of cancerous tissues to bones. In some othertype of cancers like lung cancer, expression of CD44 and CD166 has been associated withEpCAM expression. Cells that are triple positive for these markers' expression, exhibitaugmented spheroid forming ability, self-renewal capacity, clonogenicity as well as chemotherapeutic resistance. [58]

CD44 is a key signal transduction molecule which has a role in the activation of Rho-GTPases, Ras-MAP-

K, P-13/AKT pathways, etc. It is interesting to note that CD44, on its own lack kinase activity, thus it initiates signaling by adapting intracellular kinases and adaptor proteins that bind to the cytoplasmic tail of CD44 to the actin cytoskeleton. Different mechanisms exist whereby CD44 activates major signaling pathways mainly the downstream cascade kinases like p115, Rac1, c-Src and FAK, Rho and Rac upon interacting with cell surface associated growth factors, cytokines and enzymes, which helps in promoting cell migration. It has also been demonstrated that RHO-A mediated oncogenic signaling is necessary for tumour cell migration. CD44 interacts with ERM (Ezrin/Radixin/Moesin) proteins to carry out actin cytoskeletal remodelling and promote cell invasion. CD44 in breast cancer research has been studied widely since its role in breast cancer progression and metastasis depend on its various isoforms which ply through different stages of breast cancer. In some studies loss of CD44 has been shown to promote metastasis whereas gain of function in some other isoforms seemed to promote invasion and metastasis of tumour to distant site like liver from the site of origin. From another study it was observed that simultaneous upregulation of CD44 and downregulation of CD24 is associated with poor prognosis and diminished patient survival rate. With the help of microarray gene expression studies, it was observed that Cortactin, Survivin, and TGF- β 2 are some of the novel target genes behind the CD44-mediated invasion of breast cancer cells. [59] Cancerous tissue containing malignant cells exhibit diminished intracellular adhesion and enhanced cell motility coupled with lack of differentiated epithelial morphology. Mutation or downregulation of E cadherin (CDH1) gene in human cancers like loss of heterozygosity on 16q, have been found to be associated with loss of integrity in the adherens junctions. [60]

Tumour tissue in particular have stiffer extracellular matrix than normal tissue. Beta catenin in breast cancer cells translocate to the nucleus upon experiencing substrate stiffness. This drives the progression of tumour via changing the micro-RNA expression. Upon ROCK inhibition there was translocation of Beta catenin to the nucleus. This led to the activation of canonical Wnt/ β -catenin pathway. There was an inhibition in breast cancer cell migration upon downregulation of ROCK, particularly in triple negative breast cancer metastasis. [61] Local recurrence and metastasis of tumours are the major factors causing hindrance to the successful treatment in breast cancer patients. Studies have shown the presence of well-defined markers that can be associated with metastasis and local relapse. One such breast cancer cell surface marker – CD49f has exhibited itself as a better prognostic marker. CD49f+ breast tumours did not associate with age, tumour size, grade, nodal status, HER2/PR/ER status, but they were significantly associated with disease recurrence - either local or distant metastasis. CD49f+ tumours were found to be associated with markedly decreased disease-free survival [62]. CD49f (integrin α 6) has been reported to contribute to the development, differentiation, cell fate determination, migration, adhesion, survival, polarity of cancer cells [63] [64]. In breast cancer, CD49f has been observed to be involved in stem cell-like activities, such as

CD29 and CD49f mediated metastasis. CD44 and CD49f positive cells mediate stem cell properties in basal like breast cancer cells. [65]

EpCAM^{low}/CD49f⁺ subpopulation is enriched for MaSC or mammary stem cells (bipotent) progenitors and EpCAM⁺/CD49f⁺ subpopulation is enriched for luminal progenitors [66] By identifying CD49f positive cells in a tumour, patients with higher risk of distant metastatic tumours, local recurrence and poor clinical outcome can be diagnosed. [67]

1.9 Mechanotransduction in cancer

Mechanotransduction is defined as the process which senses mechanical forces extracellularly and converts them to biochemical signals intracellularly to further execute various cellular properties and behaviour. Mechano-sensation and mechano-biology therefore needs thorough research and detailed studies can help provide valuable inputs in understanding the sensory modality at the molecular level. Mechanosensitive ion channels sense the mechanical force or stimulus and are crucial in executing several biological processes like somato-sensation, sound(hearing), shear stress, etc. PIEZO1 and PIEZO2, these two mechanically activated cation channels have been identified to be expressed in many cell types. In mice, PIEZO1 has been found to be expressed in the endothelial cells of developing blood vessels. Infact embryos lacking PIEZO1 die at mid- gestation and carry defects in vascular remodelling.

When endothelial cells experience shear stress upon blood flow, PIEZO1 gets activated, the loss which causes deficits in stress fibre and defective cellular orientation in response to shear stress. Thus it seems evident that PIEZO1 is indispensable in vascular development during the growth phase of embryo. [68]

PIEZO1, the well-known mechanosensitive ion channel protein, is one of the key regulators to maintain cellular volume homeostasis in erythrocytes during circulation. Mutation in the PIEZO1 gene leads to prolonged Calcium influx and due to the disturbed Calcium homeostasis, there is erythrocytic dehydration which leads to haemolytic anaemia, a characteristic feature of hereditary xerocytosis. PIEZO1 RNA has been known to be expressed at the proerythroblast stage indicating its major role in erythropoiesis. Dysregulation in PIEZO1 channel activation leads to cell death coupled with proliferation defects in erythroid cells. [69] Both PIEZO1 and PIEZO2 are well known mechano-sensitive ion channels in mammalian cells, responsible for converting mechanical cues to biochemical signals. Genetic studies obtained from both mice and human illustrate the role of PIEZO channels in several physiological studies. Chemical agonists of PIEZO1 namely Yoda1 and Jedi1/2 have been identified via high- throughput screening assays indicating the ability of PIEZO channels to be a potential drug target. The novel drug target efficacy of PIEZO channels is yet to be properly demonstrated and understood.

Extensive research in this arena is required to pave way for better understanding into the mechanobiology of cancer cells and hence correlate it with different signaling pathways to understand the mechanism at the molecular level. [70]Breast cancer, one of the most prevalent cancers of epithelial origin, has shown the presence of PIEZO1 as a key regulator in the progression and development of breast cancer tissue. Yu et al. demonstrated the widespread expression of PIEZO1 in both normal and malignant breast cancer cells. However cancerous cells showed higher expression of PIEZO1 as compared to control. PIEZO1 knockdown studies demonstrated inhibition of fibroblast formation and expression of matrix metalloproteinases. PIEZO1 expression is negatively correlated with overall survival rate among breast cancer patients. Thus, PIEZO1 helps in regulating migration and invasion of basal cell carcinoma and can be considered as a potential therapeutic target. [71]

Cancer metastasis is characterised by two major events: migration and invasion. In certain types of cancer PIEZO1 seem to be regulating cellular migration and invasion. PIEZO1 is highly expressed in breast cancer cell (BCC) lines, whereas its role in migration of breast cancer cells has not been studied in details before. Knockdown of PIEZO1 augmented unconfined breast cancer cell migration; on the other hand, it hindered confined cell migration. Inhibition of breast cancer cell invasion by PIEZO1 is mediated by impairing invadopodium formation and suppressing expression of Matrix metalloproteinase. Through modulating cellular stiffness, motility and adhesion, PIEZO 1 regulates migration and invasion in breast cancer cells. The proliferation and cell cycle of breast cancer cells however, seemed to be unaffected by PIEZO1. This makes PIEZO1 an attractive therapeutic target. [72]

1.10 ECM and its interaction with breast cancer cells

With the help of integrins which mediate cell to matrix adhesion, the cellular homeostasis is maintained whereby cells sense and alter the mechanical cues into biochemical signals and all these interactions eventually lead to the activation of several downstream signaling pathways. Extracellular tissue forces and intracellular biological mechanisms come together via these specialized interactions. [73] Actin cytoskeleton generates forces which stretch against resisting forces of matrix fibres. This leads to change in conformation in integrins, linker proteins and nucleus. These have force sensing domains that act as mechanical switch which initiates intracellular signaling like MAPK, RHO-ROCK. The signaling pathways trigger genetic programs which eventually establish feedback loop to maintain tissue homeostasis.

To regulate normal mammary gland development, cell adhesion to the extracellular matrix (ECM) is necessary for general architecture and normal functioning. Cells adhere to ECM with the help of integrin family of transmembrane receptor proteins. This interaction helps to control gene expression and regulate clustering. This eventually activates FAK, ERK, PI3K signaling pathways, to drive proliferation and survival of the cells. A different scenario is seen in case of tumour formation, ECM is vastly remodeled and integrin signaling is altered in order to enable the cells to proliferate and invade more. It is interesting to note that the stiffness of the stromal ECM plays a key role in integrin mediated adhesion to promote tumour suppression or formation. Normal mammary gland is surrounded by loose stroma of collagen. Increased stromal ECM density makes the matrix stiffer which is then sensed by the cells with the help of Rho mediated suppression or formation. During breast carcinoma, a major risk factor associated with increase contraction of actin-myosin cytoskeleton. The surrounding ECM, when gets stiffer than the in collagen and stromal component deposition, is the greater mammographic density since ability of cell to contract it, drives the assembly of adhesion signaling complexes and integrin whereby apoptosis and epithelial phenotype gets regulated. [74]

Adhesion caused by integrin leads to the regulation in the development of a number of tissues. Upon deleting the $\beta 1$ integrin gene in luminal epithelia during different time points(stages) of mouse mammary gland (*in-vivo*) there was improper lactation and alveogenesis. Cells devoid of $\beta 1$ integrin, when cultured, showed anomalous focal adhesion, polarized acini and signal transduction. Mammary gland epithelial cells exhibited defective Stat5 activity, evaded apoptosis upon $\beta 1$ deletion. This demonstrated co-operation between cytokine and integrin signaling. [75]

Focal adhesion kinase is well known for regulating cell survival, proliferation, migration but in cancer its constitutive overexpression is central to initiate and progress tumour. Upon FAK knockout by Cre/Lox-P technique, studies proved that FAK is not essential for initiation of tumours but for their progression. Multiple signaling complexes like Src, ERK, p130Cas that are instrumental in tumour development and metastasis are regulated by FAK. Inhibiting FAK led to the interruption in the process of angiogenesis and metastasis. [76]

Another instance showed that FAK has a novel mechanism in the maintenance of cancer stemcell or progenitor cell population as seen by the marked reduction in the stem cell (percentage population of cells) expressing CD44, CD24, CD29, CD61, aldehyde dehydrogenase, etc. in FAK ablated cells. This led to marked reduction in migration and impeded self-renewal behaviour. [77]

The migrating cells with the help of surface receptors bound to the extracellular matrix generatetraction force in order to move forward and it has been well elucidated that the strength of integrin with cytoskeleton linkages, depended on the biochemical composition of the matrix aswell as its rigidity, which thus acts as a

signaling guidance in mechano-taxis. [78] A prominent feature of metastatic tumour is its ability to disseminate to distant organs with the help of angiogenesis. It is the process by which newer blood vessels are formed in an upregulated manner that are often disorganized, structurally faulty and more permeable than normal vasculature. All these factors lead to heterogeneous blood flow, heightened interstitial fluid pressure and compression of vessels. Such compromised microenvironment leads to enhanced malignant tumorigenesis. ECM stiffening in the microenvironment of tumour, alters the cell – cell adhesions and localization of VE cadherin that causes disruption of barrier function to enhance permeability. Stress induced from ECM deposition in tumour tissue, promotes vessel compression due to excess proliferation of stromal and cancer cells. When interstitial fluid pressure within the tumour exceeds that of microvascular pressure, there occurs restricted perfusion and improper flow patterns. Tumour endothelial cells are subjected to mechanically heterogeneous microenvironment as compared to normal cells. Thus, there is a constitutive change in cell-ECM force which is responsible for tumour endothelial cells being phenotypically distinct from normal endothelial cells. [79], [80], [53] Matrix metalloproteases or MMPs are responsible for ECM degradation and restructuring of basement membrane during angiogenesis. Tumour tissue abnormalities make the tumour microenvironment acidic and toxic [81].

The tumour vasculatures have heterogeneous organization, where the blood vessel distribution is more in tumour-host interface as compared to the central regions. [82] As tumour progresses, the vascular density gets reduced and all the irregular organization of structure arise due to stress build-up causing changes in ECM. [83] In fact the harsh tumour microenvironment exerts a selective pressure causing the cancer cell population to adapt to the changes in a more flexible and dynamic manner. The hypoxic condition promotes more difficult to treat tumour phenotype and aggressive behaviour. [84] Hypoxia employs selective pressure which contributes to the proliferation of cancer cells. It also induced changes in pro-survival gene expression, regulates anabolic switch in central metabolism and causes malignant progression through genomic changes in neoplastic cells. Such microenvironment affects host immune response by inducing an immuno-suppressive phenotype. In order to restore normal behaviour in tumour tissue, anti-angiogenic drugs are now being used and developed furthermore which in combination with chemotherapy increased the patient survival. We also looked at the cross talk between ERK signaling pathway and Wnt signaling pathway, as seen from the Western blot analysis in determining the role of mechanotransduction or ERK inhibition in breast cancer. The normal function of Wnt signaling include regulation of certain genes and signaling cascade in cell determination and proliferation necessary during embryonic development. Constitutive activity of Wnt leads to overexpression of genes regulating cell growth and survival eventually leading to oncogenesis. Wnt signaling also has an effect in EMT contributing to metastasis and progression of tumours. Studies have shown that when Wnt is blocked it leads to the inhibition of metastatic progression, despite the presence of other neoplastic promoters. Beta-catenin is the major force behind the dysregulation

of Wnt signaling, which consequently gave rise to protein knockdown strategies. [85]. Since matrix stiffness is identified as a critical factor in the progression of cancer, studies have related the progressive behaviour of tumours with the alterations in the mechanochemical changes of the extracellular matrix. Stiffening of tumour stroma along with change in ECM composition, include development of a dense network of collagen-rich fibres which during tumorigenesis, imparts resistance to chemotherapeutic drugs. Customized poly ethylene glycol – phosphorylcholine (PEG-PC) hydrogel systems have been developed as drug screening systems and studied to gather information on the stiffness and integrin binding profiles of tumours *in-vivo*.

Raf kinase inhibitor, Sorafenib showed reduced efficacy on stiffer microenvironments, rich in collagen. It was also seen that prolonged JNK activation facilitated the resistance, which got reversed upon treating the cells with JNK inhibitor in combination with Sorafenib, in triple negative breast cancer cells. $\beta 1$ integrin along with its downstream effector JNK mediated resistance to Sorafenib. Hence, further studies on the matrix stiffness via high throughput PEG-PC systems are beneficial for screening advanced chemotherapeutic options. [1]

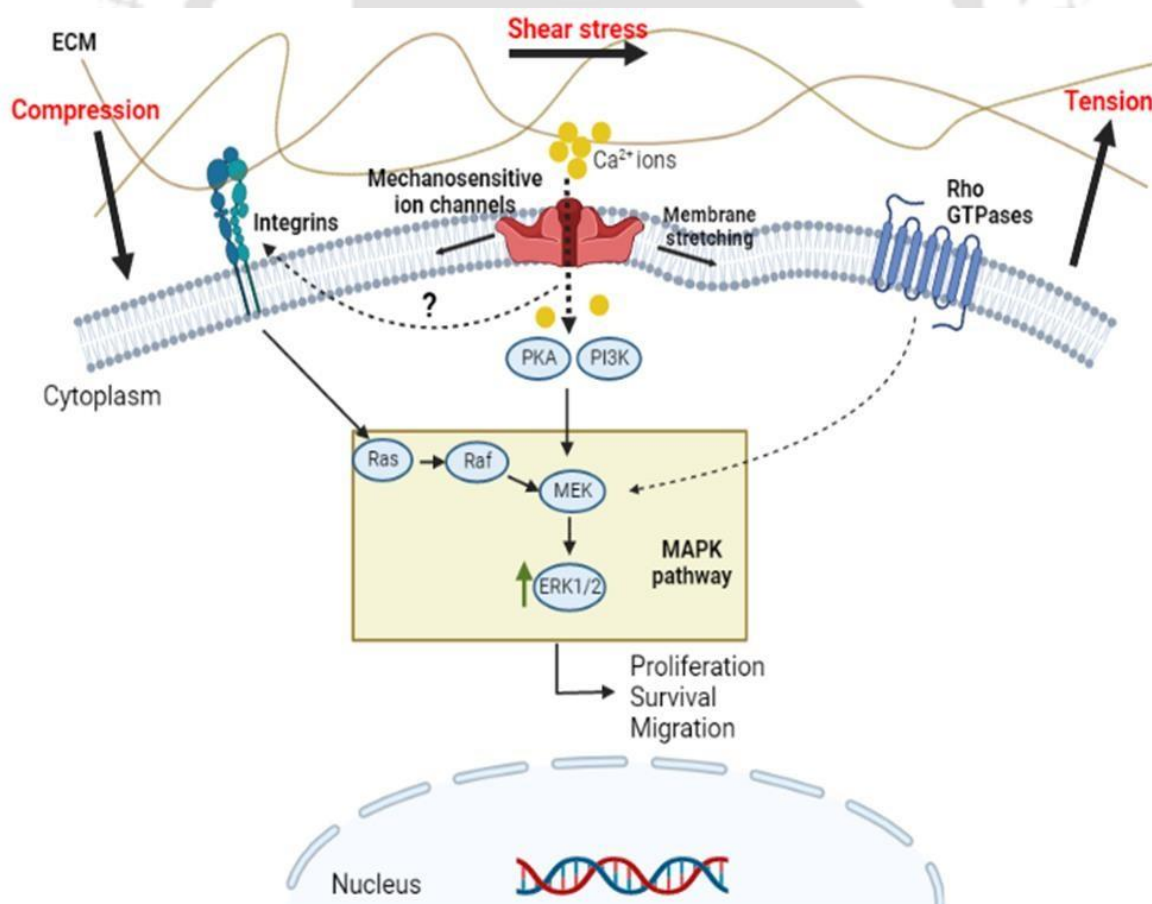


Fig 1.2 Mechanical forces in modulating ERK signaling in cancer cell

1.11 Role of PIEZO1 in regulating cancer cell behaviour

Mechanical interaction between cancer cells and their extracellular stroma provides insight into biophysical characteristics of the mechanosensitive ion channels. In breast cancer cell line MCF7, mechanosensitive ion channels got activated by negative pressure in the extracellular environment in a saturable manner. No functional mechanosensitive channels were observed with the help of patch clamp technique in MCF10A, a benign mammary epithelial cell line.

GsMTx-4 blocks the activity of mechanosensitive ion channels which led to diminished motility of MCF-7, but not in MCF-10A cells. Moreover, increase in PIEZO1 mRNA levels in the primary tumour correlated with reduced survival in patients overall. Thus, PIEZO1 is believed to have a substantial role in metastasis and invasion in cancer cells. [86]

PIEZO1 gets upregulated in gastric cancer cells and inhibits TFF1 by binding to it. PIEZO1 knockdown triggers G0/G1 cell cycle arrest which in turn inhibits proliferation. PIEZO1 showed elevated expression in prostate cancer cells in which it helps accelerating cell cycle and also activates the Akt/mTOR pathway. In other tumours, such as breast cancer, bladder cancer, osteo-sarcoma and other cancers, PIEZO1 is constitutively expressed which promoted proliferation of tumours. [71]

Poor prognosis of breast cancer is seen to be associated with higher expression of PIEZO1; particularly in breast cancer patients with lymph node positive, oestrogen receptor positive, Grade 2, luminal A, and HER2 overexpression. PIEZO1, thus can act as a prognostic marker of breast cancer. [87] PIEZO1 is found to be distributed widely in several tissues across the human body; the exact mechanism of which is still at its preliminary stage.

The malignant epithelial cancer of the oesophageal epithelium, oesophageal squamous cell carcinoma (ESCC) shows higher expression of PIEZO1 than para cancerous tissue. Proliferation, migration and invasion of ESCC cell lines were found to be inhibited by shRNA mediated PIEZO1 knockdown. Progression from G0/G1 to S phase of cell cycle was inhibited along with upregulation of cellular apoptosis upon downregulation of PIEZO1.

Tumour bearing mice studies validated the change in expression levels of PIEZO1 and p53 using immunoprecipitation, wherein the protein levels of p53, Bax, and Caspase3 were significantly upregulated by the downregulation of PIEZO1; indicating the potential of PIEZO1 protein as a therapeutic target in ESCC cells which can act via p53-BAX-Caspase3 axis to upregulate apoptosis and downregulate migration and proliferation. [88]

Prostate cancer, the major type of cancer affecting men worldwide, shows the presence of PIEZO1 as the crucial mechanosensitive ion channel responsible for sensing and transducing mechanical stimulus. The PIEZO1 expression level increased considerably in prostate cancer cell lines. PIEZO1 gene, when downregulated, led to reduction in proliferation and migration of prostate cancer cells *in-vitro* as well as led to diminished tumour growth *in-vivo*. There was reduction in Ca^{2+} signals along with inhibition of Akt and mTOR phosphorylation. There was cell cycle phase arrest at G0/G1 with simultaneous inhibition of CDK4 and CyclinD1. Therefore, in prostate cancer also PIEZO1 can be explored further as a novel therapeutic target. [89]

1.12 Yoda1—the chemical agonist of PIEZO1 and understanding its role in cancer homeostasis

PIEZO ion channels are activated by various types of mechanical stimuli and function as biological pressure sensors in both vertebrates and invertebrates. Apart from mechanical cues which are known to activate PIEZO ion channels, other modes of activation are still not much known. Scientists in 2010 screened over three million compounds to check for their ability to allow calcium ions to flow into human cells in order to identify chemical compounds that activate the PIEZO channels, using a cell-based fluorescence assay and finally a synthetic smallmolecule compound named Yoda1 was identified which acts as an agonist for both mice and human PIEZO1. Interestingly, it has been observed that Yoda1 activates PIEZO1 channels that have been purified, even in absence of other cellular components. Particularly when PIEZO1 was placed in artificial membrane devoid of any other cellular components, Yoda1 addition opened up the PIEZO1 channels. This paved way for the fact that Yoda1 can provide detailed insight to study PIEZO1 regulation and function. Another crucial research showed that Yoda 1 helped to control the red blood cell volume, paving way for the fact that Yoda1 can be helpful in providing valuable inputs in identifying role of PIEZO1 in the emerging areas of cancer mechanobiology. [2]

Yoda1 is a well-established PIEZO1 channel specific agonist. It is a pyrazine compound, the modification of this pyrazine ring led to the development of Dooku1, an analogue which reversibly antagonized Yoda1. Dooku1 inhibited Ca^{2+} entry, mediated by Yoda1 at $2\mu M$ concentration; but could not suppress constitutive PIEZO channel activity. It did not show any effect on the endogenous ATP evoked rise in Ca^{2+} or entry of Ca^{2+} in HEK293 cells via TRPV4 or TRPC4 channels over-expressed in CHO and HEK293 cells. Dooku1 also antagonizes the activity of Yoda1 responsible for dose dependent relaxation of aortic rings; mediated by endothelium and NO dependent mechanism. [90] There had been a significant reduction in proliferation in primary erythroblasts of patients with hereditary xerocytosis, as compared to normal control cells. When incubated with PIEZO1 agonist Yoda1, there is a dose dependent decrease in proliferation of erythroblasts, taken from a healthy control sample. Yoda1 treatment also induced cell death and reduced enucleation. In

Hereditary Xerocytosis patient's erythroblasts, the basal level of Ca^{2+} showed higher levels compared to normal cells. There was a dose dependent Ca^{2+} influx upon Yoda1-induced PIEZO1 activation. Erk1/2 and SAPK/JNK got phosphorylated with Yoda1. Erythroblasts, when preincubated with calcineurin inhibitor FK506, blocked Yoda1-induced NFATc2 dephosphorylation and inhibited SAPK/JNK phosphorylation as well. This indicated that PIEZO1 triggered calcium- dependent signal transduction via calcineurin activation. During erythropoiesis via calcineurin inactivation, PIEZO 1 has been observed to have a role in Calcium homeostasis regulation. [69]

There lies a mechanism to optimally balance epithelial cell division with cell death or apoptosis, in order to prevent constitutive cell growth and proliferation which can give rise to tumours. In regions of low cell density, cells are stretched which triggers the division of mammalian epithelial cells. Experimentally applied stretch on epithelia, triggered cell division via PIEZO1 channel activation; where calcium dependent phosphorylation of ERK1/2 activates cyclin B transcription which is required for the cells to enter into mitosis. Thus, two major processes namely, stretch and crowding (mechanical cues) helps to regulate cell division and death mediated by PIEZO channels. Stretch induces cell division whereas crowding induces cell extrusion. The different subcellular localisation and distribution of PIEZO1 plays an important role which affects the cell fate; in sparse epithelial regions PIEZO1 localises to plasma membrane and cytoplasm which induces cells to divide. In denser regions PIEZO1 forms bigger cytoplasmic aggregates where cells extrude. It can be said that PIEZO1 acts as homeostatic sensor to control epithelial cell numbers, thereby inducing apoptosis and extrusion in crowded regions and cell division in sparse regions. [91]

There exist several modes of migration, for a cancer cell to experience in the tumour microenvironment; whereby it leaves the primary tumour site and undergo metastasis. Amoeboid cellular migration is one such way which relies on bleb formation of cells for example in triple negative breast cancer cell line MDA-MB-231, thrombin augmented dynamic blebbing via Protease activated receptor 1 (PAR1) activation. Upon experiencing gentle contact compression while executing customised cell press for mechanical stimulation of cells, it was observed that there was a reduction in thrombin induced blebbing. A similar attenuation was observed upon Yoda1 treatment, which was impaired in cells devoid of PIEZO. Activation of PIEZO1 on the other hand reduced thrombin induced phosphorylation of ezrin, radixin and moesin of the ERM protein family which crosslink actin filaments with plasma membrane and also take part in the blebbing process. Thus, activated PIEZO1 play a major role in blocking dynamic blebbing, specifically more when induced by thrombin. [92]

Limitless replicative growth of breast cancer cells gives rise to mechanical compression which is the driving factor behind the development of a more invasive phenotype. Key regulatory events like matrix degradation and invasion are augmented upon application of compressive forces. The transmission of mechanical cues to execute intracellular changes, is carried out by PIEZO1 channel which promotes influx

of calcium ions and induces downstream Src signaling. During this mechanism, PIEZO1 was localised mainly in caveolae, which again is an important factor, given the fact that upon knocking down caveolin1 expression or reducing cholesterol content, PIEZO1 expression as well as compression induced invasive phenotype got inhibited. [93]

Thus, mechanical compression activates PIEZO1 channel to regulate increased breast cancer cell invasion that affects cellular migration along with matrix degradation, which may be instrumental in developing a potential therapeutic target. [93]

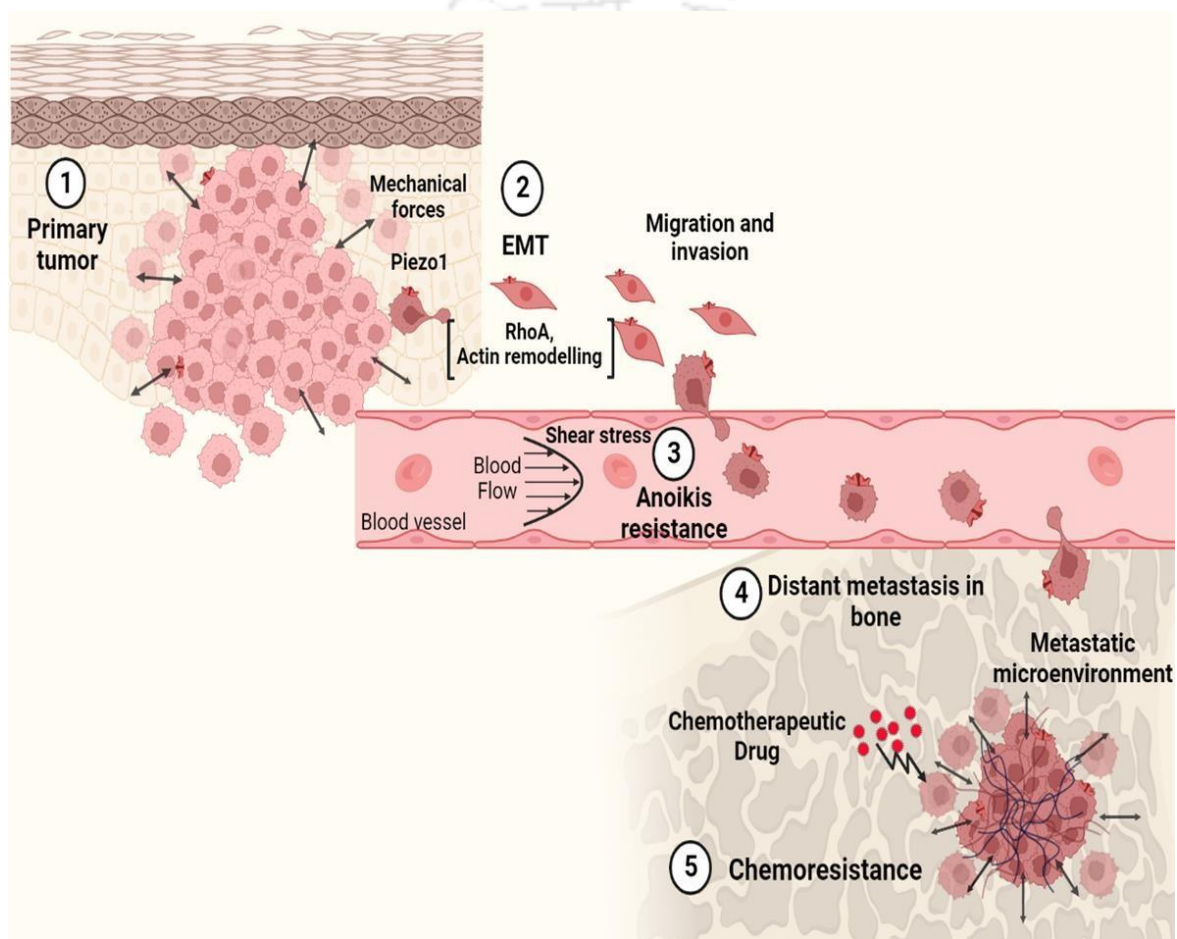


Fig 1.3 PIEZO1 in mediating mechanotransduction in various stages of breast cancer

1.13 PIEZO1 in mediating mechanical force transduction from tumour ECM into intracellular signaling pathways

In solid tumours, mechanical features of the cells get altered upon undergoing malignant transformation. A metastasising cancer tissue is characterised by extracellular matrix stiffness, invasive growth, and cell mobility which experiences positive feedbacks by inducing mechanical stimuli, which in turn favours the development of cancer. PIEZO channels have been identified as key regulators in mechanotransduction

where they convert mechanical stress to Ca²⁺ dependent signals. In certain cancers like gastric, bladder and breast cancers an overexpression of PIEZO1 have been reported alongside downregulation of PIEZO1 in other types. [94] Mechanotransduction process is indispensable in maintaining homeostasis in normal cells, for several cellular processes like proliferation, migration and apoptosis, sensory and tactile perception, regulation of blood pressure and micturition process via bladder volume regulation. However, PIEZO1 dysregulation has been reported to promote progression of cardiomyopathies, fibrosis and cancer. [94]

PIEZO1 expression has been found to be higher in the invasive ductal breast carcinoma MCF7 as compared to MCF-10A, normal mammary cell line model. It has been reported that MCF7 cell lose their motility upon application of tarantula toxin (Grammostola spatulate) mechano- toxin-4(GsMTx-4), which blocks PIEZO channels non-specifically. In fact, higher levels of PIEZO1 mRNA in primary tumours of breast cancer patients was found to correlate with overall less survival time and higher hazard ratios, this implies PIEZO1 can possibly have an oncogenic role since it promoted invasion and metastatic spread. [86] Mechanical stretch induced gating of PIEZO1 channel triggers Calcium influx that in turn activates Akt as well as m-TOR pathways. This helps in the upregulation of cell cycle regulator molecules like cyclin D1 and CDK4 and thereby helps in cell proliferation, migration and cell cycle progression. [89]

Body weight, often, plays an important role in determining the underlying cause of matrix stiffness of breast cancer tissues. Previously density of extracellular matrix and obesity were considered as independent risk factors for breast cancer patients which later proved otherwise, as increased weight enhances the content of local myofibroblast in mammary adipose tissue. Alterations in the stroma therefore increased malignant potential as observed with elevated interstitial ECM stiffness. Both diet and genetically induced obese mouse models showed enriched myofibroblasts and stiffness augmenting ECM components in mammary fat samples.

Adipose stromal cells isolated from obese mice models were found to have more amount of myofibroblasts and deposited stiffer and denser ECMs as compared to control lean mice.

Decellularized matrices from obese ASCs were found to enhance mechano-signaling and thus the malignant potential of breast cancer cells. On the other hand, caloric restraint in mouse model reduced myofibroblast content in mammary fat, implying that mammary ECM mechanics has potential role in anticancer therapies. YAP/TAZ pathway is responsible for the regulation of cellular events like autophagy. In some types of aggressive breast cancers YAP/TAZ are found to be activated due to the presence of stiffer extracellular matrix owing to excess collagen deposition. This imparts increased autophagy thereby providing them growth, invasion and metastatic advantage. [95] In regions of cell with higher confluency, YAP/TAZ gets inhibited which reduces both proliferation and basal autophagy. This limits general cell metabolism downstream of m-TORC1 inhibition. This also leads to the accumulation of aggregate prone

proteins which in turn is dependent on YAP/TAZ's autophagy activity. In areas of high cell confluency and softer matrix, autophagy gets inhibited on the other hand there is activation of autophagy on stiffer matrix. All these regulate downstream consequences of altered Hippo signaling that depends upon altered YAP/TAZ signaling.[96] Epithelial cells have a unique mechanism to preserve their barrier function while still removing excess cells by extrusion. Cells, supposed to undergo apoptosis, emits Sphingosine-1-Phosphate (S1P), that binds to the G-protein-coupled receptor Sphingosine-1- Phosphate receptor 2 (S1P2) of the adjacent cells. This binding activates contraction of an actomyosin ring circumferentially and basally, mediated by Rho-A. The contraction helps in squeezing out the specific cell apically and simultaneously pulls together neighbouring cells without leaving any space in between. Thus, crowding induced live cell extrusion is the major type of cell extrusion that helps maintain constant cell numbers. Defective extrusion leads to the loss of contact inhibition of the epithelial cells which then go on to form masses. [97]

Preserving epithelial barrier is essential since it acts as the first line of defence against pathogens from entering inside the body. The process by which mechanotransduction transduce bio-physical stimuli to biochemical response is executed by mechanically gated ion channels; these are essential for maintaining regular indispensable activities necessary for physiological functions such as touch pain (sensory), temperature regulation, auditory function. High resolution structure details of PIEZO1 may help reveal the molecular factors of ion permeation and gating. PIEZO1 is one of the major mechanosensitive ion channels but least understood in details. With the help of cryo-EM structural knowledge, the modularity and function of PIEZO1 channel is determined by constructing deleting proteins. The minimal amino acid sequence of the PIEZO1 channel which has the ability to fold and function as the channels pore domain between E2172 and last residue E2547. Addition of anchor region has negligible effects on permeation properties. The pore domain of PIEZO1 is not pressure sensitive and affixation of PIEZO Repeat A failed to restore pressure dependent gating. Thereby it has been elucidated that the sensing module exist between residues 1 to 1952. [98]

As already known, PIEZO1 serves as the crucial mechano-sensitive ion channel, ubiquitously in all cell types. The change in its structure or conformation in response to external mechanical force has been put forward and the role of the anchor domain has been thoroughly explored in the process of mechanically gated ion channels. Thus, inserting glycine residues at each corner of triangle shaped anchor domain in order to decouple the domain, has been proven the fact that this anchor region is crucial for mechano-gating by PIEZO1. In between the anchor and outer helix of Human PIEZO1, inserting two excess glycine residues resulted in inactivation and inhibited mechano-sensitivity. Surprisingly, inserting two glycine residues at the apex of anchor domain at the conserved amino acid P2113 led to augmented sensitivity to membrane forces. There exists a strong correlating evidence suggesting that larger volume amino acid residues reduce mechano-sensitivity whereas smaller volume residues increase the sensitivity of PIEZO1 mediated force

transduction. [99]

Cytokinesis, the final stage of cellular division requires the presence of mechanosensitive PIEZO1 ion channel, which is activated at the intracellular bridge connective two daughter cells at the time of abscission. PIEZO 1 is also found to be a crucial regulator of endosome trafficking.

[100] Cells under normal culture conditions showed that a minute fraction of filopodia exhibited considerable PIEZO1 signal change with response to Yoda1. The mechanism of Yoda1 in assisting opening of PIEZO1 is majorly to affect the membrane tension by lowering it; which is observed by the fact that if the resting cellular tension is extremely low, Yoda 1 cannot help open PIEZO1. On the contrary channels which are closed yet in a pre-stressed state have a greater chance to respond to Yoda1. In live cells there has been flattening of PIEZO1 during activation. [101]

Different biological processes like immune response and tissue response to pathogens and injury are carried out by macrophages. The study in the role of PIEZO1 in macrophage polarisation and microenvironment stiffness sensing, demonstrated that there has been a reduction in inflammation and augmented wound healing exhibited by macrophages lacking PIEZO1. Calcium ion influx is dependent on PIEZO1, modulated by soluble signals and promoted on stiffer substrates, as revealed by transgenic Ca²⁺ reporter expressing macrophages. PIEZO1 is essentially required by in-vitro stiffness dependent macrophage activity as well as biomaterial implantation *in-vivo*. Positive feedback between PIEZO1 and actin leads to the activation of macrophages. PIEZO1 act as mechano-sensor of stiffness in macrophages, where stiffer substrates induce inflammatory activation via MyD88-dependent pathways and enhanced NFκB. Chemical agonist of PIEZO1, Yoda1 induces stiffness dependent increase in Ca²⁺ influx and IFN-γ/LPS stimulation. Stiffness enhanced both inflammation and healing but not in a similar manner where inflammation scaled with increasing stiffness unlike healing. Interestingly PIEZO1 depletion reduced inflammation but enhanced healing pathway mechanism. In cells, cultured on stiffer substrate, PIEZO1 mediated Ca²⁺ influx inhibited IL4/IL13 induced activation of the transcription factor STAT6. STAT6 signaling pathway is essential to maintain the process of healing even on softer matrices. Thus, Calcium signaling mediated by PIEZO1 enhances inflammation in stiff surroundings, whereas the same cannot be said in regulation of healing pathways that seem to be a complex interplay.

At the time of development and progression of any disease including cancer or fibrosis or cardiovascular disease, macrophages alter the mechanical cues. Upsurge in inflammatory activation in cardiovascular disease and healing activation in cancer and fibrosis have been associated with enhanced stiffness. [102]

Mechanical properties of tumour tissues are often altered by matrix stiffness, which can be sensed by mechanosensors or mechanotransducers. ECM stiffening causes mechanical perturbations in the lipid

bilayer which in turn activate TRP and PIEZO channel proteins. These are evolutionary conserved channels linking tissue stiffening to cell signaling pathways like Ca^{2+} in tumour and stromal cells. PIEZO has been known to activate transmembrane receptor integrin that promotes drug resistance and cancer stemness properties. Interaction between the extracellular matrix proteins and the extracellular domains of integrins promote the assembly of cytoplasmic complexes made up of scaffold proteins like FAK (focal adhesion kinase), Src, talin, paxillin, vinculin, etc. This helps in coordination of cytoskeleton assemblage and focal adhesion with matrix mechanical signals. Thus, diverse signaling pathways in tumour and stromal cells triggered by stiffening of ECM promote cell growth, metastasis, angiogenesis, evasion from immunity and drug resistance. Upon the advent of tumour formation, ECM gets degraded and growth factors, sequestered by ECM promote inflammation, tumour growth and angiogenesis. Other surveys provide the fact that mammographic density is directly correlated with the risk of breast cancer association. [103].

Mechanotransduction arise as a result of interaction between the cells and extracellular matrix microenvironment, involving force sensitive cellular proteins which are related to cytoskeleton. Some of these proteins adhesion sensors whereas some other are non-adhesion force sensors like PIEZO1, LIM. [104]. Tumour tissue are generally found to have stiffer matrix but have softer cellular cores. Thus, according to some hypothesis cancer cells generate traction force on rigid substrate in order to migrate while being soft at the same time to glide through the narrow spaces to metastasize. [105]

It is therefore difficult to draw a general idea about the mechanisms of cancer based mechanotransduction across different cell types or even within the same cancer type. Majority of the studies have put forward the notion of cancer tissue being more rigid than their normal counterparts, but substrate stiffness has negligible effect on cell spreading, proliferation and migration. Softer matrices have been shown to promote programmed cell death, while on the other hand, stiffer matrices induce Epithelial to mesenchymal transition as well as angiogenesis. It will be feasible to elucidate the underlying mechanism of mechanotransduction regulation, using polyacrylamide or biopolymer gels with adjustable stiffness. This may help to study a variety of cell-based events like migration, proliferation, invasion and apoptosis. Newer approaches comprising mainly of 3D scaffolds, micropillars, microfluidic devices imitating tumour microenvironment shall help in providing broader insight into the role of mechanotransduction in cancer. [74]

Tumour formation arises as a result of limitless cellular proliferation, gene mutations altering expression and upregulation of certain signaling pathways. Tumour advancement at the stage of tissue is characterised by proteolysis and disruption of the basement membrane, followed by enhanced deposition of stromal extracellular matrix. Extracellular matrix helps in binding the cells together in the differentiated state, acting as a tumour suppressor. Tumours have specific stiffened ECM remodelling in general. Studies have shown that breast tumours at the initial stages have collagen crosslinking and ECM stiffening coupled with

enhanced focal adhesions. Increase in collagen crosslinking helped the ECM to stiffen and promote focal adhesion accompanied by increased PI3K activity. It was also observed that integrin signaling upon inhibition, suppressed the premalignant epithelium invasion into crosslinked, rigid ECM. On the contrary, enforced integrin clustering augmented PI3-K signaling, focal adhesions as well as invasion of premalignant epithelium. In correlation with the above statement, it was also observed that reduction of lysyl-oxidase mediated crosslinking of collagen effectively decreased PI3K activity and focal adhesions, which eventually led to the decreased tumour incidence and hindered malignancy. [106]

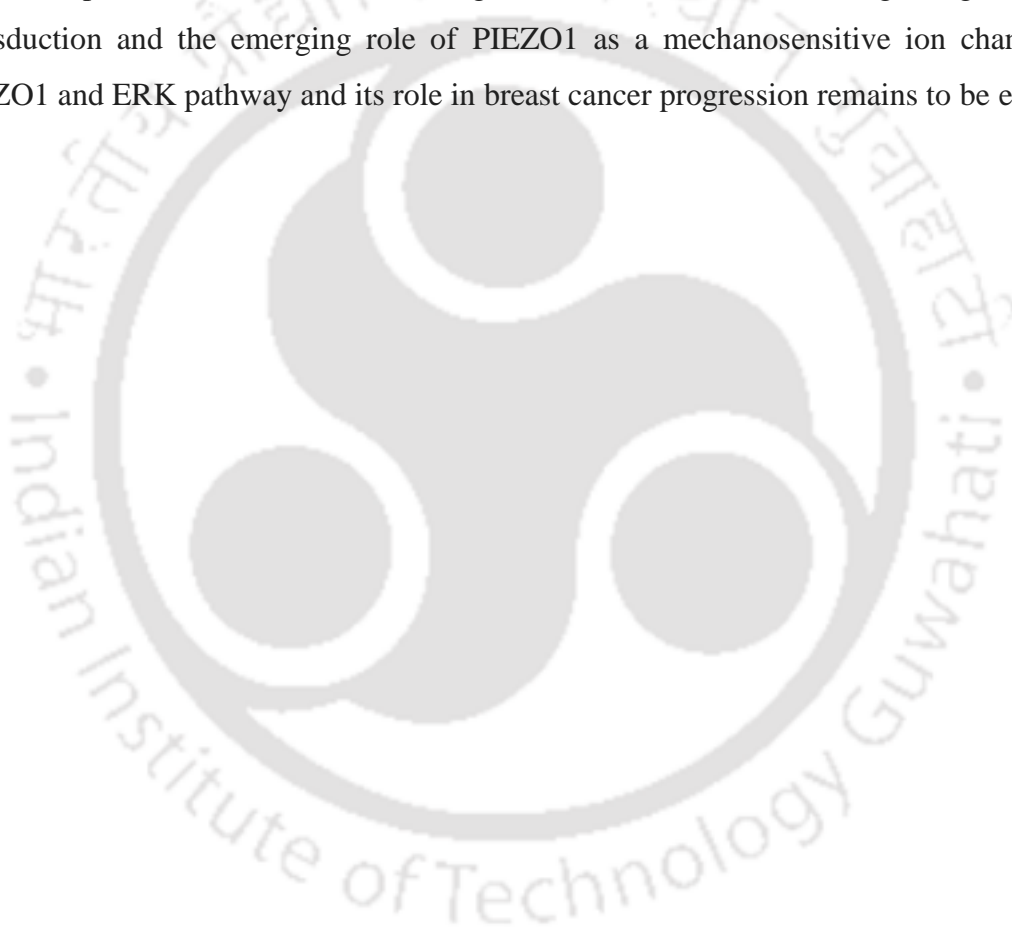
Presence of hormone receptors like ER, PR, HER2, etc act as well-known biomarkers for breast cancer which aids to predict the outcome of treatment. This poses a problem for patients with triple negative breast cancers that do not express any hormone receptor and also for those where predictably disease progression is not clear. It has been found that alterations in the deposition of collagen, tumour associated collagen signature - TACS helps in invasion in mouse models, manifested early in development and progression of tumour.

The need for the identification of new biomarkers will help in collagen deposition and arrangement. In animal (mouse models) of mammary tumour progression, TACS enables the concerned to predict relapse and survival in human patients. One needs to have a proper understanding on the way in which collagen alignment helps in the process of cell invasion. This will pave way into the development of better therapeutic strategies to hinder tumour development and help gain as much information in which cells invade along aligned matrices. Better approach from therapeutic perspective can be attained which aims to target the cell-ECM interactions or at the matrix level to curb down collagen deposition [107].

Improper epithelial to stromal interactions help in augmenting tumour formation, especially in breast cancer cells the migration of metastatic epithelial cells occurs in direct contact along the stromal collagen fibres. ECM adjacent to the epithelial cells of the mammary tissue has been studied extensively and it has been examined that maximum amount of stroma is fibrillar collagen which further exert physical stress and generate mechanical signals across a flat basement membrane which is thinner than 200 nm. There are certain gaps which prevent the basement membrane from completely spanning and isolating the epithelial cells, thereby leading to the occurrence of direct interactions of collagen with epithelial cell microregions. [108] Tumour cells have been found to have a tendency to localize adjacent to dense collagen. They frequently create a desmoplastic response which in turn contract and localize collagen that is followed by tumour growth and stretching of the collagen matrix. All these events eventually initiate matrix reorganisation, often by proteolytic cleavage in order to enable local invasion. Thus, the increase in expression levels of Rho and ROCK found in cancer with invasive phenotypes, is associated with greater motility and contractility of tumour cells. The detailed mechanisms behind the local invasion have been elucidated in the light of matrix rearrangement via GTPase dependent tumour cell contractility.

Beta1 integrin interaction with laminin in the basement membrane, generates signals which contribute to the differentiation and morphogenesis of mammary epithelial cells. Cytoplasmic domain of beta1-integrin subunits is associated with integrin-linked kinase (ILK), whose mutated form when expressed under experimental conditions, altered mouse epithelial cell morphogenesis. Constitutive expression of wild type ILK resulted in loss of E-cadherin molecule which enabled the cells to become invasive. This also led to the alteration of cytoplasmic stress fibres from an epithelial cytokeratin to a mesenchymal vimentin intermediate filament phenotype. [109] Thus ILK promotes disruption of cell-to-cell junctions and helps in inducing mesenchymal transformation of mammary epithelial cells.

Considering the present evidences indicating involvement of ERK signaling in mediating mechanotransduction and the emerging role of PIEZO1 as a mechanosensitive ion channel, the link between PIEZO1 and ERK pathway and its role in breast cancer progression remains to be explored.



OBJECTIVES

From the literature, it is clear that ERK signaling pathway regulates proliferation, migration, invasion and chemoresistance in cancer cells and dysregulation leads to poor clinical outcome in breast cancer patients. The frequency of RAF/MAP-K pathway mutations in breast cancer, specifically, is lower compared to other cancers, despite the role of ERK signaling as a key player in breast cancer malignancy and poor prognosis. This makes ERK signaling pathway an attractive therapeutic target for breast cancer and identifying drugs specific to the ERK signaling molecules can help combat the progression of breast cancer and prevent distant metastasis. Upon analyzing various factors that modulate ERK signaling, it was found that mechanotransduction is a crucial regulator of ERK pathway. Under physiological conditions, several cell types express PIEZO1, a mechanosensitive ion channel protein, at an optimum level and is required for normal cellular functioning. PIEZO1 acts to convert the extracellular mechanical stimuli into biological signals. Reports have suggested that ERK pathway not only senses growth factors but also regulates mechanical stiffness induced phenotype changes in cancer cells. Thus, understanding the relation between mechanotransduction and ERK signaling pathway in breast cancer with respect to the mechanosensitive ion channel PIEZO1 can pave way for the development of better therapeutic targets for breast cancer patients across all stages. Given the important role of ERK signaling pathway in several cancers, we hypothesized that ERK signaling will play a crucial role in breast cancer progression. Thus, inhibition of ERK signaling pathway might have a therapeutic benefit in inhibiting cancer progression. Cancer cells are exposed to mechanical stimulus, which regulate their proliferation, migration and survival. During metastasis, the cells enter the circulation and are subjected to shear stress which activate the mechanosensors and their survival. We hypothesize that mechanostimuli and mechanotransduction might play an important role in cancer progress, especially metastasis and thus targeting mechanotransducers might have therapeutic benefits.

Based on the review of literature, the following objectives were formulated to understand the role of ERK signaling and its relationship with the mechanosensitive ion channel protein PIEZO1:

To understand the role of ERK signaling in breast cancer

- 2.1 *Effect of ERK inhibition in breast cancer cells by multi-kinase RAF inhibitor - Sorafenib.*
- 2.2 *Effect of ERK inhibition in breast cancer cells by ERK1/2 specific inhibitor - BVD-523.*

To understand the role of mechanotransduction in breast cancer

- 2.3 *Effect of PIEZO1 activation by chemical agonist Yoda1 in breast cancer cells.*
- 2.4 *Effect of PIEZO1 inhibition through PIEZO1 silencing in breast cancer cells*

MATERIALS AND METHODS

3.1. MATERIALS

3.1.1 Chemicals and reagents

3.1.1.1 Stains and dyes

- **Phalloidin-tetramethyl rhodamine isothiocyanate (TRITC)** - 1mg/ml solution was made in dimethyl sulphoxide (DMSO) (w/v) and aliquots stored at -20°C until use. Working solution (1:3000) was made from stock solution by diluting with 2% FBS and protected from light.
- **Propidium Iodide (PI)** - 1 mg/ml stock solution of PI was dissolved in PBS and stored at 4°C and protected from light.
- **4',6-diamidino-2-phenylindole (DAPI)** - DAPI powder was reconstituted in double distilled water to make 1mg/ml stock solution and stored at -20°C until use. For working solution (1:2000), DAPI was dissolved in PBS.

3.1.1.2 Inhibitors and activators

- **Sorafenib** – Sorafenib tablets were purchased as Sorafenib Tosylate IP equivalent to Sorafenib 200mg manufactured by Natco Pharma Ltd. A stock solution of 50mM was prepared by dissolving each tablet in sterile water. A working stock of 5mM was prepared to obtain working concentrations in growth medium as per the requirements.
- **BVD-523** – BVD-523 was reconstituted in DMSO to prepare 5mM working stock solution and working concentrations were used in growth medium as per the requirements.
- **EGF** – Recombinant human epidermal growth factor (EGF) purchased from Thermofisher Scientific. A working stock of 20µg/ml was prepared in 1%FBS in PBS and working concentration of 20ng/ml in growth medium was used for experiments.
- **Yoda1** – Yoda1, purchased from Sigma Aldrich was reconstituted in DMSO to prepare 20mM stock solution. A working stock of 5mM was prepared in DMSO and used to obtain the working concentrations in growth medium as per the requirements.
- **Dooku1** - Dooku1, purchased from Sigma Aldrich, was reconstituted in DMSO to prepare 10mM working stock solution and working concentrations in growth medium was prepared as per the requirements.

3.1.1.3 Antibodies

Fluorescent dye conjugated antibodies - CD24-APC, CD44-FITC, CD49a-PE, CD49b-FITC, CD49d-PE, CD49e-PE, EpCAM-APC, phosphorylated form of p38 MAPK, and STAT5 were purchased from BD Biosciences.

3.1.2 Cell lines

Breast cancer cell lines – **MCF7** (ER⁺PR⁺HER2⁻) and **MDA-MB-231** (ER⁻PR⁻HER2⁻) were purchased from National Center of Cell Sciences (NCCS, Pune, India). Both the cell lines were maintained in High Glucose DMEM-culture media supplemented with 10% FBS, L-Glutamine (100x) and Penicillin/Streptomycin (100x), as mentioned in methods section.

Human Epithelial Kidney 293FT (293FT) Cells - 293FT cells were obtained from Invitrogen and maintained with the DMEM-HG media, supplemented with 2mM L-Glutamine (100x), MEM Non-Essential Amino Acids (1x), Sodium Pyruvate (1x) and Penicillin-Streptomycin (1x). The culture dishes were maintained at 37°C and 5% of CO₂ incubator.

3.1.3 Cell culture media and reagents

Mammalian cell culture growth Media - High Glucose DMEM - DMEM-HG is supplemented with 3.7 g/L sodium bicarbonate, 10% FBS and 1X Penicillin/Streptomycin sterilized with 0.22 µM filter paper and stored at 4°C.

3.1.4 Solutions and Buffers

3.1.4.1 Buffers and solutions for cell culture

- **Phosphate Buffered Saline (PBS)** - The mixture of 137 mM NaCl, 2.7 mM KCl, 10 mM Na₂HPO₄ and 2 mM KH₂PO₄ was dissolved in sterile distilled water and adjusted pH to 7.2-7.4 by adding 1N HCl. Sterilized by autoclave at 121°C and stored at room temperature.
- **Trypsin solution** - 2.5% Trypsin solution was diluted in PBS and stored at -20°C until use.

3.1.4.2 Buffers and solutions for Immunocytochemistry

- **0.1% Triton-x-100** - 0.1% Triton-x-100 solution prepared with PBS (v/v)
- **4% Paraformaldehyde solution** - Paraformaldehyde (4%) solution was prepared by dissolving paraformaldehyde powder in PBS (w/v) and warm at 55°C by setting up waterbath. When pH of the solution was adjusted to the range of 7.2 to 7.4, the solution became clear and dissolves completely, make aliquot and stored at -20°C until use.

3.1.4.3 Buffers, solutions and reagents for SDS-PAGE and Immunoblotting

- **Acrylamide:** 29:1 (acrylamide: bisacrylamide) - 40% (w/v) - stored at room temperature. Final working concentrations used are - 12.01% for resolving gel and 4% for stacking gel
- **Resolving gel buffer:** Stock concentration- 1.5 Molar Tris buffer pH-(8.8)-Working

- concentration – 0.375M
- **Stacking gel buffer:** Stock concentration- 0.5 Molar Tris HCl buffer pH-(6.8)- Working concentration – 0.125M
 - **10% APS:** Final working concentration- 0.1%
 - **TEMED:** (1:1000) dilution) (All the products mentioned above were purchased from Invitrogen)
 - **SDS Sample Loading Buffer 5X:** 250Mm Tris-HCl (6.8), 50% Glycerol, 10% SDS (from MERCK Specialities Private limited);10% Beta mercaptoethanol, 0.5% Bromophenol blue (from HIMEDIA)
 - **1X TbsT (Tris buffered saline with tween):** 50mM Tris Base- pH 7.6, 150mM NaCl, Tween 20 (0.1%)-(from MERCK Specialities Private limited)
 - **10X Running buffer recipe:** pH 8.3- 0.025 M Tris Base, 0.192 M Glycine (from HIMEDIA), 1%SDS (w/v) - (from MERCK-MIOM602345) – Diluted to 1X (1:9) with deionised water before running the samples.
 - **10X Transfer buffer:** Tris base-250mM, Glycine-192mM. 1X buffer was prepared using 10% of 10X Transfer buffer, 20% Methanol and 70% De-ionised water.
 - **Nitrocellulose Blotting Membrane roll-** Pore size 0.45micron (from HIMEDIA) was used for protein transfer from SDS-PAGE gel.

3.2.METHODS

3.2.1 Cell culture

Breast cancer cell lines MCF7 and MDA-MB-231 were grown in High Glucose DMEM media supplemented with 10% FBS and Penicillin-Streptomycin antibiotics (Gibco). Cells were seeded with a density of about $3-5 \times 10^3$ cells/cm² and sub-cultured every 3-4 days when cells were about 70-80% confluent. Briefly, cells were trypsinized for 3-5 minutes at room temperature and centrifuged at 300g for 5 minutes. The culture dishes were maintained at 37°C in a 5% of CO₂ incubator.

3.2.2 Cell counting

Cells were counted using trypan blue exclusion assay. Cells were initially trypsinized at room temperature and resuspended in growth media. 10µl aliquot was mixed with equal volume of 0.4% trypan blue and loaded into Haemocytometer chamber. The number of live cells in 4 quadrants, each having a total volume of 0.1 µl, was counted and averaged to calculate the cell density as follows.

$$\text{Cell density (cells/ml)} = \frac{\text{Average quadrant count} \times 1000 (\mu\text{l/ml}) \times 2}{0.1 \mu\text{l}}$$

The doubling time was calculated using the following formula.

$$\text{Doubling time} = \frac{\text{Culture duration} \times \log_{10} 2}{\log_{10} \frac{\text{Final cell number}}{\text{Initial cell number}}}$$

3.2.3 Apoptosis analysis

Apoptosis analysis was performed by staining the cells with Annexin-V and PI (Annexin-V staining kit, Invitrogen – Thermo-Fisher Scientific) according to the manufacturer's instructions and analysed using flow cytometry. Briefly, the cells were collected and washed with ice-cold PBS. The cells were resuspended in 100 μ l of 1X Annexin V binding buffer at a concentration of 1×10^5 cells/100 μ l buffer; anti annexin V antibody was added to the cells and incubated in dark for 15 mins at room temperature. Additional 200 μ l of annexin-V binding buffer containing PI was added to the cells and analysed with FACS LSR Fortessa. During analysis the cells were visualized in FSC versus SSC plot and gated to select the cells and to remove the cell debris. The gated population was plotted to visualize the fluorescence in respective channels. Quadrant gate was created to separate the live cells, early apoptotic, late apoptotic and dead cells.

3.2.4 Ki67 staining and Cell cycle analysis

The cell cycle analysis was performed using propidium iodide (PI) staining. The cells were collected and washed with PBS. The cells were then fixed with ice-cold 70% ethanol. The ethanol was added drop-wise to the cell pellet while vortexing to avoid cell clumping. The cells were incubated at -20°C overnight. After overnight fixation, cells were washed with PBS by centrifugation at 500g to pellet the cells. RNase A (100 μ g/ml) was added to the cells and incubated at 37°C for 30 minutes. The G0 cell cycle stage of the cells was analysed by Ki67 staining. FITC conjugated Anti-Ki67 antibody (BD Biosciences) in 100 μ l staining buffer (2% FBS in PBS), was added to the cells at the recommended concentration and incubated at room temperature for 1 hour in dark. PI (30 μ g/ml) was added to the cells and incubated on ice for 20 minutes. The cells were analysed with FACS Calibur to detect PI fluorescence which shows the cell cycle profile. During FACS analysis, first the cells were gated using forward vs side scatter plot to remove the cell debris. The cells were gated in PI-area versus PI- height to remove cell doublets. The cell cycle profile was visualized in PI channel in the linear scale. The cells which were negative for Ki67 at the G0 position of the cell cycle were considered as quiescent or non-cycling cells.

3.2.5 Phenotyping

The expression of various cell surface markers was assessed by flow cytometry. For each marker studied, cells were trypsinized, washed once with ice cold PBS to remove the media and resuspended in ice-cold FACS buffer (PBS with 2% FBS) at a density of 1×10^5 cells/100 μ l. The cells were then stained with FITC, PE or APC (fluorescent dye) conjugated anti-human monoclonal antibodies,

against the specific cell surface antigen. The antibody incubation was done for 30 minutes at 4°C in dark. After the incubation, cells were washed and stained with 2µg/ml of Propidium Iodide in FACS buffer to differentiate between live/dead cells. The processed samples were analyzed with BD FACS calibur. First the cells were gated for live cells and the gated cells were plotted into FSC versus SSC plot. The cells were again gated to remove cell debris and the viable cells were visualized in the fluorescent channels for which the cells were stained. Gating for the positive cells were done based on the isotype control.

3.2.6 Phospho flow cytometry

The phosphorylated levels of signaling proteins were analyzed through Phospho flow cytometry by specifically staining with antibodies against the phosphorylated forms of the proteins. Cells were collected by brief trypsinization at 37°C and fixed with 2% formaldehyde in PBS for 10 minutes. Cells were then washed and incubated with ice cold methanol at -20°C for 4 hrs. The cells were washed with staining solution - 0.5% Bovine serum albumin (BSA), counted and equal number of cells from different treatments were added to the FACS tubes. Equal amount of fluorescent conjugated phospho specific antibodies (BD Biosciences) were added to the samples and incubated at room temperature for 1 hour. The cells were washed with the staining solution and analyzed with FACS LSR Fortessa.

3.2.7 ROS analysis

The level of mitochondrial superoxide molecules produced in the cells, was determined using MitoSOX Red mitochondrial superoxide indicator (Molecular Probes). The media of the cells for different treated conditions were changed after the required treatment time, washed with PBS and replaced with MitoSOX reagent containing serum starved media. The cells were incubated with 5µM MitoSOX reagent in cell culture incubator for 30 minutes at 37°C. The MitoSOX reagent was then washed once with warm PBS, trypsinized and collected by centrifugation at room temperature, then resuspended in 2% FBS in PBS at room temperature and finally processed for analysis in flow cytometer. The MitoSOX fluorescence level in the cells was compared with the unstained cells as control.

3.2.8 Colony formation assay

Hundred to five hundred cells were plated in each well of a 6-well/12-well/24-well plate according to the experimental requirements and treated with test materials for 48 hours. Fresh media was added after treatment or the cells were incubated with treated media for 7-10 days in case of continuous treatment conditions. After completion of the treatment, the colonies formed, were washed with ice cold PBS after removing the media. Colonies were then fixed with 100% ice cold methanol for 10 minutes at 4°C and then stained with 0.1% crystal violet. The number of colonies were counted microscopically and the images of single cell colonies were documented microscopically and image area were analyzed

with the help of Image Lab software.

3.2.9 Spheroid formation assay

Breast cancer cell spheroids were prepared by seeding cells at a density of $0.5-2 \times 10^4$ cells/ml. Prior to cell seeding, the wells of a U-bottomed 96-well plate were coated with 1% noble agar (dissolved in PBS). Test materials were added along with growth media at the time of seeding the cells. The plate was kept in cell culture incubator at 37°C with 5% CO₂, undisturbed for 4-5 days to allow the formation of spheroids. After 4 days of seeding, the spheroid area was monitored for 14 days and documented microscopically. Spheroid area of all the conditions were analyzed as described in details in the following subsection 20c.

3.2.10 Migration assay

The migration of breast cancer cells *in vitro* was evaluated by wound healing assay. Cells were seeded at a density of 20,000 – 30,000 cells/cm² to obtain a confluent monolayer of cells after 24 hours. The growth media was replaced with serum-free medium for 12- 16 hours to induce growth arrest so as to impede the effect of proliferation on wound closure. The cell monolayer was scratched with sterile 200 µl pipette tip and washed once with Phosphate buffered saline (PBS). Cells were then replenished with growth medium with indicated concentration of drugs and allowed to migrate. Images were taken every 4 hours. Open wound area was calculated at each time-point using T-scratch software and migration speed of cell front was calculated as described in the subsection 20d.

3.2.11 Spheroid migration assay

Breast cancer cell spheroids were prepared by seeding cells at a density of $0.5-2 \times 10^4$ cells/ml. Prior to cell seeding, the wells of a U-bottomed 96-well plate were coated with 1% noble agar (dissolved in PBS). The plate was kept in cell culture incubator at 37°C with 5% CO₂, undisturbed for 4-5 days to allow the formation of spheroids. After 4-5 days, in case of spheroid migration assay, the spheroids were transferred to collagen (50µg/ml)-coated flat bottomed 96-well plates. The collagen coating was done in a sterile flat bottomed 96 well plate for 2 hours and then washed with PBS, prior to the transfer of spheroids. Test materials were added to the wells in DMEM with 2% FBS and spheroids were allowed to migrate. Migration of the cells from the spheroid into the collagen matrix was monitored and documented microscopically.

3.2.12 SDS-PAGE and Immunoblotting

Total protein was isolated with RIPA buffer (25 mM Tris-HCl [pH 7.4], 150 mM NaCl, 1mM EDTA, 1% NP-40, 1% sodium deoxycholate, 0.1% SDS) containing protease inhibitor and phosphatase inhibitor (ThermoFisher). Protein concentration was determined using Precision Red reagent

(Cytoskeleton Inc., USA) according to manufacturer's protocol. 20–30µg of protein was loaded in each well and proteins were resolved on 10% SDS-PAGE and transferred onto a nitrocellulose membrane using a semi-dry electroblotting apparatus. Membrane was blocked with 5% BSA or skimmed milk in Tris-buffered saline with 0.1% tween-20 for 1 hour at room temperature. It is then incubated with primary antibody (1:1000/2000/5000 dilution depending on the primary antibody type) for indicated proteins for 24-36 hours at 4°C. After washing, the membrane was again incubated with HRP-conjugated secondary antibody for 1 hour at room temperature. The chemiluminescent signal was recorded after incubation with ECL substrate (Biorad) using Biorad Chemi-Doc imager. The band intensity for each protein was calculated using Biorad Image Lab software, and normalized using lane normalization factor calculated using band intensity of GAPDH (house-keeping control protein).

3.2.13 Immunocytochemistry

Cells were seeded at a density of 3000 cells/cm² on coverslip bottom dishes. After the completion of different treatment conditions, cells were washed twice with PBS and fixation was done with 4% paraformaldehyde for 20 minutes at room temperature. The fixative was removed and the cells were washed with PBS. After washing, the cells were permeabilized with 0.1% triton-x-100 in PBS for 15 minutes at room temperature. The cells were then washed with PBS for 5 minutes and incubated for blocking with 5% FBS in PBS for 1 hour at room temperature. The F-actin or filamentous actin in the cells were observed by staining the cells with fluorescent conjugated Phalloidin since Phalloidin specifically binds to F-actin. The cells were then stained with phalloidin-TRITC (1:2000 / 1:3000) in 2% FBS in PBS and incubated at 4°C overnight in dark. Cells were then washed with PBS for 5 times (5 minutes each). Nucleus was stained with DAPI for 5 minutes and washed with PBS for 5 times (5 minutes each). The cells were finally documented using Zeiss Axio observer and CCD camera (Zeiss).

3.2.14 Gene silencing

a. Plasmid transformation

Lentiviral packaging system consisting of two helper plasmids, psPAX2 and pMD2.g, and transfer plasmids pLKO.1 puro shPIEZO1 and scramble were transformed into competent E. coli TOP10 strain by heat shock method. Briefly, 100 µl of competent cells were incubated with 1-2 µg of plasmid on ice for 30 minutes and then briefly subjected to heat shock at 45 °C for 45 seconds, followed by another 5-minute incubation on ice. 200 µl of SOC media was

added to the cells followed by an incubation at 37 °C for 1 hour. Cells were then plated on agar containing 100 µg/ml ampicillin and incubated for 16 h at 37 °C.

b. Plasmid isolation

Individual growing colonies of transformed cells were picked to inoculate up to 300 ml of liquid broth for plasmid isolation. Plasmids were isolated from cultures in exponential growth phase using Midi-DNA extraction kit by Invitrogen as per the manufacturer's protocol. Plasmid concentration and purity was determined using Nanodrop spectrophotometer. Plasmids were diluted in nuclease free water to obtain final concentration of 1 µg/µl and stored at -20 °C.

c. Lentiviral packaging and production

HEK293T cells were used to produce lentiviral particles with transfer plasmids pLKO.1 puro shPIEZO1 or Scramble. Briefly, HEK293T cells were seeded at a density of 70000 cells/cm² in a 6 well plate and incubated at 37 °C in 5% CO₂ for 24 hours. Cells were fed fresh growth media 2 hours prior to transfection using Polyethylenimine (PEI). Transfection mix was prepared in serum free growth media by adding 12 µl of PEI (1 µg/µl in H₂O) to the plasmid mix consisting of 2.5 µg transfer plasmid, 1.5 µg psPAX2 and 0.7 µg pMD2.g. The transfection mix was pulse vortexed and incubated at room temperature for 10 minutes. Transfection mix was topped with 650 µl of pre-warmed growth media and added to the cells gently along the walls of the well. Cells were incubated for 2 hours at 37 °C, after which additional 2 ml growth media was added to the cells. After 24 hours, the media was replaced with lentivirus harvesting media consisting of growth media of target cells supplemented with 2% FBS only. Lentivirus was harvested twice following a 24-hour incubation each and used for transduction directly.

d. Lentiviral transduction

MCF7 and MDA-MB-231 cells were seeded at appropriate density to obtain 50 % confluency after 24 hours. Lentiviral harvest media was diluted in 1:1 ratio with fresh growth media and supplemented with FBS at final concentration of 10% and 4 µg/ml Polybrene to obtain the transduction media. Cells were incubated with transduction media for 14 hours at 37 °C in 5% CO₂ to obtain stably transduced cell lines.

e. Selection of transduced cells

Control (non-transduced) cells were treated with 1-4 $\mu\text{g/ml}$ Puromycin in growth media for 48 hours to obtain the minimum dosage required for selection. Subsequently, shPIEZO1 and Scramble transduced cells were selected with 2 $\mu\text{g/ml}$ Puromycin for 5 days. Cells were selected again after each thawing and at regular intervals to ensure stable expression of transduced genes.

3.2.15 Calcium flux analysis

The change in intracellular concentration of calcium ions was assessed using Fura-2-AM indicator. Briefly, cells were washed with Ca^{2+} free buffer and loaded with 2 μM Fura-2-AM using Pluronic® F-127 as permeabilizing surfactant for 1 hour at 37°C. Cells were again washed and incubated in Ca^{2+} free buffer for 20 minutes to remove excess dye. The fluorescence was recorded for emission at 510nm after excitation at 340nm (F340) and 380nm (F380) with shortest interval possible (~1.7s) on Tecan infinite M200 pro. The ratio of F340/F380, which is proportional to Ca^{2+} bound Fura-2, was corrected for each well by subtracting the average baseline value recorded for 20 cycles. The fluorescence was recorded for additional 180 cycles after addition of indicated drug.

3.2.16 Shear stress experiment

In order to mimic the shear forces experienced by cells *in vivo*, cells were subjected to orbital shaking culture. Briefly, 10,000 cells for colony formation assay or 1×10^6 cells for RNA/protein extraction were seeded in 1 ml of growth media in 50 ml conical tubes and incubated at 37 °C with orbital shaking at 100RPM for 24hours.

3.2.17 Anoikis culture

Cells were seeded in agar coated 12-well plates and treated with different conditions as per the requirement of the experiment. The duration of treatment is generally kept for 48 hours. The principle of this assay is based on the fact that agar coating, inhibits the adhesion of the cells to the culture surface; thereby maintaining the cells in suspension and enabling the study of anoikis resistance of cancer cells. The cells were then analyzed for self-renewal through colony formation assay. During colony formation, test materials were either removed from the pre-treated cells or added again throughout the colony formation period.

3.2.18 Gene expression analysis**a. RNA extraction**

RNA extraction was performed using the RNA extraction kit by Invitrogen according to the manufacturer's protocol. Briefly, up to 1×10^6 cells were lysed and the extracted RNA was quantified using Nanodrop spectrophotometer and stored at -80°C until reverse transcription.

b. Reverse transcription

1-2 μg of RNA was converted to cDNA in three technical replicates, using the reverse transcription kit by Invitrogen according to the manufacturer's protocol. The reaction was performed on Eppendorf thermomixer as per the following protocol.

Step	Temperature	Time
Stage 1	25°C	10 min
Stage 2	37°C	120 min
Stage 3	85°C	5 min
Stage 4	4°C	∞

The cDNA obtained was diluted 10 times in nuclease free water and stored at -20°C .

c. Real-time PCR

Real-time PCR was done for all the genes on CFX96 Real time PCR system by Bio-Rad. Each $10\ \mu\text{l}$ reaction mixture consisted of $3\ \mu\text{l}$ of 1:10 diluted cDNA, $0.25\ \mu\text{l}$ of Forward and Reverse primer each, $5\ \mu\text{l}$ of 2X SYBR green mix, and $1.5\ \mu\text{l}$ of Nuclease free water. The reaction protocol was setup as follows.

Step	Temperature	Time
Initial denaturation	95°C	10 min
40 cycles:		
Denaturation	95°C	15 sec
Annealing, Extension, plate read	60°C	45 sec
Melt Curve:		
Final Extension	72°C	10 min
Denaturation	95°C	15 sec
Plate read from 60 to 95°C with 0.5°C increment every 5 sec	$60-95^\circ\text{C}$	

Storage (optional)	4 °C	∞
--------------------	------	---

3.2.19 Data analysis

a. Flow cytometry data

Flow cytometry data generated as FCS files were analyzed using FCS Express 5 by Denovo Software, and results were tabulated in Excel for further analysis. The results are shown as the Mean \pm standard error (SE) as applicable.

b. Immunoblot quantification

Immunoblot quantification was done using Image Lab software by Bio-Rad. Lanes and bands were detected and the background correction was done using the software tools. The adjusted band intensity values were then tabulated and further analyzed in Excel. The Lane normalization factor was calculated for each condition by dividing the GAPDH band intensity of each lane by the maximum GAPDH band intensity obtained for the given blot

$$\text{Lane normalisation factor} = \frac{\text{GAPDH band intensity for the lane}}{\text{Maximum GAPDH band intensity on the blot}}$$

Subsequently, the band intensity for probed proteins was normalized by dividing with its respective lane normalization factor.

$$\text{Normalised protein expression} = \frac{\text{Observed band intensity}}{\text{Lane normalisation factor}}$$

Finally, the protein expression level of experimental conditions was normalized with the values obtained for control conditions and averaged across replicate blots. The results are shown as the mean \pm SE obtained for n>3 replicate blots.

c. Colony and spheroid growth/migration assay analysis

The microscopic images obtained for colonies or spheroids were analyzed using ImageJ by NIH. The colony/spheroid area was calculated by drawing the boundaries using the free-form area selection tool. The obtained area data was tabulated in Excel for different conditions and the results are shown as the mean \pm SE.

d. Wound healing assay analysis

The 2D-migration analysis was done using the T-Scratch software provided by ETH Zurich. The open image area data obtained from T-Scratch for each time point was imported into Excel and the average migration speed of the cell front

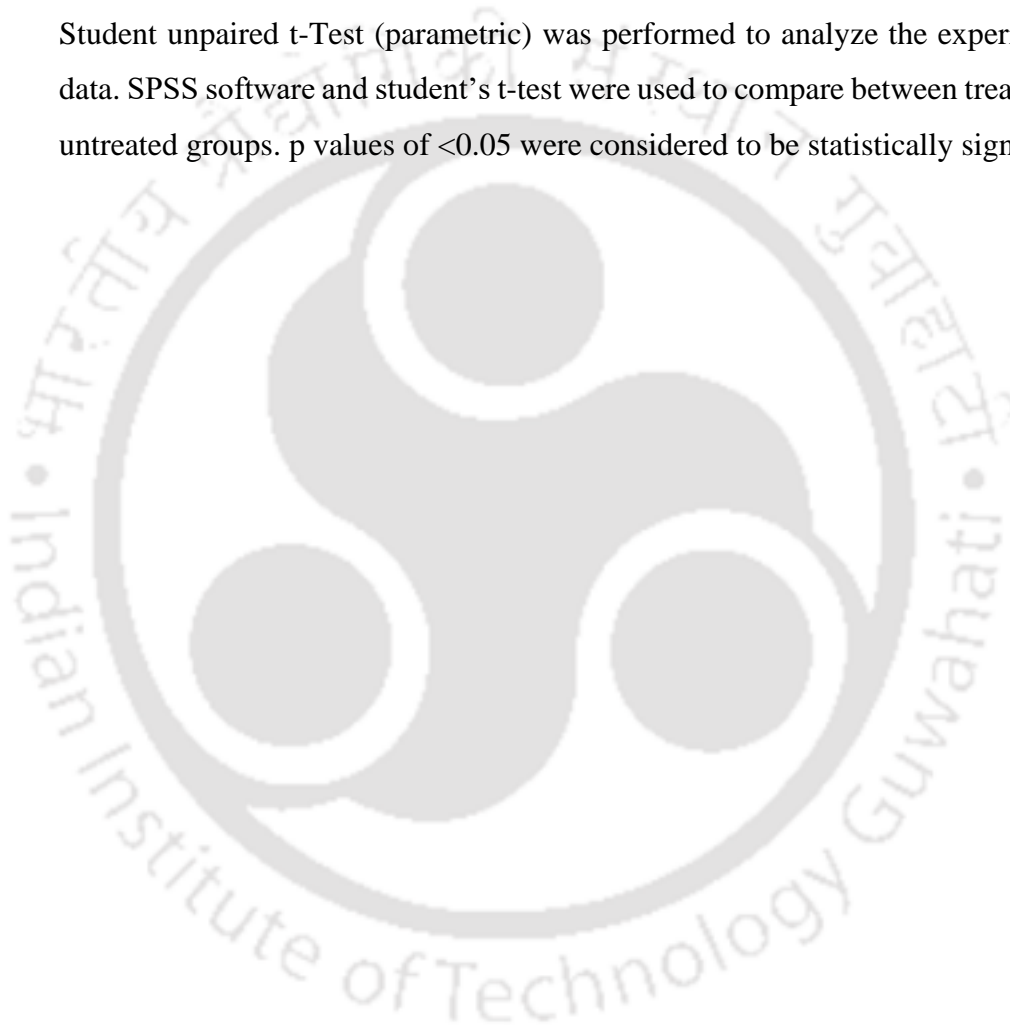
was calculated using the following equation.

$$\text{Migration speed } (\mu\text{m/hr}) = \frac{\Delta\text{Open image area (pixel}^2) \times \text{scale factor } (\mu\text{m/pixel})}{\text{Image height (pixel)} \times \Delta\text{Time (hr)} \times 2}$$

The migration speed was averaged for $n > 3$ regions for each condition and reported as mean \pm SE.

e. Statistical test

Student unpaired t-Test (parametric) was performed to analyze the experimental data. SPSS software and student's t-test were used to compare between treated and untreated groups. p values of < 0.05 were considered to be statistically significant.



RESULTS

4.1 Effect of ERK1/2 inhibition in breast cancer cells by multikinase RAF inhibitor Sorafenib

Activation of ERK1/2 and p38 MAPK pathways have been attributed to induce tumor progression and chemoresistance in breast cancer. To understand the role of ERK1/2 pathway in breast cancer progression, in this study, sorafenib, an FDA-approved multi-kinase inhibitor, is utilized to inhibit ERK1/2 pathway. Sorafenib is an effective inhibitor of cell surface receptor tyrosine kinases such as VEGF and PDGF receptor kinases, Flt-3, and c-kit and intracellular serine/threonine kinases such as Raf-1. Although sorafenib has shown promise as a therapeutic agent alone or in combination with other cytotoxic drugs, the molecular mechanism of sorafenib in breast cancer cells is not well understood. Further, sorafenib was utilized in this study to understand how the ERK1/2 signaling pathway modulation can impact breast cancer progression and chemoresistance.

To evaluate the effect of sorafenib the breast cancer cell lines MCF7 and MDA-MB-231 were treated with increasing concentration of sorafenib (**Fig.4.1.1a-b**) (0.01 μ M to 50 μ M) for different time periods ranging from 24 – 96 hours (**Fig.4.4.1c**) to determine the IC50 concentration of sorafenib and the appropriate treatment time. Sorafenib inhibited the proliferation of MCF7 and MDA-MB-231 cells in a concentration-dependent manner (**Fig.4.4.1a**).

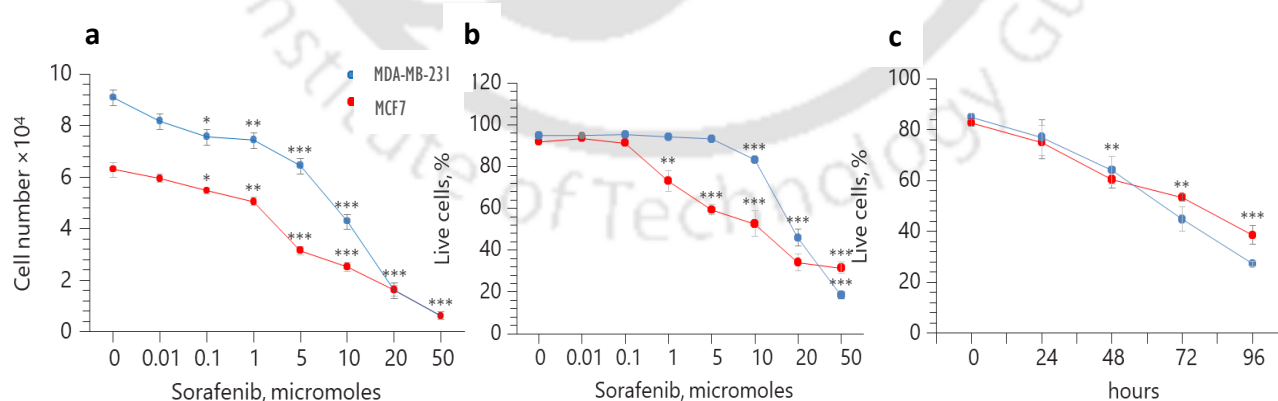


Fig.4.1.1 Effect of sorafenib on proliferation and survival of breast cancer cells. MCF7 and MDA-MB-231 breast cancer cells were treated with different concentrations of sorafenib and its effect on proliferation was determined by cell counting (**a**) and survival (**b**) was determined by propidium iodide (PI) staining through flow cytometry. (**c**) MCF7 and MDA-MB-231 cells were treated with sorafenib (10 μ M) for the indicated time points and

live cell percentage was determined by PI staining through flow cytometry. Values are mean \pm SD, $n = 3$ independent experiments, * $p < 0.05$, ** $p < 0.005$, *** $p < 0.0005$.

Furthermore, MCF7 cells exhibited higher sensitivity to sorafenib compared to MDA-MB-231 cells. MCF7 cells showed 4-fold higher sensitivity to sorafenib with an IC₅₀ value of 5 μ M for MCF7 and 20 μ M for MDA-MB-231 cells. A significant decrease in the percentage of live cells was observed when the cells were treated 48 hours. Hence, the rest of the study was performed with a standard concentration of 10 μ M of sorafenib and 48 hours of treatment for both MCF7 and MDA-MB-231 cells.

As sorafenib was reported to inhibit ERK1/2 [44], the level of phospho ERK1/2 (pERK1/2) was determined by immunoblotting in sorafenib treated MCF7 and MDA-MB-231 cells. The cells were treated with epidermal growth factor (EGF) as a positive control. While EGF treatment increased the pERK1/2 levels as expected, sorafenib treatment significantly inhibited phospho proteins levels of ERK1/2 (**Fig.4.1.2 a-b**). Reduced levels of pERK1/2 were also accompanied by reduction in KI67 and PCNA expression suggesting that sorafenib treatment has the potential to inhibit cell proliferation in addition to inducing cell death (**Fig.4.1.2 c**).

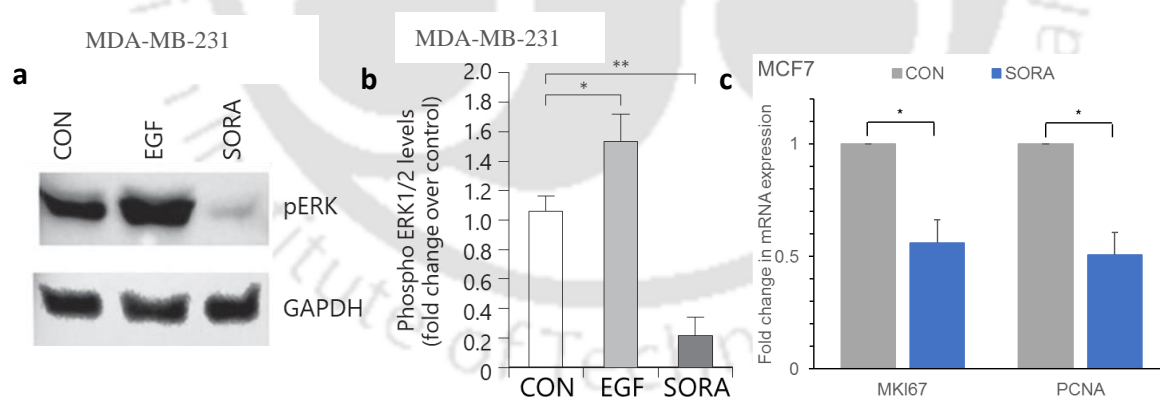


Fig.4.1.2 Gene expression and signaling pathway changes due to sorafenib treatment

Phospho-ERK1/ERK2 (Thr185, Tyr187) levels in MDA-MB-231 cells left untreated(CON) or after treatment with EGF or sorafenib (SORA) for 48 h was determined by Western blotting. **(b)** Expression was normalized to GAPDH expression levels in each sample. Values are mean \pm SD, $n = 3$, * $p < 0.05$, ** $p < 0.005$. **(c)** Fold change in mRNA -levels of KI67 and PCNA were determined by q-PCR.

In order to evaluate the effect of sorafenib treatment on proliferation further, the cell cycle profiles of sorafenib treated cells was determined (Fig.4.1.3a-b). Sorafenib induced cell cycle arrest in both MCF7 and MDA-MB-231 cells with a significant increase in the percentage of cells at G0/G1 stage of the cell cycle. Treatment with sorafenib also increased the mitochondrial superoxide levels in the MDA-MB-231 (Fig.4.1.3c-d) cells suggesting that ROS production is one of the mechanisms through which sorafenib might inhibit breast cancer cell proliferation and survival.

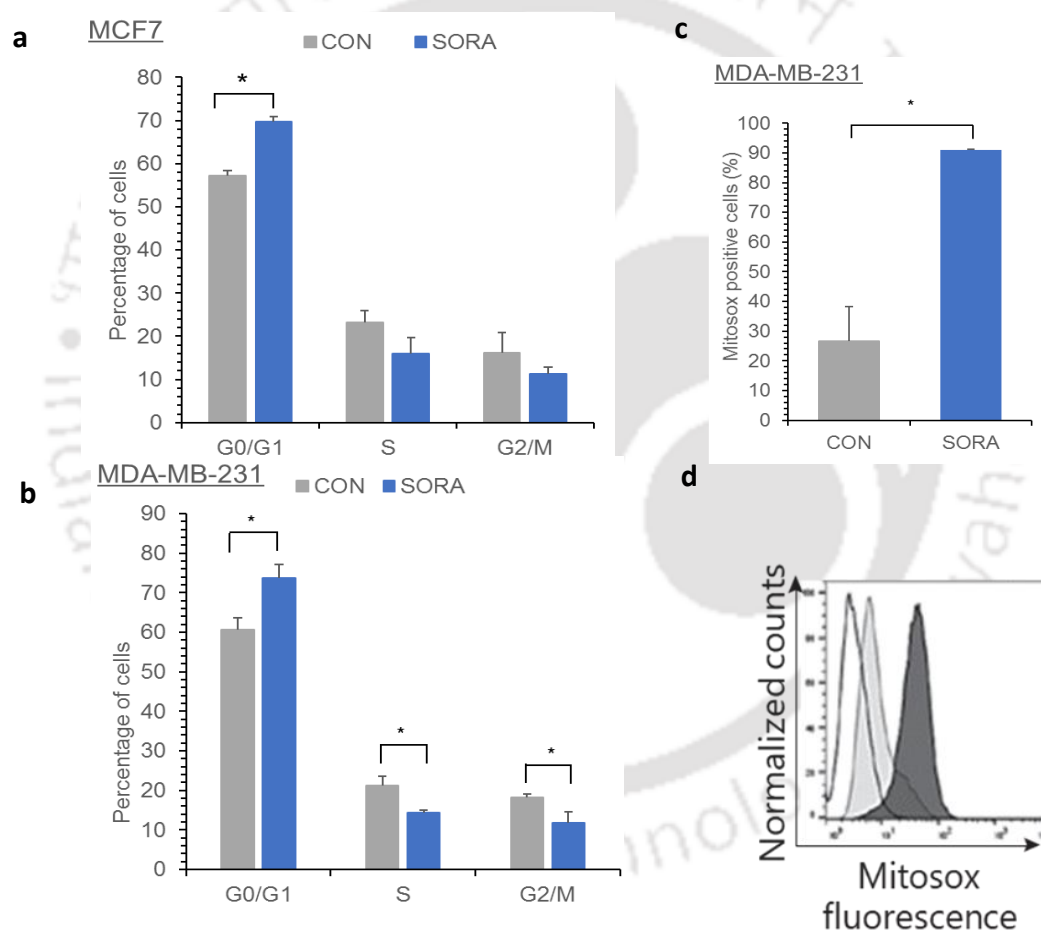


Fig.4.1.3 Effect of Sorafenib on proliferation and survival. (a) MDA-MB-231 and (b) MCF7 cells were left untreated (CON) or were treated with EGF (20 ng/ mL) or sorafenib (SORA, 10 μ M) for 48 h and the cell cycle profile was analyzed by flow cytometry. (c) Percentage of cells containing mitochondrial superoxide, in sorafenib (SORA, 10 μ M) treated and untreated (CON) MDA-MB-231 cells was assessed by staining the cells with Mitosox and quantified by flow cytometry. (d) Representative flow cytometry histogram showing the Mitosox-positive cells in control (gray histogram), and sorafenib-treated cells (black histogram). Black line represents the unstained cells. Values are mean \pm SD, *n*

= 3 independent experiments, * $p < 0.05$, ** $p < 0.005$, *** $p < 0.0005$.

To further evaluate the inhibitory effect of sorafenib (reduction in p-ERK levels of MDA-MB-231 cells), MDA-MB-231 were allowed to form 3D spheroids (Fig.4.1.4a-b) and proliferate as spheroids during treatment with sorafenib. This was done to closely mimic the *in vivo* conditions where the cancer cells proliferate as a tumor mass. As observed with the 2D culture, sorafenib significantly and irreversibly inhibited the proliferation of MDA-MB-231 3D spheroids. The cells formed significantly smaller spheroids and were unable to proliferate even though the treatment with sorafenib was performed at the time of spheroid formation. The spheroid size did not increase even until 14 days of the observation period, clearly indicating that sorafenib irreversibly arrests the growth of breast cancer cells.

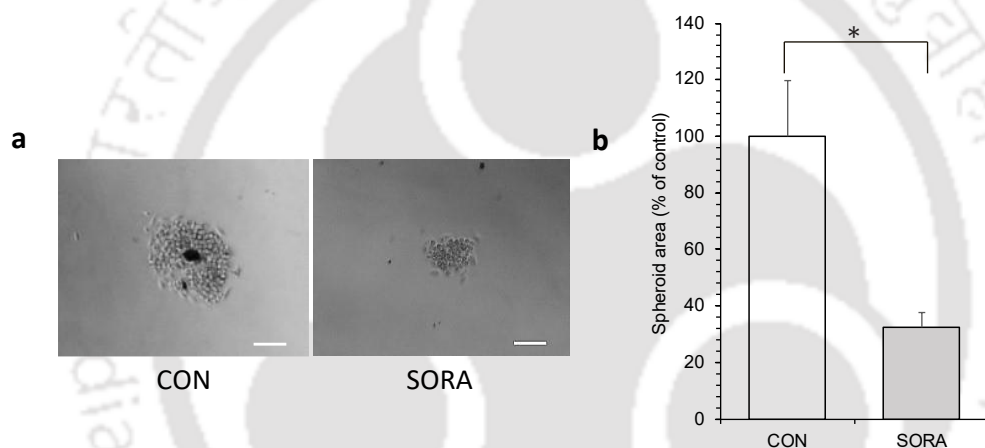
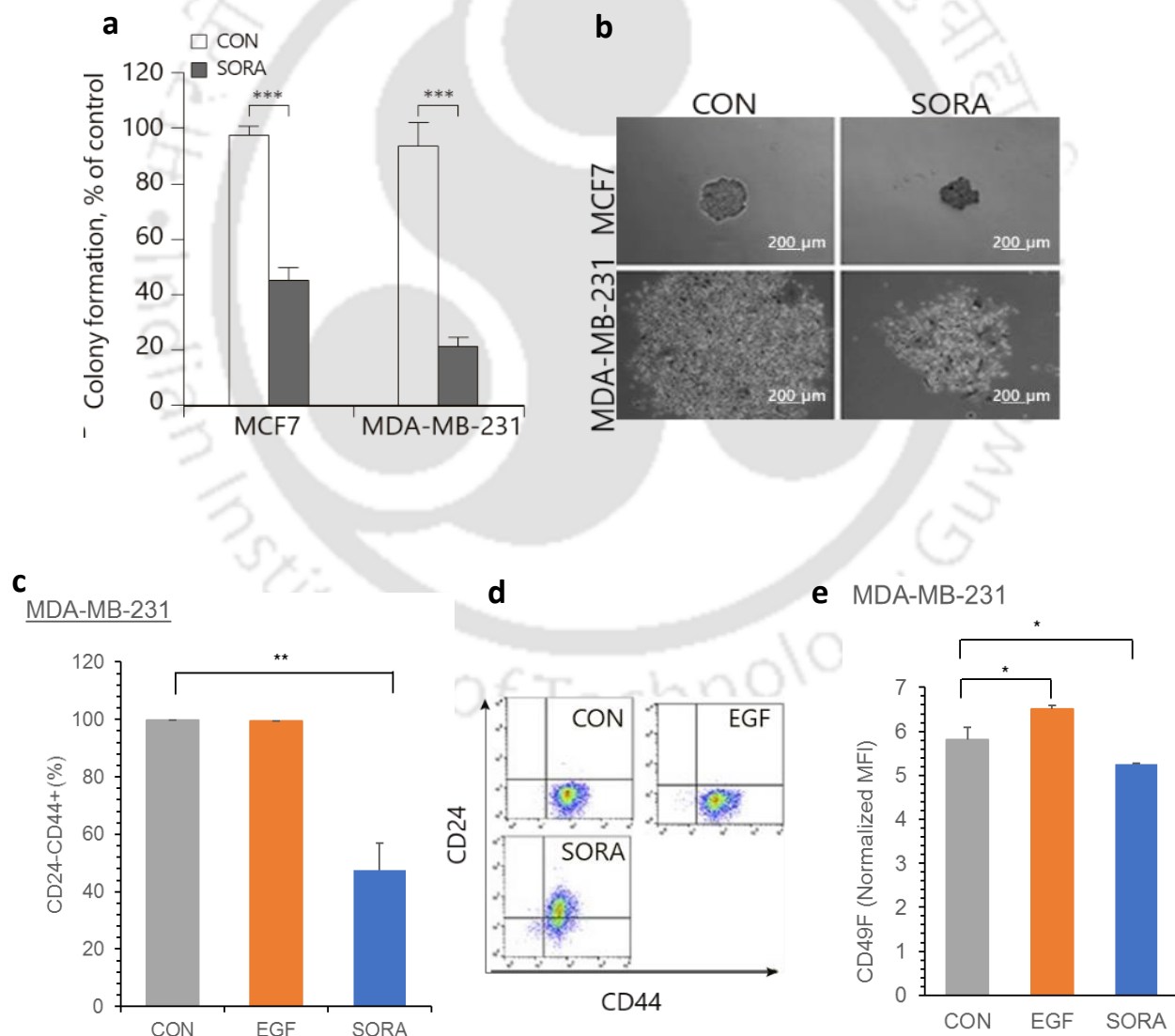


Fig.4.1.4 Effect of Sorafenib treatment on spheroid growth (a) Representative images of 3-D spheroids of MDA-MB-231 cells **(b)** Percentage of spheroid growth area in Sorafenib treated MDA-MB-231 showing significant reduction in size of spheroids compared to untreated (CON) condition.

However, several studies have shown that cancer progression and metastasis are mediated by cancer stem cells with high self-renewal and proliferation abilities. The breast cancer stem cells and their self-renewal ability during sorafenib treatment was determined by colony-formation assay (Fig.4.1.5a-b), and changes in the stem cell population was analyzed by flow cytometry (Fig.4.1.5c-e). Sorafenib treatment significantly decreased the self-renewal ability of both MCF7 and MDA-MB-231 cells, with the treated cells forming fewer colonies. Here, the cells were treated only for the initial period of 48 hours during colony formation, however, the cells formed fewer colonies, and were smaller in size compared to the control untreated conditions (Fig.4.1.5a-b). Studies have shown that cancer stem cells in breast cancer is defined by CD44⁺/CD24^{-/lo} and CD49F-expressing cells [62] [110],

and the percentage of CD44⁺/CD24^{-/lo} and CD49F⁺ cells was determined by flow cytometry (Fig.4.1.5c-e).

In line with the reduction in the colony formation ability, sorafenib treatment significantly increased the CD24 expression (Fig.4.1.5c, f) indicating a reduction in the breast cancer stem cell population. Similarly, gene expression analysis showed a significant increase in CD24 transcript levels during sorafenib treatment (Fig 4.1.5f, g), in both MCF7 and MDA-MB-231 cells. In MDA-MB-231 cells, EGF treatment did not affect either CD44 or CD24 expression. This was accompanied by a significant decrease in the transcript levels of CD49F (Fig.4.1.5e) in MDA-MB-231 cells, however, expression of ALDH1A3 (Fig.4.1.5g), a marker for stem cells was unaffected in both EGF and sorafenib-treated MDA-MB-231 cells.



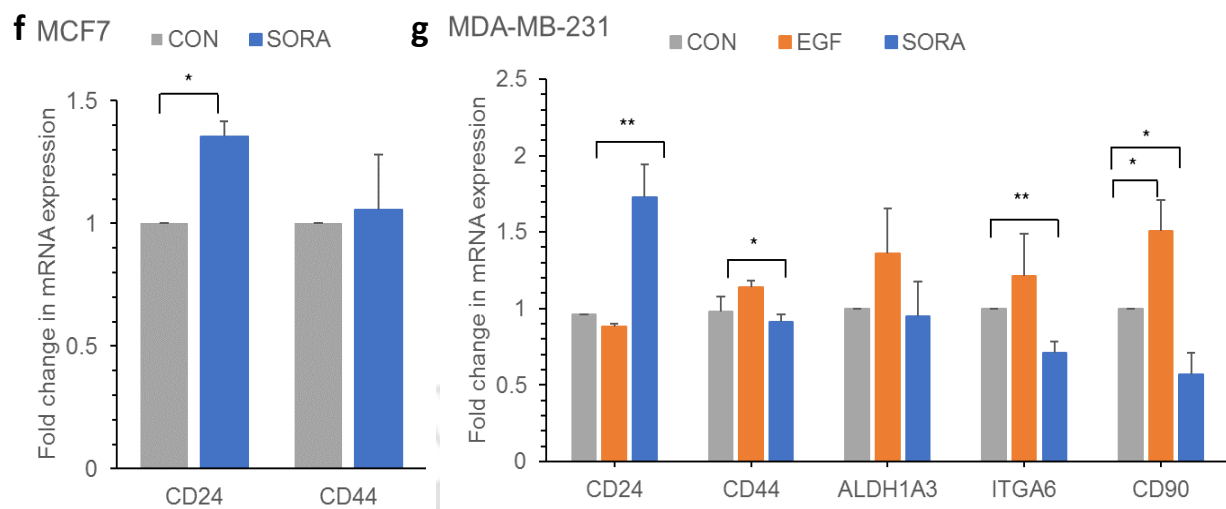
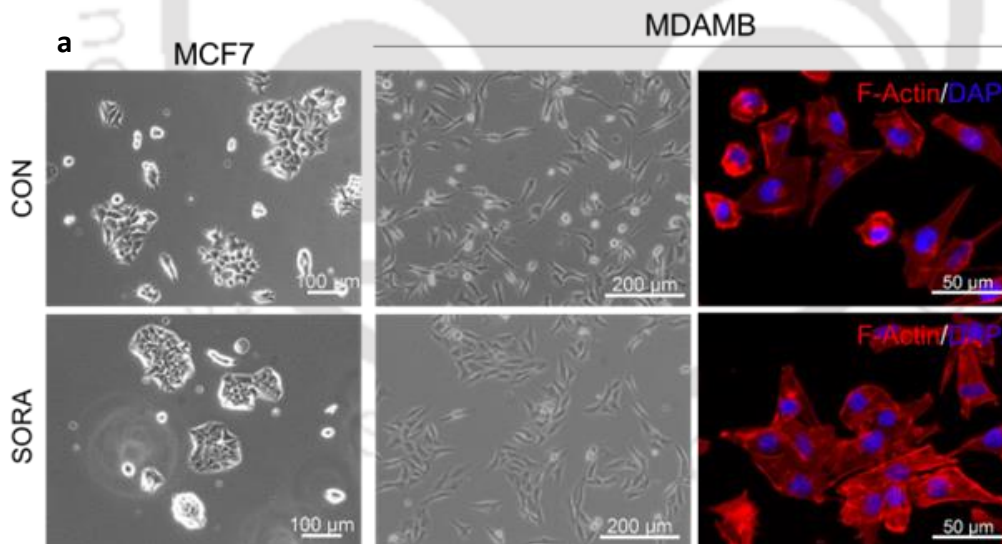


Fig.4.1.5 Effect of Sorafenib treatment on breast cancer stem cells (a) Clonogenic assay was performed for sorafenib (SORA) and untreated (CON) MCF7 and MDA-MB-231 cells and the percentage of colonies obtained after sorafenib treatment is shown. **(b)** Representative images showing colonies after sorafenib treatment of MCF7 and MDA-MB-231 cells. **(c)** Percentage of MDA-MB-231 cells with the phenotype CD44⁺CD24⁻ in untreated (CON), EGF (20 ng/mL) or sorafenib (SORA, 10 μ M) treated cells. **(d)** Representative flow cytometric dot blot showing CD44, CD24 expression pattern in MDA-MB-231 under different treatment conditions. **(e)** Graph showing CD49F expression in control (CON), EGF or sorafenib (SORA) treated MDA-MB-231 cells. **(f)** Gene expression analysis by real-time PCR showing expression levels of CD24, CD44, ALDH1A3 and ITGA6 in control (CON), EGF and sorafenib (SORA) treated MDA-MB-231 cells. **(g)** Gene expression analysis by real-time PCR showing expression levels of CD24 and CD44 control (CON), EGF and sorafenib (SORA) treated MCF7 cells. Values are mean \pm SD, n > 3 independent experiments, *p < 0.05, **p < 0.005, *** p < 0.0005.

One of the hallmarks of cancer cells is metastasis, the ability of the cells to migrate and invade distant tissues and organs. Metastasis is initiated by epithelial-mesenchymal transition (EMT) which induces changes in the morphology and gene expression profile of the migrating cells. In order to understand whether sorafenib treatment could interfere with the metastatic ability of the breast cancer cells in addition to its cytotoxic effects, the migration of breast cancer cells in 2D monolayer culture and 3D spheroids was studied (**Fig.4.1.7**). Moreover, the actin cytoskeleton plays an important role in regulating the migration of cells, and EMT is accompanied by changes in the cell morphology and the rearrangement of F-actin in the cells. Interestingly, sorafenib treatment increased the cell-cell contact and reduced actin projections in MCF7 and MDA-MB-231 cells, suggesting its anti-migratory effect (**Fig.4.1.6a**). In MCF7 cells, filopodia formation and loss of E-cadherin expression induced by EGF treatment were reversed when sorafenib was added along with EGF (**Fig.4.1.6b**).



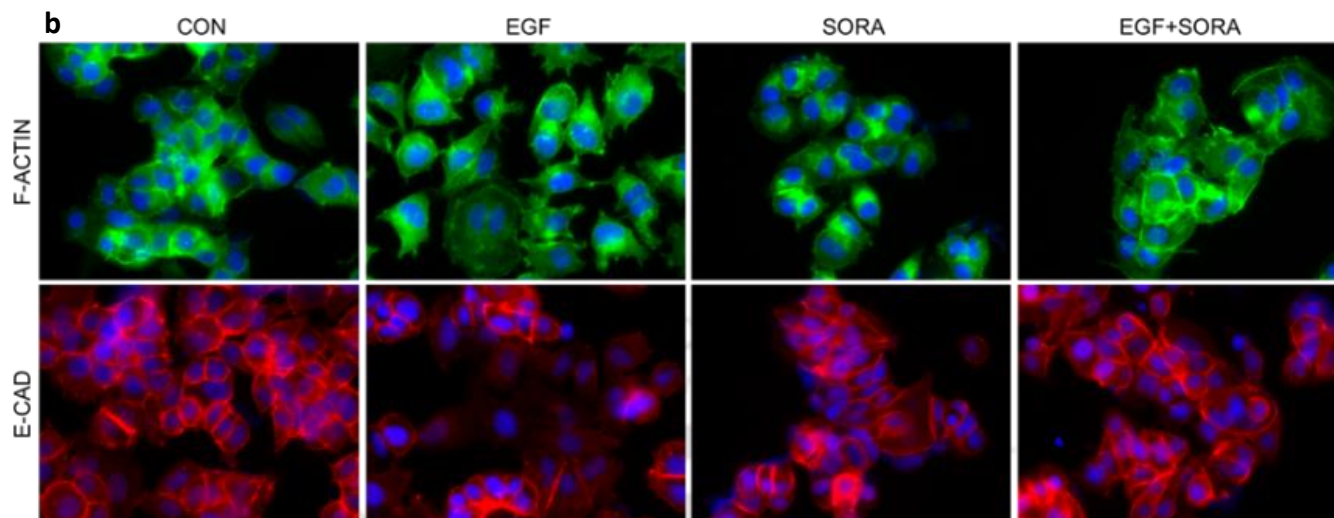
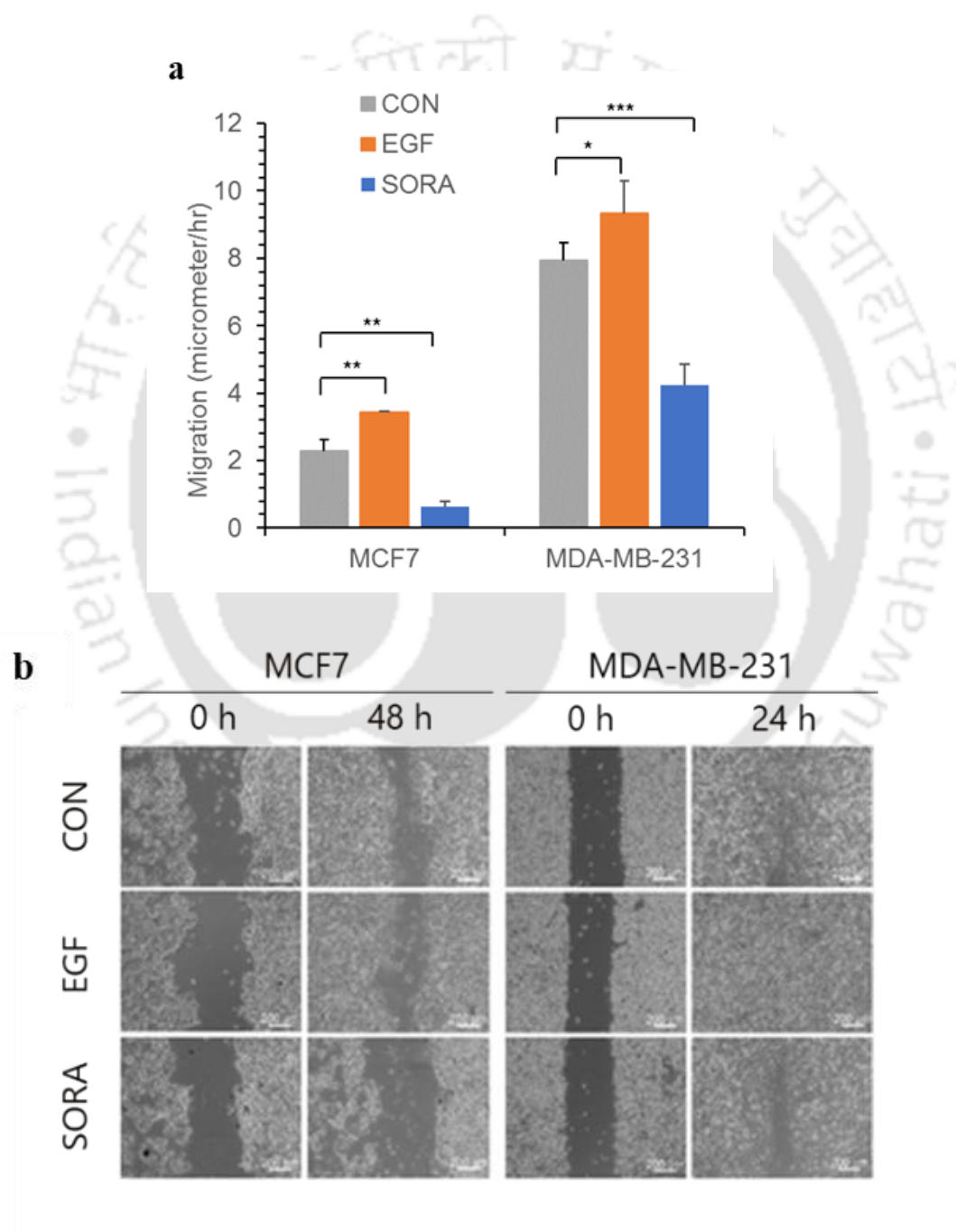


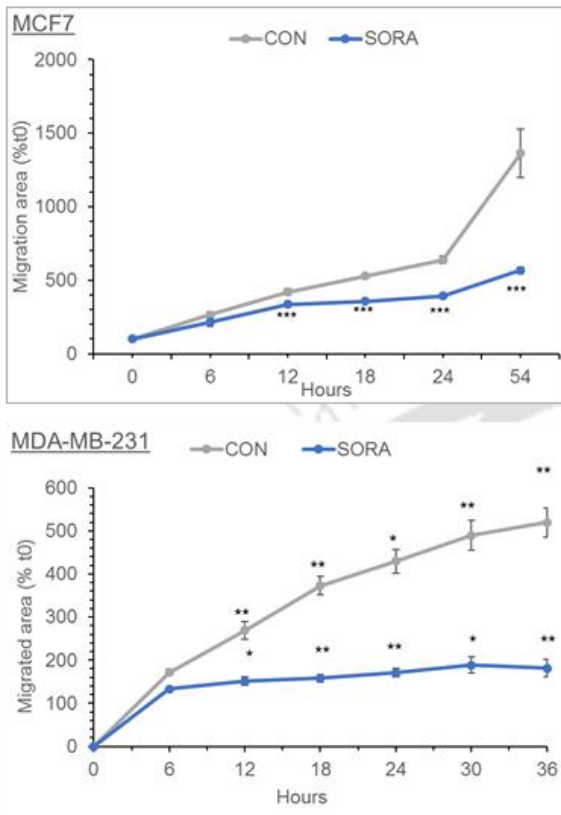
Fig.4.1.6 Effect of Sorafenib treatment on cytoskeleton of breast cancer stem cells (a) Phase contrast microscopic images of MCF7 and MDA-MB-231 cells treated with sorafenib (SORA) or left untreated (CON). The bottom panel shows fluorescent microscopic images of MDA-MB-231 stained with F-actin and DAPI after treatment with sorafenib. **(b)** Fluorescent microscopic images of MCF7 control (CON) cells or treated with EGF, sorafenib (SORA) or a combination of EGF and SORA (EGF + SORA). The top panel shows F-actin staining and the bottom panel shows E-cadherin (E-CAD) staining for the treated cells.

Similarly, while EGF treatment significantly increased the migration of MCF7 and MDA-MB-231 cells, sorafenib treatment inhibited the migration potential of both MCF7 and MDA-MB-231 cells (**Fig.4.1.7a-b**). In order to evaluate the effect of sorafenib on the migration of breast cancer cells further, a 3D spheroid invasion assay (**Fig.4.1.7c-d**), which closely mimics the migration of cancer cells in *in vivo* conditions was performed. Similar to that observed in 2D conditions (**Fig.4.1.7a-b**), the invasion of MCF7 and MDA-MB-231 cells from the 3D spheroids on the collagen matrix (**Fig.4.1.7c-d**) was drastically reduced in the presence of sorafenib. The migration inhibitory effect of sorafenib was more profound in the highly metastatic cell line MDA-MB-231, and the effect was sustained over several hours. The reduction in the migration ability of the cells was accompanied by an increase in the Ep-CAM expression a marker that represents the loss of migration potential in breast cancer cells (**Fig.4.1.7e-f**). Furthermore, gene expression analysis (**Fig.4.1.7g-i**) showed that sorafenib treatment significantly induced E-cadherin, Ep-CAM, TIMP2, TIMP3 and TIMP4 expression in MDA-MB-231 cells. In contrast, EGF induced the

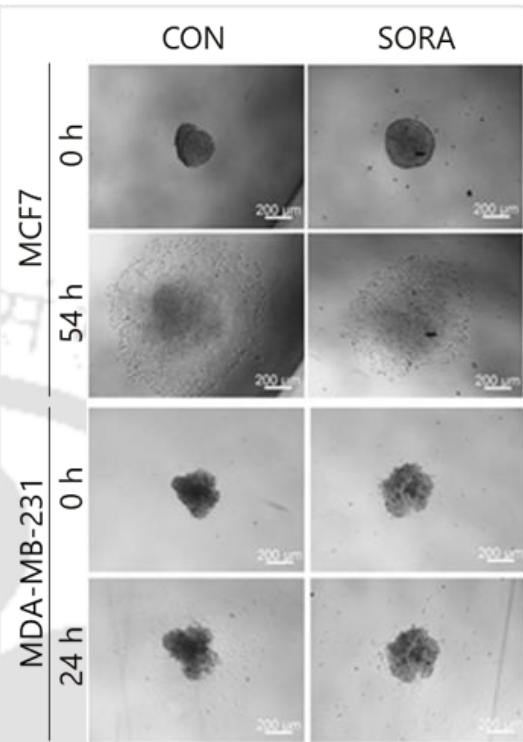
expression of matrix metalloproteinases (MMP) MMP1 and MMP9; sorafenib treatment diminished the expression of MMP1 and MMP9 in MDA-MB-231 cells. Expression of vimentin (VIM) was unaffected in MDA-MB-231 cells; however, sorafenib significantly reduced the expression of migration-related marker EREG at the transcript level. In MCF7 cells, (Fig.4.1.7j), there was a significant downregulation in the expression of EMT markers VIM and N-cadherin (CDH2).



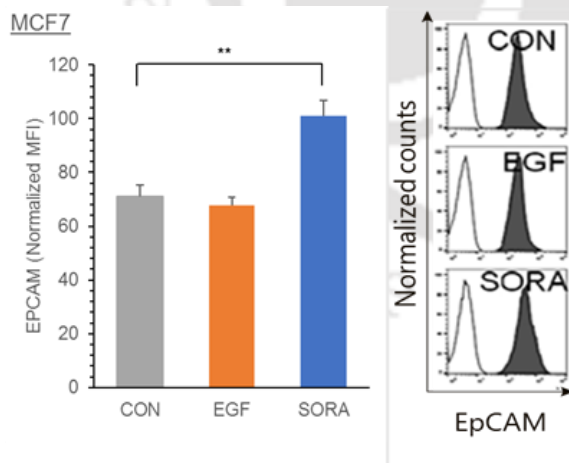
c



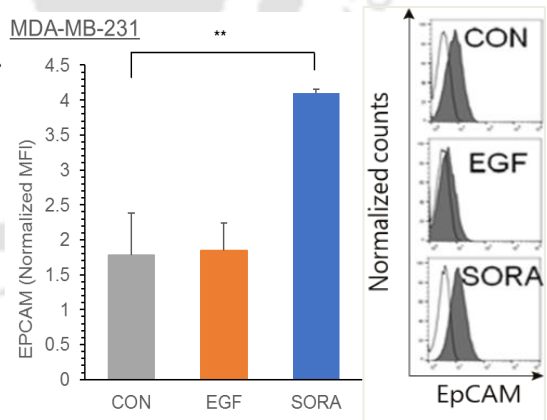
d



e



f



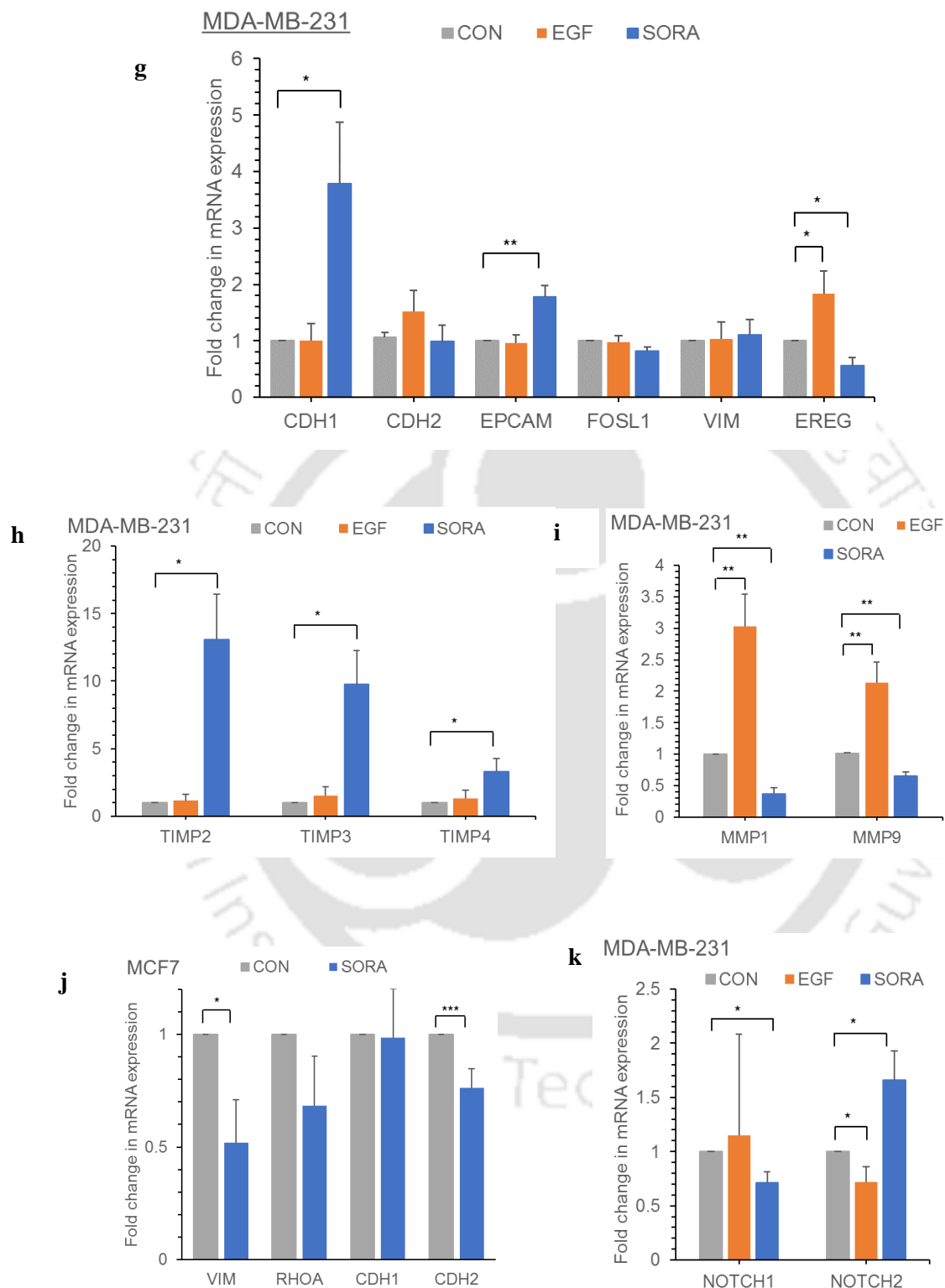


Fig.4.1.7 Effect of Sorafenib treatment on migration and invasion of breast cancer stem cells (a) MCF7 and MDA-MB-231 cells were subjected to wound healing assay during treatment with EGF or sorafenib (SORA), migration speed was calculated and

compared with untreated control (CON) cells. **(b)** Representative images of wound healing migration assay. Values are mean \pm SD, $n = 3-6$. **(c)** 3D spheroid invasion was performed with MCF7 and MDA-MB-231 cells on collagen (50 μ g/ml) coated wells during treatment with sorafenib (SORA) or in control (CON) untreated conditions. Migration of the cells out of spheroid was documented at regular intervals and the mi-grated area was normalized to the spheroid area at $t = 0$. The migration area at different time points for MCF7 and MDA-MB-231 are shown in the representative images **(d)**. Values are mean \pm SD, $n = 4-7$. **(e-f)** EpCAM expression in MCF7 **(e)** and MDA-MB-231 **(f)** cells treated with EGF or sorafenib (SORA) for 48 h, compared with control (CON) cells along with representative flow cytometric histograms showing EpCAM expression under different treatment conditions for MCF7 and MDA-MB-231 cells. Isotype control is represented by black line and antibody-stained cells are represented by grey histogram. Values are mean \pm SD, $n = 3-4$. **(g-i)** Gene expression changes of cell migration markers due to sorafenib treatment was determined by expression levels of represented genes through real-time PCR in MDA-MB-231 cells left untreated (CON) or treated with EGF and sorafenib (SORA) for 24 h. Expression levels were normalized to the respective GAPDH levels and fold change with respect to the control untreated cells were determined. Values are mean \pm SE, $n = 3$, $*p < 0.05$, $**p < 0.005$.

In order to determine whether sorafenib treatment impacts cancer-related signaling pathways, the expression levels of phospho P38MAPK (pP38MAPK) and phospho STAT5 (pSTAT5) were analyzed by flow cytometry **(Fig.4.1.8)**. Sorafenib treatment significantly reduced the expression levels of pP38MAPK and pSTAT5 in MDA-MB-231 cells, further confirming its anti-tumorigenic effects.

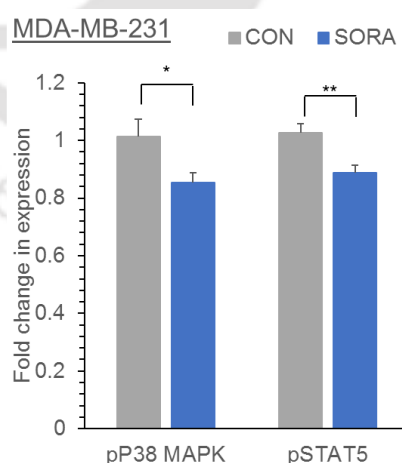


Fig.4.1.8 Gene expression and signaling pathway changes due to sorafenib treatment Phospho-p38 MAPK (pT180/pY182) and phospho-STAT5 (pY694) levels in control untreated (CON) or sorafenib (SORA) treated MDA-MB-231 cells after 24 h of treatment was determined by phospho-protein flow cytometry. Values are mean \pm SD, $n = 3$, $*p < 0.05$, $**p < 0.005$.

In conclusion it can be said that Sorafenib significantly and irreversibly inhibited the proliferation and migration of MCF7 and MDA-MB-231 both in 2D monolayer culture and 3D spheroids along with cell cycle growth phase arrest, indicating that sorafenib irreversibly arrests the growth of breast cancer cells. Sorafenib treatment significantly decreased the self-renewal ability of both MCF7 and MDA-MB-231 cells, with fewer and smaller colonies observed after sorafenib treatment. Sorafenib treatment significantly increased the CD24 expression, indicating a reduction in the breast cancer stem cell population. This was accompanied by a significant decrease in the transcript levels of CD49F in sorafenib treated MDA-MB-231 cells. Sorafenib treatment increased the cell-cell contact and reduced actin projections in MCF7 and MDA-MB-231 cells, suggesting its anti-migratory effect, as determined by immunocytochemistry. In MCF7 cells, filopodia formation and loss of E-cadherin expression induced by EGF treatment were reversed when sorafenib was added along with EGF. Gene expression analysis showed that sorafenib treatment significantly induced E-cadherin, EpCAM, TIMP2, TIMP3 and TIMP4 expression and diminished the expression of EREG, MMP1 and MMP9 in MDA-MB-231 cells. Sorafenib treatment significantly reduced the expression levels of phospho P38MAPK and phospho STAT5 in MDA-MB-231 cells, determined by flow cytometry, further confirming its anti-tumorigenic effects.

4.2 Effect of ERK1/2 inhibition in breast cancer cells by ERK1/2 specific inhibitor BVD-523

It was clear from the earlier data that sorafenib, a multi-kinase inhibitor significantly reduces the proliferation, migration and metastatic abilities of breast cancer cells. To understand the specific role of ERK1/2 signaling in breast cancer progression, the study was extended to include BVD-523 (BVD) a first-in-class ERK1/2 inhibitor BVD-523 (BVD) which is under clinical trial in several cancer types [44]. Firstly, the dose response analysis of different concentrations of BVD (0.001 μ M to 20 μ M) was performed for the MCF7 and MDA-MB-231 cell lines (**Fig.4.2.1a-b**). A dose-dependent decrease in the cell number was observed with BVD treatment after 48 hr of treatment. Although a significant reduction in cell number was observed at a concentration of 5 μ M and more, the cell viability was not significantly affected.

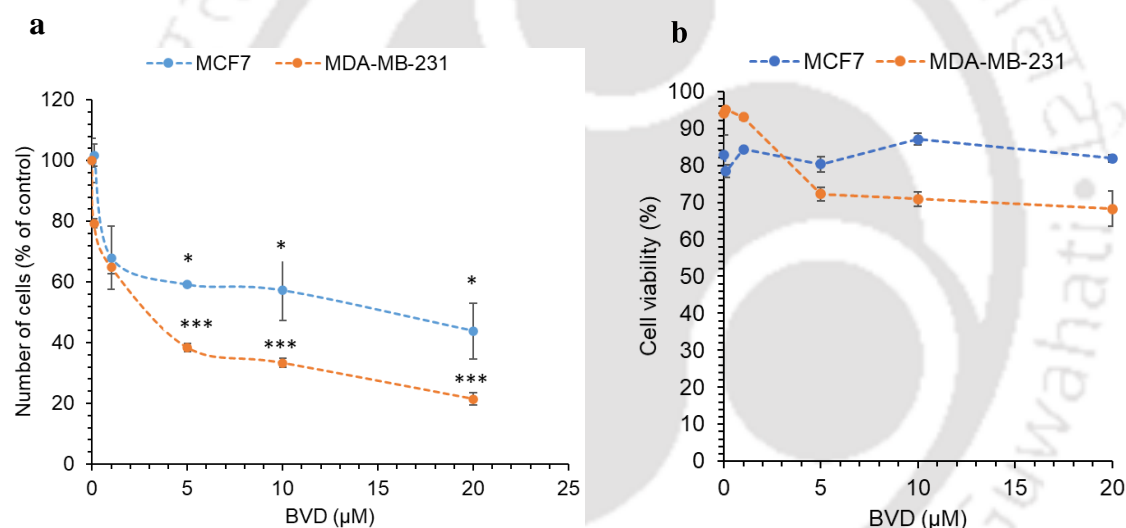


Fig.4.2.1 Effect of ERK1/2 inhibition on cell proliferation and survival Proliferation assay of MCF7 and MDA-MB-231 cells with increasing concentrations of BVD-523 with (0.001 to 20) μ M range. As observed, (a) **number of cells** showed a dose dependent decrease in both the cell lines and (b) **percentage of cell viability** in MDA-MB-231 reduced by 20% upon treatment with more than 1 μ M concentration, whereas in MCF7 cells there was no such effect after 48 hours of treatment. Thus, 10 μ M concentration of BVD-523 has been selected for further studies. Values are mean \pm SD, $n > 3$ independent experiments, * $p < 0.05$, ** $p < 0.005$, *** $p < 0.0005$.

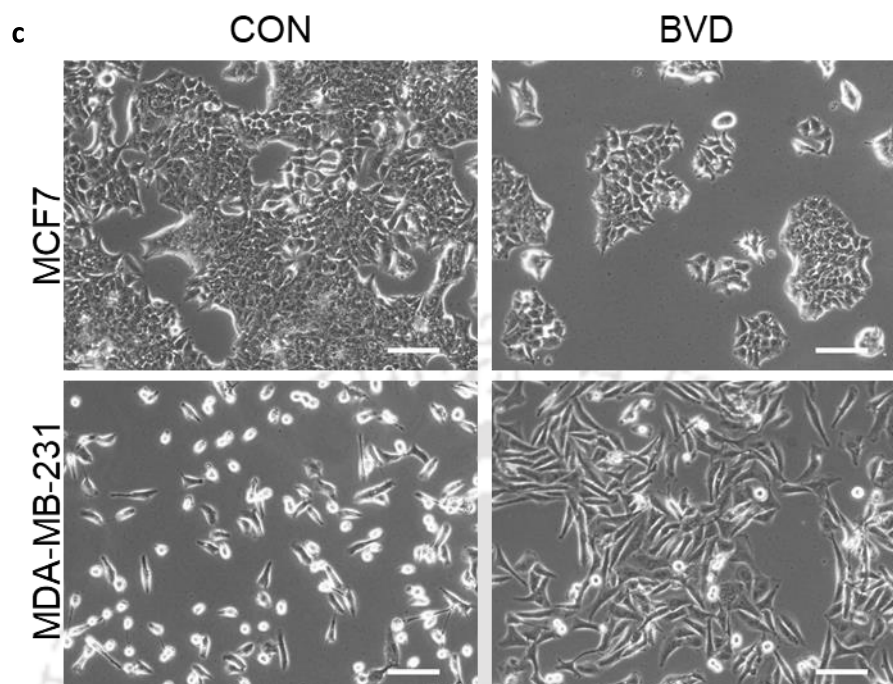


Fig.4.2.1 Effect of ERK1/2 inhibition on morphology (c) BVD treatment showed a marked effect on the morphology of MDA-MB-231 cells. BVD-treated MDA-MB-231 cells assumed a clustered and flattened morphology, whereas, MCF7 cells showed a reduction in cell density, consistent with their reduced proliferation potential.

The inhibitory effect of BVD on cell proliferation was also seen during the 3D growth of cells. MCF7 cells treated with BVD during spheroid formation, exhibited smaller spheroids and the spheroid size did not significantly increase during the 14 days observation period. Here, only a single dose of BVD was added during the spheroid formation and its effect on growth inhibition could be observed until 14 days (**Fig.4.2.2 a-b**).

Given the fact that cell proliferation was inhibited without significant changes in the cell viability, cell cycle analysis was done for BVD treated MDA-MB-231 and MCF7 cells. A significant increase in the G1 phase was observed in BVD treated MCF7 and MDA-MB-231 cells with a concomitant decrease in the percentage of cells in S and G2/M stages. (**Fig.4.2.3 a-b**).

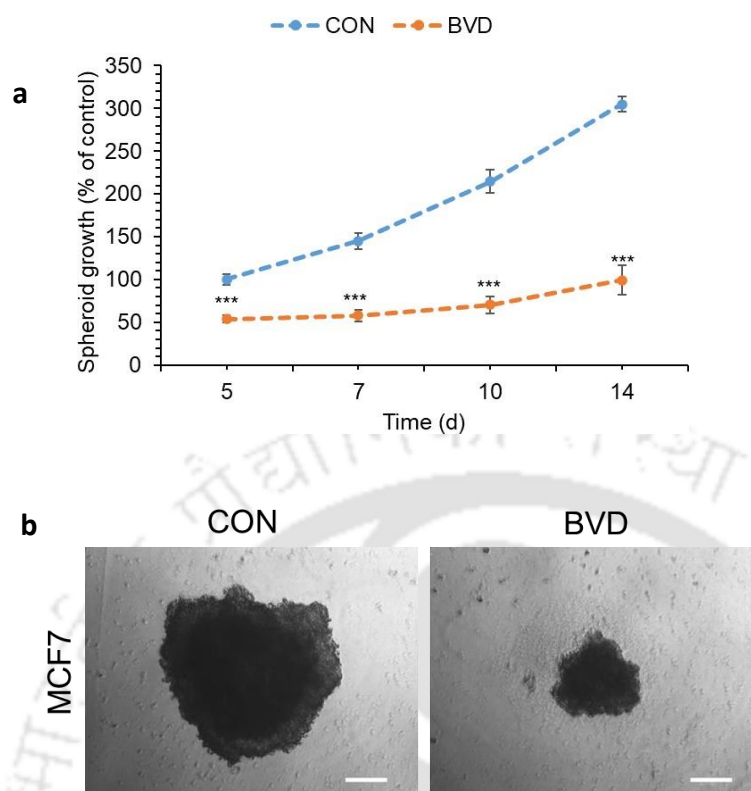


Fig.4.2.2 Effect of ERK1/2 inhibition on spheroid growth (a) BVD treatment showed a significant decrease in growth of MCF7 cell-spheroids over time. Spheroid growth areas of BVD treated cells were calculated as compared to untreated (CON) conditions starting from day 5 to day14. **(b)** Representative images of spheroids as observed under microscope.

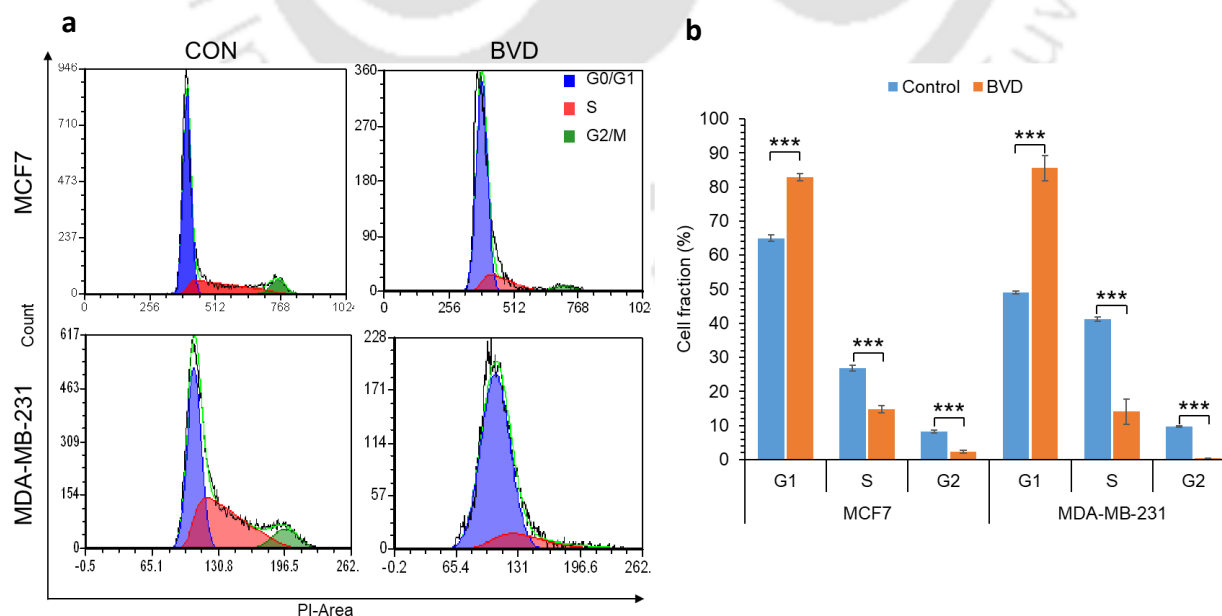
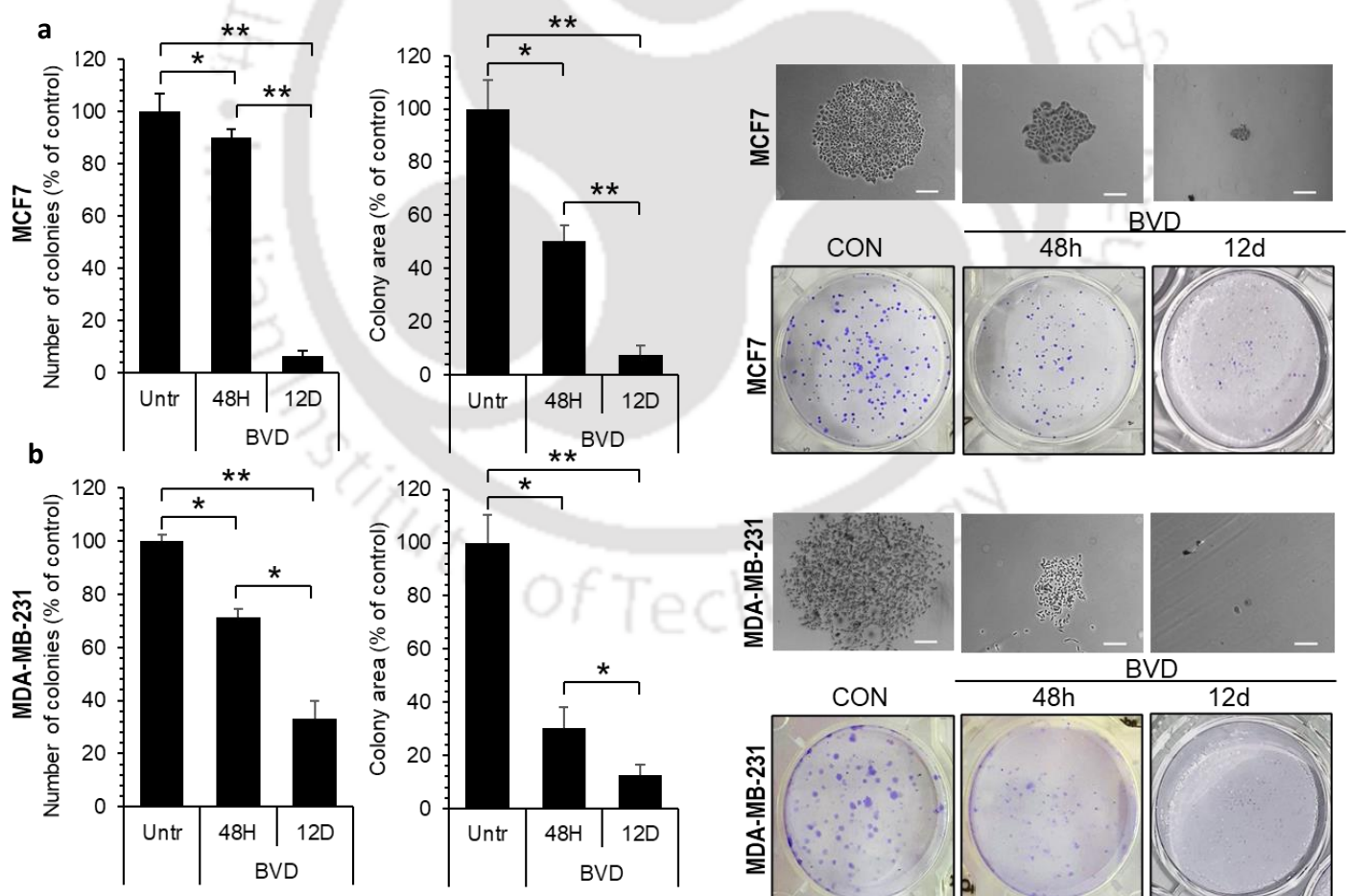


Fig.4.2.3 Effect of ERK1/2 inhibition on cell cycle (a-b) -The cell cycle status of breast cancer cells upon treatment with BVD showed growth arrest in G1 phase. MCF7 and MDA-

MB-231 cells showed increase in cell fraction G1 phase and reduction in S and G2 phase upon BVD treatment; * $p < 0.05$, ** $p < 0.005$, *** $p < 0.0005$.

To determine whether BVD treatment can inhibit the proliferation of self-renewing cancer stem-cell like cells, the self-renewal ability was determined by colony-formation assay. Treatment of cells with BVD for initial 48 hr was sufficient to significantly inhibit the colony formation, however, continuous treatment with one dose of BVD for 10-12 days resulted in 15-fold and 3-fold reduction in the colony formation ability in the MCF7(**Fig.4.2.4a**) and MDA-MB-231(**Fig.4.2.4b**) cells respectively. Taken together, these results indicate that ERK1/2 inhibition with BVD significantly impairs breast cancer cell proliferation and self-renewal.

The phenotype of the BVD treated cells was determined, especially the markers that define the breast cancer stem cell population. BVD treatment significantly reduced the CD44 and CD49F cell surface expression in MDA-MB-231(**Fig.4.2.4c-d**) cells and an upregulation of EPCAM expression was observed in these cells.



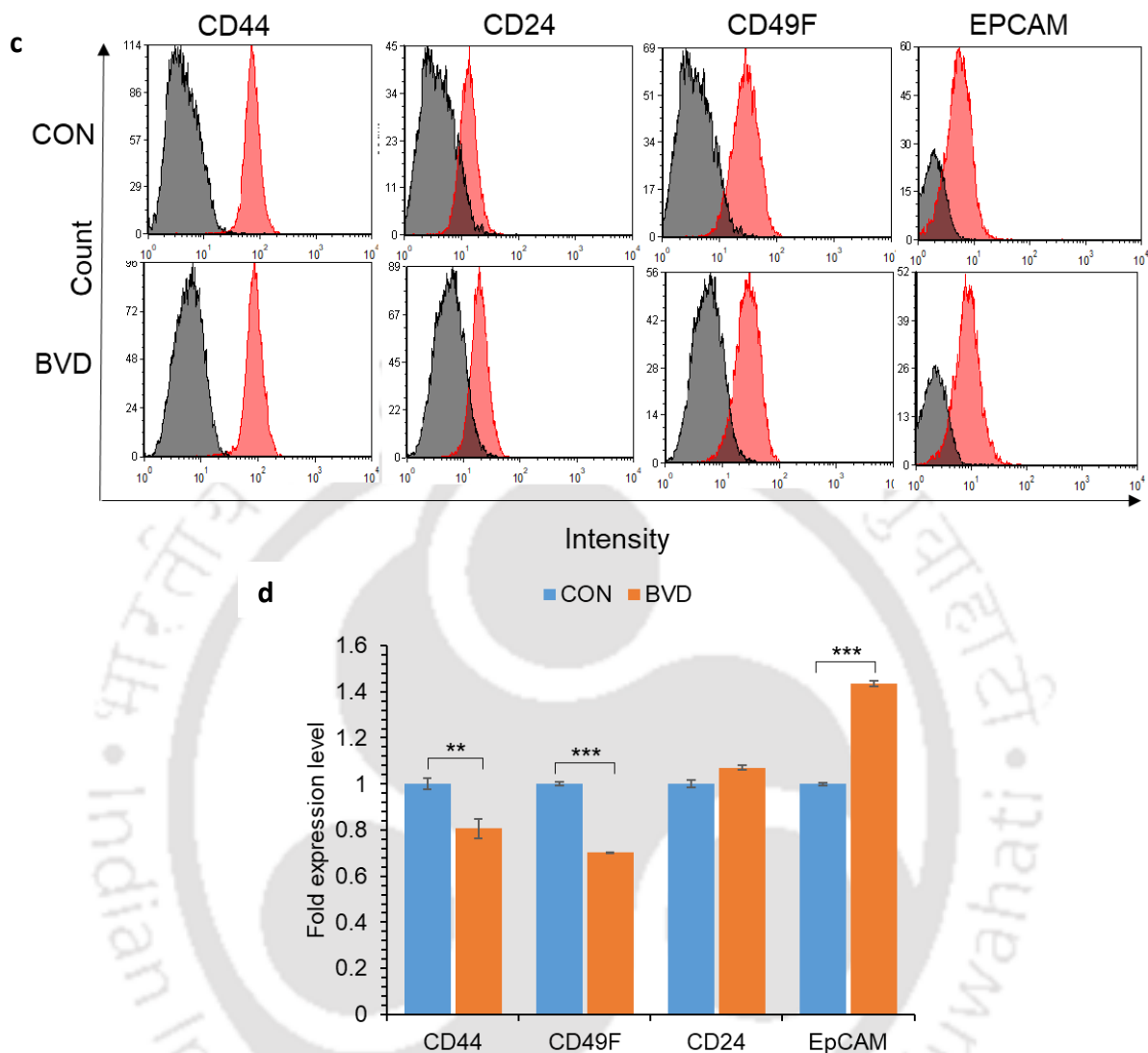


Fig.4.2.4 Effect of ERK1/2 inhibition on self-renewal ability Colony formation assay showed a significant decrease in the self-renewal ability of both **a)** MCF7 and **b)** MDA-MB- 231 cells after BVD-523 treatment. The number of colonies as well as area of the colonies reduced after 48 hours and furthermore in case of 12 days of continuous treatment, implying BVD-523 was effective in reducing the self-renewal ability as well as proliferation of the breast cancer cells. Effect of ERK1/2 inhibition on cell surface marker expression was observed in **c)** Representative flow cytometry histogram plots of MDA-MB-231 cells. **d)** MDA-MB231 cells showed a significant decrease in stemness markers CD44 and CD49f, but a significant increase in Ep-CAM upon treatment with BVD as compared to untreated (CON) cells; *p < 0.05, **p < 0.005, *** p < 0.0005.

To understand whether ERK1/2 inhibition through BVD treatment could impair the migration ability of breast cancer cells, wound healing migration assay was performed. A wound was created in the cell monolayer and BVD was added to the cells and the cells were allowed to migrate and the cells were documented periodically. BVD treatment had a moderate effect on inhibiting the migration of both MCF7 and MDA-MB-231 cells (**Fig.4.2.5a-b**).

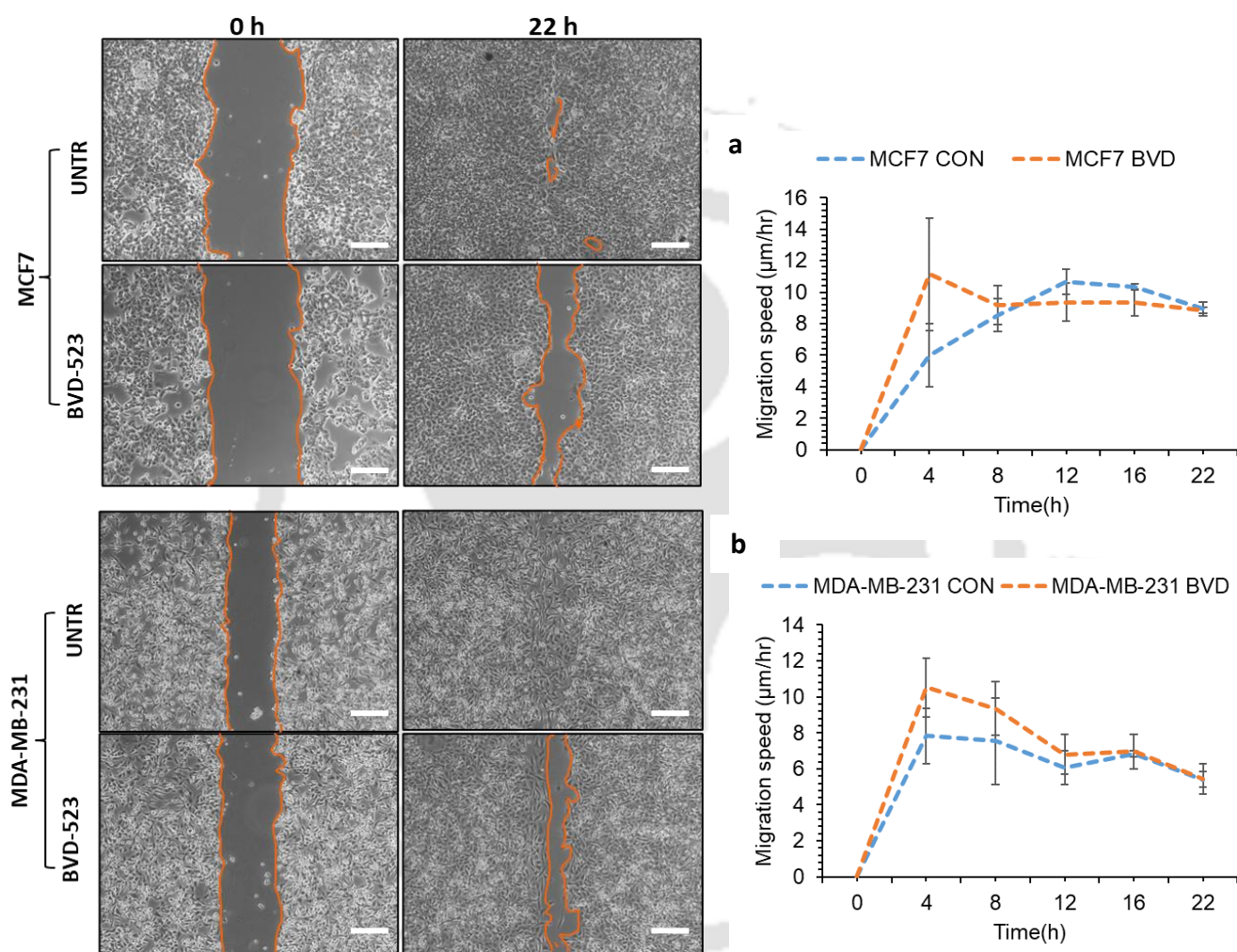


Fig.4.2.5 Effect of ERK1/2 inhibition on migration Wound healing assay showed a decrease in the migration of both **a**) MCF7 cells and **b**) MDA-MB-231 after BVD-523 treatment. Images were taken at 5X magnification. Percentage of open image area was calculated in comparison to untreated (CON) cells.

BVD-523 effectively inhibited proliferation and migration of both MCF7 and MDA-MB-231 cells. Both the cell lines showed a significant dose-dependent decrease in cell number. PI-stained MDA-MB-231 cells showed ~20% reduction in cell viability upon treatment with BVD. In addition to this, cell cycle analysis of the breast cancer cells showed accumulation of greater percentage of cells in G1 phase followed by simultaneous reduction in S- phase and G2/Mphase suggesting cell cycle arrest and growth inhibition upon treatment of breast cancer cells with BVD in-vitro. In line with these data, marked inhibition of spheroid growth rate upon BVD treatment was observed. BVD treatment of either cell type for 48 hours or continuous treatment for a period of twelve days, showed a significant reduction in the number and area of the colonies compared to the control cells. BVD treated MDA-MB-231 cells showed significant downregulation in expression of CD44 and CD49F and increased expression of CD24 and EpCAM. These indicate an effective role of ERK signaling in regulating cell behaviour in different subtypes of breast cancer and how different ERK1/2 specific inhibitors can be further developed as a good therapeutic option.

4.3 Effect of PIEZO1 activation by chemical agonist Yoda1 in breast cancer cells

During cancer progression, the cells in the tumor are subjected to crowding and extensive mechanical stress. Studies have reported that the stiffness of the breast tumor increases as the cancer progresses [111]. The mechanical stress experienced by the cancer cells activate the mechanosensors which in turn activate several signaling pathways and cancer associated gene expression. PIEZO-type mechanosensitive ion channel component 1 (PIEZO1) is a mechanosensitive ion channel involved in regulating survival, proliferation and migration of cancer cells. Several studies have shown that PIEZO1 plays an important role in cancer progression. A dual role for PIEZO1 is reported in the literature where the activation of PIEZO1 at lower cell density promotes proliferation whereas at higher density. It induces cell death in epithelial cells. The mechanosensitive cation channel protein PIEZO1 is expressed in breast cancer cells and are necessary to sense the mechanical properties of the tissue. Mechanosensing is an important step during metastasis and interrupting the mechanosensing ability of cancer cells might have therapeutic benefits for the treatment of metastatic cancers.

To understand the role of PIEZO1 in breast cancer progression, the PIEZO1 channel was activated by using the chemical agonist YODA1 (YODA) and inhibited with the antagonist DOOKU1 (DOOKU). Previous studies have reported that DOOKU1 competitively inhibits PIEZO1 activation by YODA1. Firstly, the optimum concentration of YODA1 and DOOKU1 was determined by treating both MCF7 (**Fig.4.3.1a**) and MDA-MB-231(**Fig.4.3.1b**) with either YODA1 or DOOKU1 or in combination with a concentration ranging from 0.01 to 20 μM . The cell viability was not significantly affected in both MCF7 and MDA-MB-231(**Fig.4.3.1c**), however, proliferation of the cells was significantly inhibited with increasing concentrations of YODA1. No significant effect on viability or proliferation was observed upon treatment with YODA1 and DOOKU1 failed to reverse the inhibitory effects observed with YODA1 treatment. Treatment with either YODA1 or DOOKU1 did not affect the morphology of MCF7 cells whereas MDA-MB-231 cells assumed more spindle shaped morphology upon treatment with YODA1 alone or in combination of YODA1 and DOOKU1 (Y+D) (**Fig.4.3.1d**). To understand whether YODA1 treatment affects the calcium flux, which measures the PIEZO1 channel activity, the calcium flux in the presence of YODA or Y+D was determined. While YODA increased the

calcium flux, DOOKU failed to inhibit the increased calcium flux, on the contrary, DOOKU in combination with YODA further increased the calcium flux in MCF7 cells.

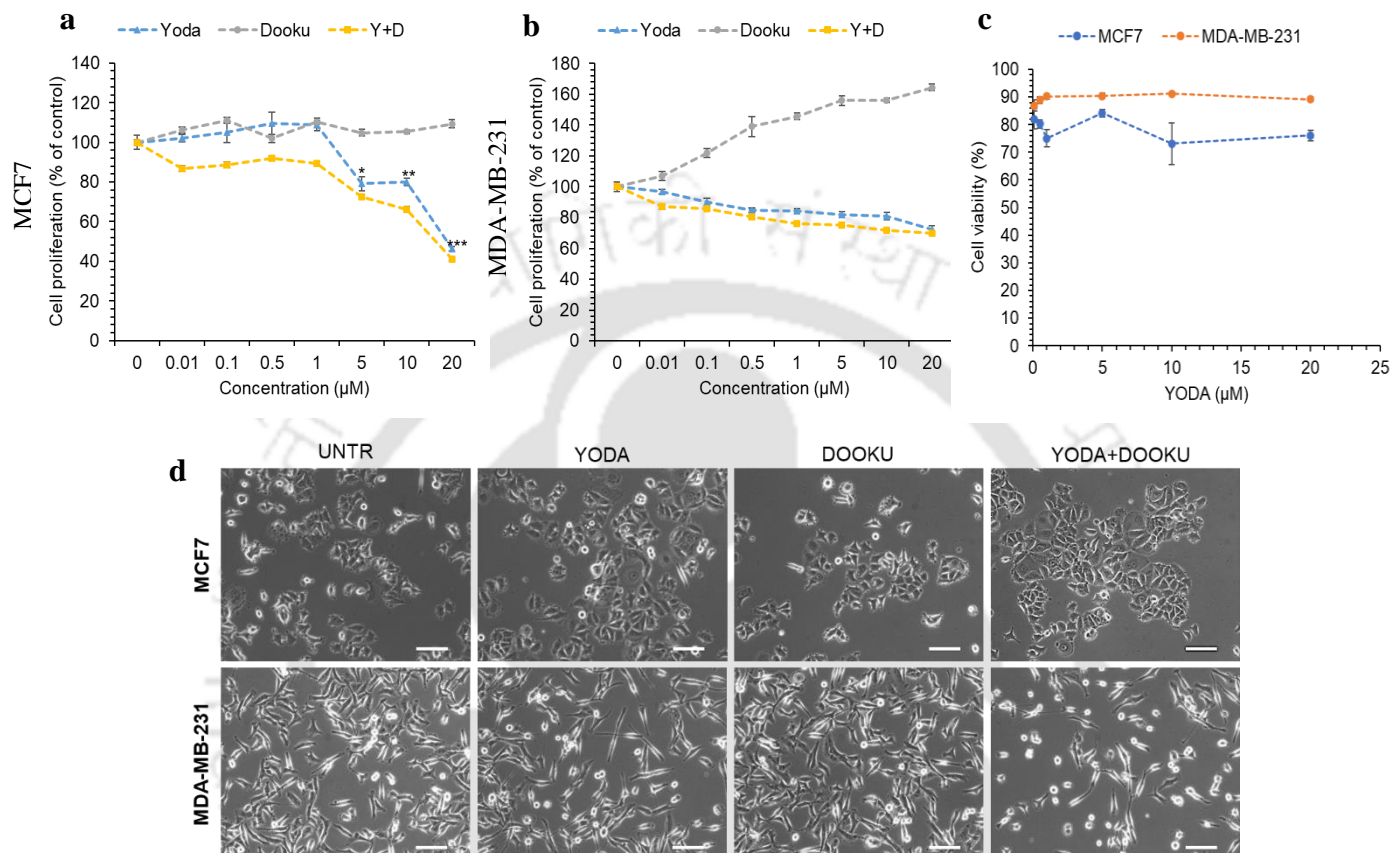
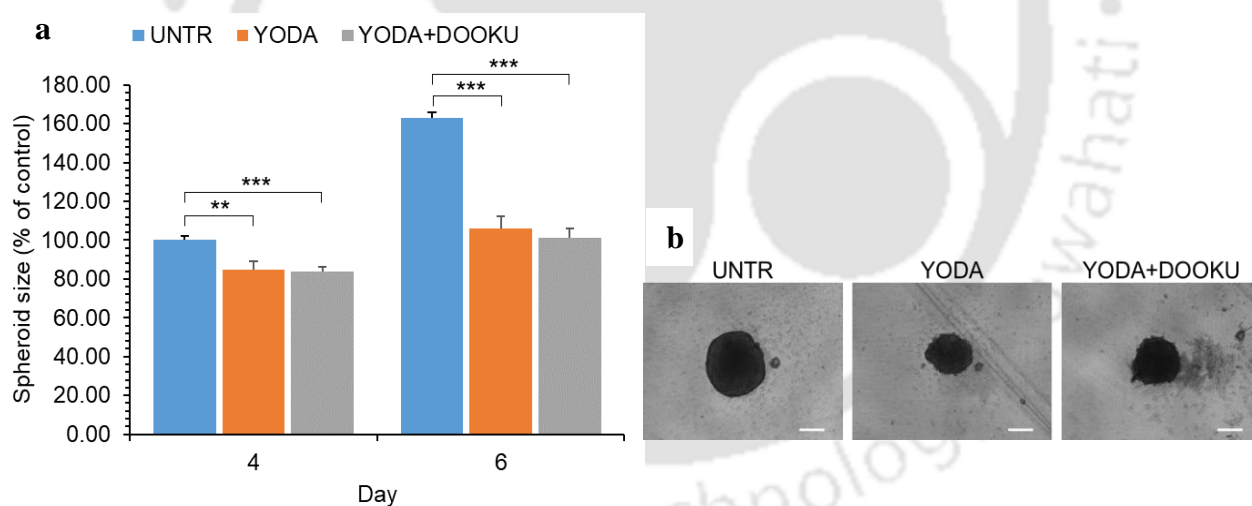


Fig.4.3.1 Effect of PIEZO1 activation on proliferation of breast cancer cells (a) MCF7 and **(b)** MDA-MB-231 cells were treated with different concentrations of Yoda1, Dooku1 and Yoda+Dooku (Y+D) in combination and the effect on proliferation was determined by cell counting **(a-b)** and survival was determined by propidium iodide (PI) staining through flow cytometry. **(c)** MCF7 and MDA-MB-231 cells were treated with concentrations ranging from 0.01 µM to 20 µM as indicated and live cell percentage was determined by PI staining through flow-cytometry. **(d)** Microscopic morphology images of MCF7 and MDA-MB-231 cells left untreated (UNTR) and treated with Yoda or Dooku. Values are mean ± SD, $n = 3$ independent experiments, * $p < 0.05$, ** $p < 0.005$, *** $p < 0.0005$

The effect on YODA1 in inhibiting the proliferation of MCF7 was also observed when MCF7 were grown as 3D spheroids in the presence of YODA or YODA+DOOOKU (**Fig.4.3.2a-b**). However, either YODA or DOOKU treatment did not significantly affect the 3D growth of MDA-MB-231 cells. Further the colony-forming ability of MCF7 and MDA-MB-231 cells were significantly inhibited when they were treated with either YODA or YODA+DOOKU continuously for a period of 10-14 day. However, pre-treatment of the cells during initial 48 hr of colony formation did not affect the colony forming ability of MCF7 cells but YODA treatment resulted in a moderate inhibition of colony formation ability of the cells. While pre-treatment and continuous treatment of MCF7 cells with either YODA or YODA+DOOKU resulted in cells forming significantly smaller colonies, the colony size was not affected when MDA-MB-231 cells treated continuously. However, pre-treatment with YODA+DOOKU resulted in MDA-MB-231 cells forming smaller colonies compared to control, or DOOKU treated conditions. (**Fig.4.3.2c-e**).



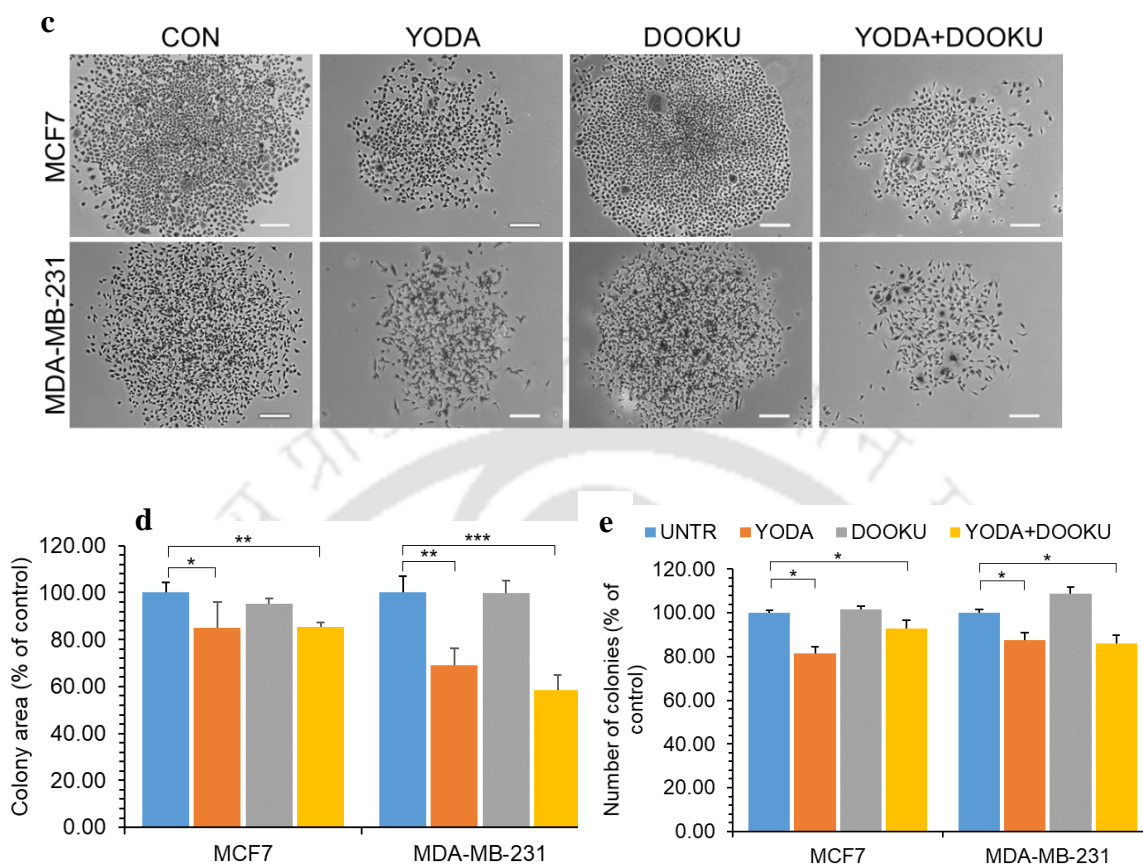
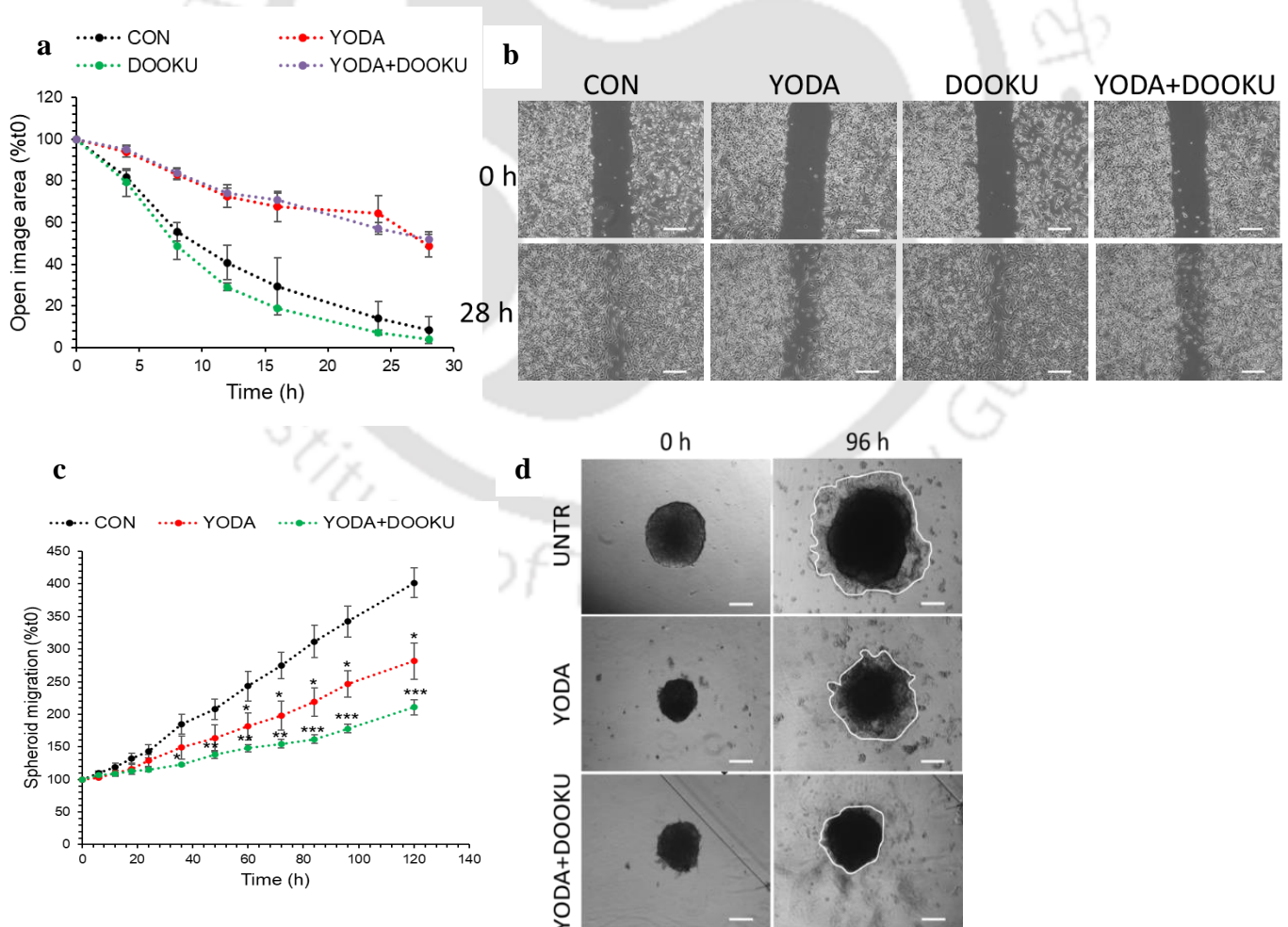


Fig.4.3.2 Effect of PIEZO1 activation on proliferation and self-renewal in breast cancer Spheroid area analysis of MCF7 cells with Yoda treatment and Yoda Dooku combination treatment for 6days is shown. **(a)** Representative images of MCF7 cells showing spheroid growth area analysis. **(b)** MDA-MB-231 and MCF7 cells were left untreated (CON) or were treated with Yoda1(YODA) Dooku1(DOOKU) or Yoda1 Dooku1 combination (YODA+DOOKU) for 10 days and clonogenic assay was performed **(d-e)**. The percentage of colony area of the treated conditions with respect to the control cells is shown. **(c)** Representative images showing colonies after Yoda and Dooku treatment of MCF7 and MDA-MB-231 cells. Values are mean \pm SD, $n = 3$ * $p < 0.05$, ** $p < 0.005$, *** $p < 0.0005$.

Since PIEZO1 senses the mechanical properties of the microenvironment and can modulate the migration and invasion of the cancer cells, the migration of MCF7 and MDA-MB-231 cells in the presence of YODA or YODA+DOOKU was determined (Fig 3a-d). PIEZO1 activation through YODA treatment significantly inhibited the invasion of MCF7 into collagen matrix (**Fig.4.3.3a-b**) and migration of MDA-MB-231 (**Fig.4.3.3c-d**) in a wound healing assay. As observed with colony formation or proliferation, DOOKU treatment did not produce any effect on migration when treated alone but inhibited migration when treated with YODA (YODA+DOOKU). YODA-treated MCF7 cells showed a significant downregulation of EMT associated gene SNAI2. However, YODA treatment also resulted in significant downregulation of CDH1, which is associated with low migratory phenotype. YODA/DOOKU treated MCF7 cells showed a similar mRNA expression of CD44, ALDH1A3, RAC1 and RHOA as control cells (**Fig.4.3.3e**).



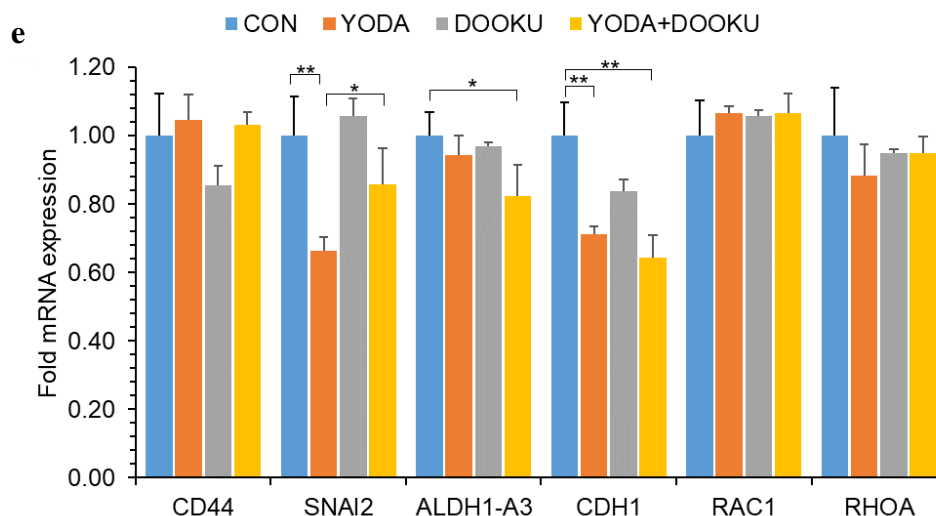


Fig.4.3.3 Effect of PIEZO1 activation on migration and invasion in breast cancer (a-b) MDA-MB-231 cells were subjected to wound healing assay in monolayer culture with a manually made scratch(2D) during treatment with Yoda1(YODA), Dooku1(Dooku) and Yoda1+Dooku1combination (YODA+DOOKU) and migration speed was calculated and compared with untreated control (CON) cells. **(b)** Representative images of wound healing migration assay are shown. **(c-d)** 3D spheroid migration was performed with MCF7 cells on collagen (50 μ g/ml) coated wells during treatment with Yoda1(YODA), Yoda1+Dooku1(YODA+DOOKU) and untreated (CON) conditions. Migration of the cells out of spheroid was documented at regular intervals and the migrated area was normalized to the spheroid area at $t = 0$. The migration areas at different time points are shown in the representative images. Values are mean \pm SD, $n = 3-6$. **(e)** q-PCR analysis of migration related genes in MCF7 cells with Yoda1, Dooku1 and Yoda+Dooku treatment along with control cells is represented graphically. Values are mean \pm SD, $n = 3$ independent samples, * $p < 0.05$, ** $p < 0.005$, *** $p < 0.0005$.

The effect of PIEZO1 activation on anoikis resistance was determined in MCF7 and MDA-MB-231 cells where the cells were culture in the presence of YODA, DOOKU or YODA+DOOKU conditions in the anoikis culture. The cells after anoikis culture were assessed for the colony formation ability. The treatment with YODA, DOOKU or YODA+DOOKU was continued while the cells were seeded for colony formation or grown in the normal growth media. In all the different conditions, treatment with YODA alone or in combination with DOOKU (YODA+DOOKU) resulted in the formation of fewer and smaller colonies in both MCF7 and MDA-MB-231 cells. Treatment with DOOKU alone did not change the colony formation ability in terms of the size or the number of colonies formed. In order to understand the mechanism of growth arrest induced by YODA1, cell cycle analysis was performed for YODA/DOOKU-treated MCF7 and MDA-MB-

231(**Fig.4.3.4a-b**). MDA-MB-231 cells treated with YODA or DOOKU alone exhibited a similar cell cycle profile as control cells. However, when YODA and DOOKU were added together, MDA-MB-231 cells showed a 20% increase in percentage of cells in G0/G1 phase ($p=0.01$) and a decrease in S-phase population indicating a growth arrest in G0/G1 phase. YODA-treated MCF7 cells saw a marginal 10% decrease in G0/G1-phase fraction ($p=0.02$) and a concomitant increase in S-phase population ($p=0.04$) compared to control cells. Treatment with DOOKU did not significantly affect the distribution of cells in different phases, albeit the statistical significance of the difference obtained with YODA treatment was lost when DOOKU was added in combination. Considering the growth inhibitory effect of YODA on MCF7, the higher proportion of cells in S-phase in YODA-treated MCF7 cells hints at S-phase arrest. To further elucidate the molecular basis of growth difference observed in YODA/DOOKU treated MCF7, mRNA expression levels of cell cycle related genes was evaluated by qPCR (**Fig.4.3.4c**). YODA-treated MCF7 cells showed a 20% reduction in CCND1 expression ($p<0.05$), with no significant difference in the expression of CCNE2. YODA-treated MCF7 cells also showed a 25% reduction in the expression of cell cyclin inhibitor CDKN1A ($p<0.0005$). Treatment with DOOKU did not show any significant effect on the expression of CCND1 and CCNE2 as the expression levels of DOOKU-treated MCF7 were similar to control cells and YODA+DOOKU-treated cells were similar to YODA-treated cells. However, YODA+DOOKU-treated MCF7 cells had a higher expression of CDKN1A ($p<0.05$) than YODA-treated cells. The effect of YODA/DOOKU treatment on the stemness-related genes was further studied for MCF7 cells (**Fig.4.3.4d**). YODA-treated MCF7 cells showed a significant upregulation of NANOG and OCT4 ($p<0.05$), and this increase in expression was also observed in YODA+DOOKU condition but statistical significance was not achieved. A similar expression level of SOX2, ID1 and ID2 was observed across all treatment conditions, which may indicate that Yoda might help the cells to achieve quiescence and this property of stemness might be correlated with upregulation of NANOG and OCT4. This is in line with the reduced proliferation of cells and cell cycle arrest upon Yoda treatment of MCF7 cells. YODA or DOOKU treatment alone did not affect the ID4 expression, however, their combination produced a statistically significant increase in ID4 expression, indicating that YODA and DOOKU can act synergistically to affect expression of some genes.

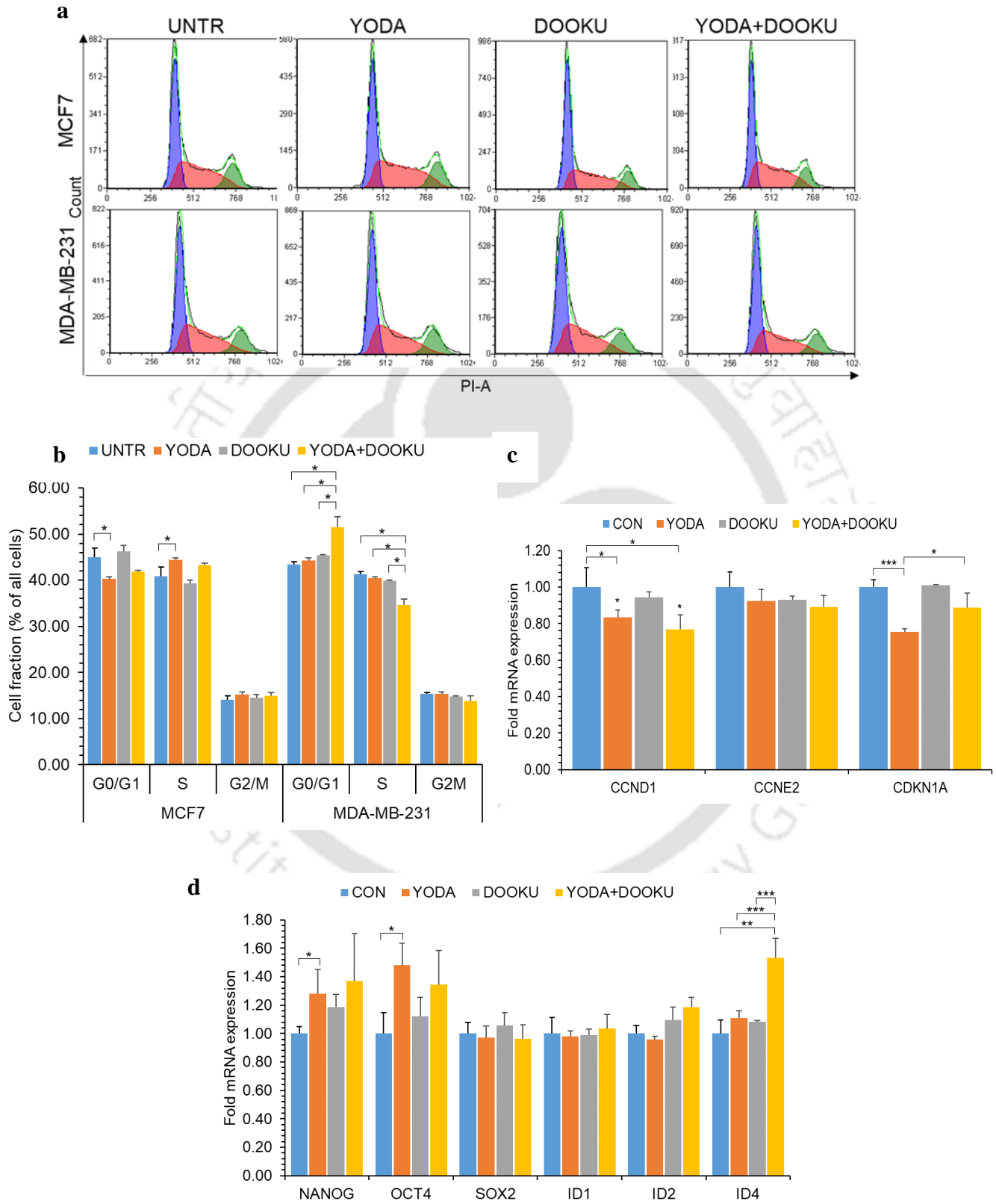
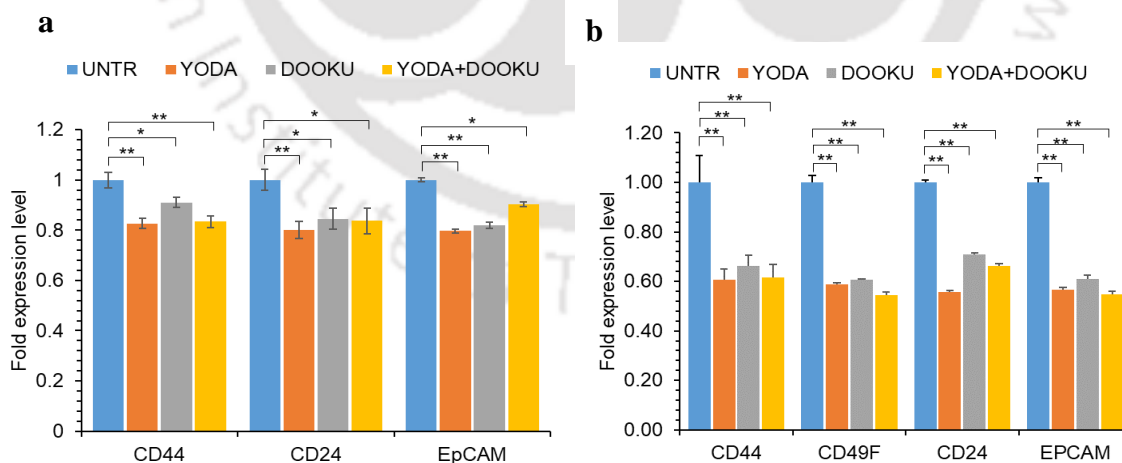


Fig.4.3.4 Effect of PIEZO1 activation on cell cycle and expression of proliferation genes in breast cancer MDA-MB-231 and MCF7 (a-b) cells were left untreated (CON) or were treated with Yoda, Dooku and combination Yoda+Dooku (10 μ M) for 48 h and the cell cycle profiles were analyzed by flow cytometry. **(a)** Represents flow cytometric histogram plots and **(b)** represents graphical analysis of percentage cell fraction in different phases of cell cycle for different conditions for both MCF7 and MDA-MB-231 cells. **(c)** Gene expression changes of cell cycle related genes due to Yoda or Dooku treatments were determined by expression levels of represented genes through real-time PCR in MCF7 cells left untreated (CON) or treated with YODA/DOOKU/YODA+DOOKU for 24 h. Expression levels were normalized to the respective GAPDH levels, and fold change with respect to the control untreated cells were determined. **(d)** Gene expression changes of stem cell markers due to Yoda1 and Dooku1 treatment was determined by expression levels of represented genes through real-time PCR in MCF7 cells left untreated (CON) or treated with EGF and sorafenib (SORA) for 24 h. Expression levels were normalized to the respective GAPDH levels and fold change with respect to the control untreated cells were determined. Values are mean \pm SE, $n = 3$, * $p < 0.05$, ** $p < 0.005$, *** $p < 0.0005$.

The expression of stemness markers was evaluated in YODA/DOOKU-treated MCF7(**Fig.4.3.5a**) and MDA-MB-231(**Fig.4.3.5b**) by flow cytometry. Both cell lines showed a significant downregulation of CD24, CD44 and EPCAM upon treatment with YODA/DOOKU or their combination. Furthermore, MDA-MB-231 also showed a drastic reduction in expression of CD49F when treated with either YODA, DOOKU or their combination.



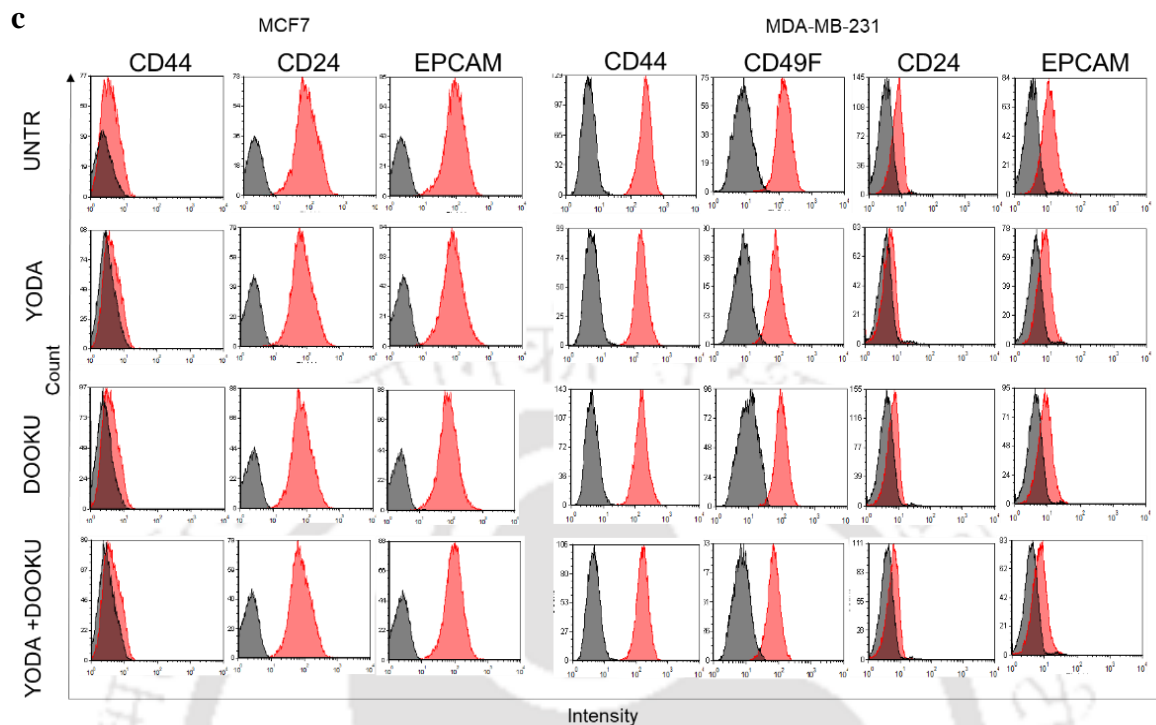


Fig.4.3.5 Effect of PIEZO1 activation on stemness in breast cancer (a) Fold expression levels of stemness markers in MCF7 and (b) MDA-MB-231 cells, treated with Yoda1 and Dooku1 at 10 μ M for 48h, are determined by flow cytometry. (c) Representative histogram plots of MCF7 and MDA-MB-231 cells expressing different stemness markers are shown. Values are mean \pm SE, $n = 3$, * $p < 0.05$, ** $p < 0.005$, *** $p < 0.0005$

PIEZO1 activation can induce intracellular ROS accumulation in different cell types like cardiomyocytes and stem cells [112], [113], [114]. Mitochondrial superoxide is a source of ROS generation and oxidative damage which can hamper the normal cellular processes [115]. The mitochondrial superoxide levels in YODA-treated breast cancer cells were quantified by MitoSOX staining of the cells (**Fig.4.3.6**). While, MDA-MB-231 cells treated with YODA or DOOKU alone showed similar percentage of MitoSOX positive cells as non-treated cells; MDA-MB-231 cells treated with combination of YODA and DOOKU showed a two-fold ($p < 0.0005$) increase in MitoSOX positive fraction compared to control cells. MCF7 cells showed a significant increase in percentage of MitoSOX positive cells up on treatment with YODA ($p < 0.005$), with an even higher increase for DOOKU-treated cells ($p < 0.05$). Similar to MDA-MB-231 cells, MCF7 cells treated with combination of YODA and DOOKU showed a two-fold increase ($p < 0.0005$) in the

percentage of MitoSOX-positive cells compared to non-treated cells, which was highest among all conditions. These results indicate that Yoda1-induced PIEZO1 activation can induce ROS damage in breast cancer cells and the role of DOOKU as a YODA-antagonist needs to be reevaluated.

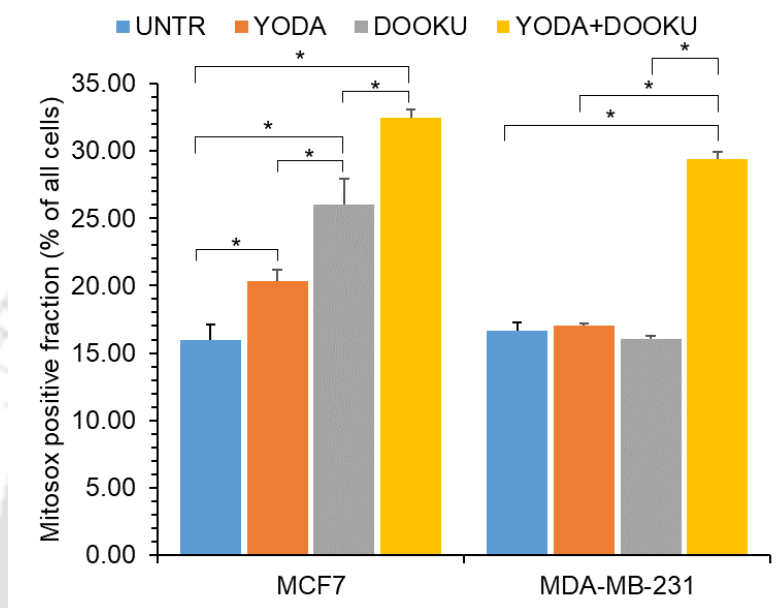


Fig.4.3.6 Effect of PIEZO1 activation on mitochondrial ROS generation in breast cancer Percentage of cells containing mitochondrial superoxide, in Yoda1(YODA), Dooku1(DOOKU), Yoda1+Dooku1(YODA+DOOKU) at 10 μ M concentration for each, in case of treated, and untreated (CON) MDA-MB-231 and MCF7 cells were assessed by staining the cells with MitoSOX and quantified by flow cytometry. Values are mean \pm SD, $n = 3$, $*p < 0.05$.

PIEZO1 activation is known to modulate ERK phosphorylation in several cell types. The effect of Yoda-induced PIEZO1 activation on the phosphorylation of ERK1/2 in MCF7 and MDA-MB-231 was assessed by immune-blotting (**Fig.4.3.7a-d**). Both MCF7(**4.3.7a-b**) and MDA-MB-231 cells (**4.3.7c-d**) treated with Yoda (Y) for 48 hours showed a significant upregulation of p-ERK1/2 levels compared to control cells. While, Dooku-treatment(D) did not show any significant effect on ERK1/2 phosphorylation in MDA-MB-231 cells, alone or in combination with Yoda; MCF7 cells showed marginally higher p-ERK1/2 level in Dooku than untreated (Untr) and Yoda+Dooku (Y+D)-treated condition than only Yoda-treated condition respectively, albeit the difference did

not attain statistical significance. Furthermore, Yoda-treated cells also showed alterations in the expression of key pathway proteins involved in proliferation and migration of cells. Yoda-treatment significantly reduced the expression of RHOA in both MCF7 and MDA-MB-231 cells, which could not be rescued by Dooku. Treatment of MDA-MB-231 cells either with Yoda or Dooku showed a significant reduction in the expression of β -catenin, and their combination showed a marginal additive effect. Since, Yoda-treated MCF7 cells showed a marked reduction in mRNA expression of CDH1 (E-CAD) despite reduction in their migratory potential, the effect of Yoda-treatment on E-CAD protein expression was evaluated. Yoda-treated MCF7 showed a significant reduction in expression of E-CAD compared to non-treated cells, whereas, treatment with Dooku did not show any significant effect on E-CAD expression.

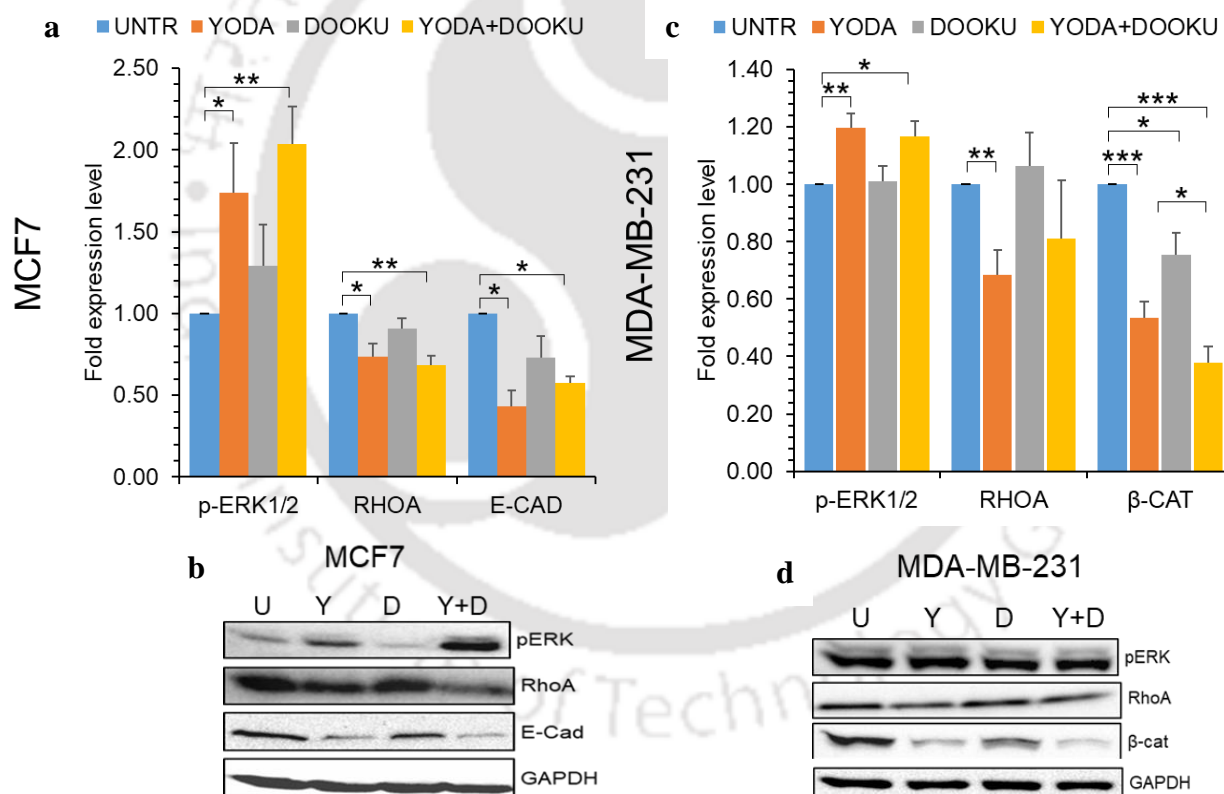
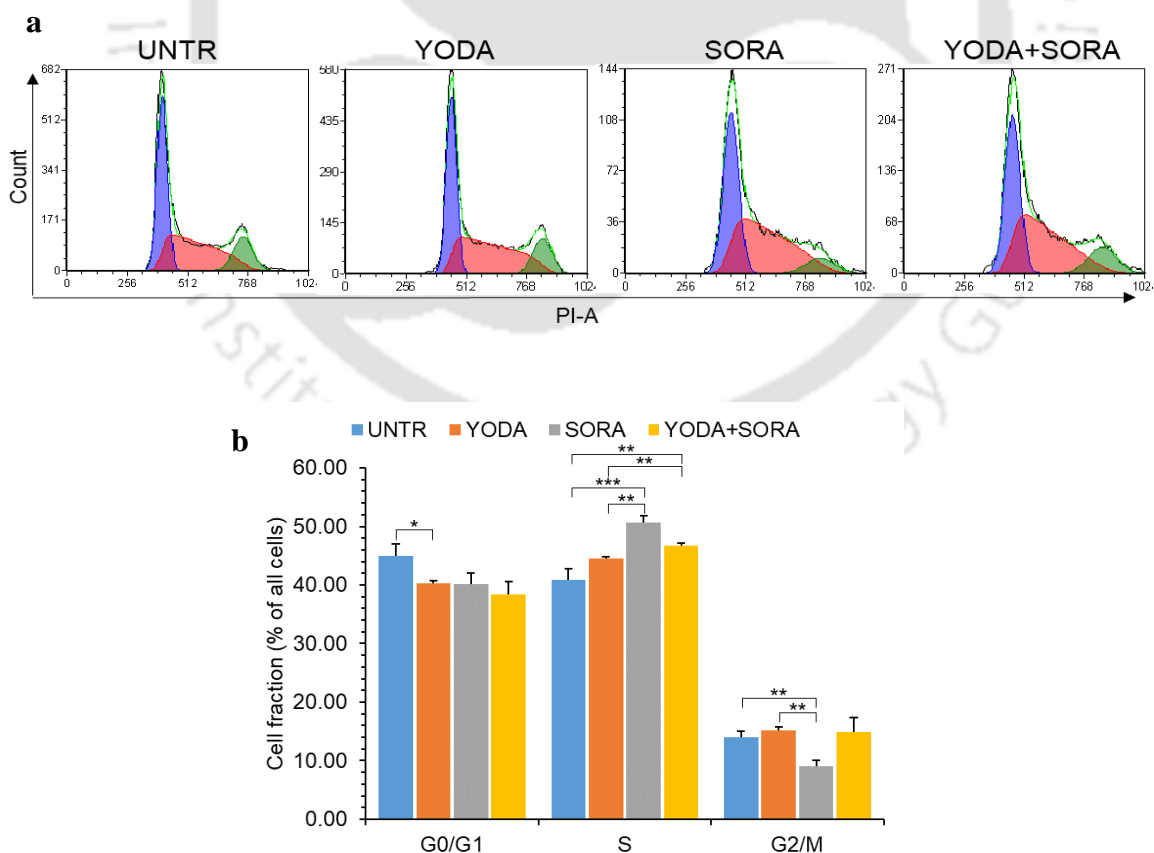


Fig.4.3.7 Effect of PIEZO1 activation on signaling pathways in breast cancer Phospho-ERK1/ERK2 (Thr185, Tyr187), Rho-A and E-cadherin in MCF7(**a-b**) and β -catenin along with phospho-ERK and Rho-A in MDA-MB-231 cells (**b-c**), left untreated (U) or after treatment with Yoda1(Y)/Doku1(D)/Yoda1+Dooku1(Y+D) for 48 h was determined by immunoblotting. Expression was normalized to GAPDH expression levels in each sample. Values are mean \pm SD, $n = 3$, * $p < 0.05$, ** $p < 0.005$, *** $p < 0.0005$.

Previous studies have suggested that PIEZO1 activation through YODA1 treatment modulates ERK signaling pathway in several cell types. Raf kinase inhibitor, Sorafenib showed reduced efficacy on stiffer microenvironments, rich in collagen [1]. Considering the effect of YODA-induced PIEZO1 activation on the ERK-phosphorylation in breast cancer cells, the role of PIEZO1 activation in mediating the Sorafenib-sensitivity of MCF7 and MDA-MB-231 cells was assessed. MCF7 and MDA-MB-231 cells were subjected to colony formation assay (**Fig.4.3.8c-d**) under treatment with YODA/SORA or their combination. In case of MDA-MB-231 cells, addition of YODA did not affect their response to SORA treatment, as indicated by similar reduction of colony size in SORA and SORA+YODA condition compared to control cells. Whereas, MCF7 cells treated with combination of YODA and SORA produced significantly larger colonies than SORA-treated MCF7 cells. Cell cycle analysis of MCF7 cells (**Fig.4.3.8a-b**) treated with YODA/SORA or their combination revealed that addition of YODA could rescue the G2/M population abrogated by SORA treatment. Together these results indicate that PIEZO1-activation may impart resistance against the action of sorafenib in some subtypes of breast cancer.



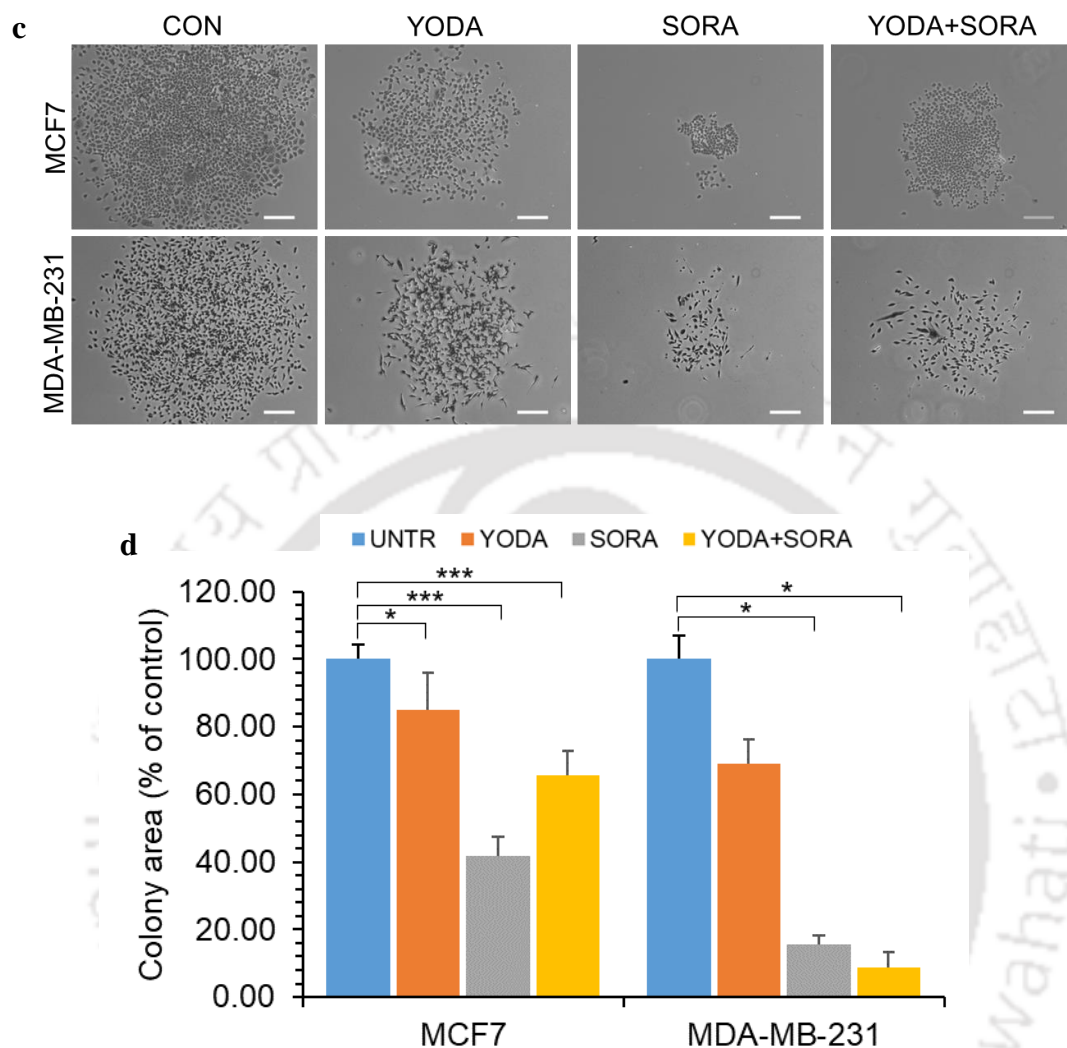


Fig.4.3.8 Effect of PIEZO1 activation on cellular self-renewal ability and growth progression in breast cancer MCF7 (a-b) cells were left untreated (CON) or were treated with Yoda1(YODA) Sorafenib (SORA) or Yoda1 Sorafenib combination (YODA+SORA) for 48 h and cell cycle was analyzed by flow cytometry. (a) Representative histogram plots showing G0/G1, S and G2/M phases of cell cycle in MCF7. (c-d) MDA-MB-231 and MCF7 cells were left untreated (CON) or were treated with Yoda1(YODA) Sorafenib (SORA) or Yoda1 Sorafenib combination (YODA+SORA) for 48 h and clonogenic assay was performed. The percentage of colony area of the treated conditions with respect to the control cells is shown. (c) Representative images showing colonies after Yoda and Sorafenib treatment of MCF7 and MDA-MB-231 cells. Values are mean \pm SD, $n = 3$ * $p < 0.05$, ** $p < 0.005$, *** $p < 0.0005$.

PIEZO1 activation by Yoda1 inhibits proliferation and induces cell cycle arrest in breast cancer cells with a rise in mitochondrial superoxide levels. Yoda1 effectively inhibited both 2D and 3D migration in breast cancer cells. Yoda1 treatment in MCF7 cells showed upregulation in Nanog and Oct4 indicating quiescence maintenance by breast cancer cells in line with inhibition on proliferation and inducing cell cycle arrest. Both MCF7 and MDA-MB-231 cells treated with Yoda for 48 hours showed a significant upregulation of p-ERK1/2 levels compared to control cells. Yoda-treatment significantly reduced the expression of RHOA in both MCF7 and MDA-MB-231 cells, which could not be rescued by Dooku. Treatment of MDA-MB-231 cells either with Yoda or Dooku showed a significant reduction in the expression of β -catenin, and their combination showed a marginal additive effect. Considering the effect of YODA-induced PIEZO1 activation on the ERK-phosphorylation in breast cancer cells, the role of PIEZO1 activation in mediating the Sorafenib-sensitivity of MCF7 and MDA-MB-231 cells was assessed. In case of MDA-MB-231 cells, addition of YODA did not affect their response to SORA treatment, as indicated by similar reduction of colony size in SORA and SORA+YODA condition compared to control cells. Whereas, MCF7 cells treated with combination of YODA and SORA produced significantly larger colonies than SORA-treated MCF7 cells. Cell cycle analysis of MCF7 cells treated with YODA/SORA or their combination revealed that addition of YODA could rescue the G2/M population abrogated by SORA treatment. Together these results indicate that PIEZO1-activation may impart resistance against the action of sorafenib in some subtypes of breast cancer. Thus it will be interesting to further study the role of PIEZO1 in regulating breast cancer cell proliferation, migration and stemness based on their subtypes.

4.4 Effect of PIEZO1 inhibition through PIEZO1 silencing in breast cancer cells

The studies with PIEZO1 activator Yoda1 showed that PIEZO1 activation leads to a reduction in migration and proliferation of breast cancer cells. Although Dooku1 was reported as a PIEZO1 inhibitor, as per the data shown in the previous section, Dooku1 failed to reverse the effects of Yoda1.

So, a different strategy was followed to downregulate PIEZO1 expression. For this, lentiviral-mediated gene silencing method was utilized to downregulate PIEZO1. The breast cancer cells MCF7 and MDA-MB-231 were transduced with lentiviral particles containing scramble sequence (Control) or shRNA against PIEZO1 (MCF7^{shPIEZO1}, MDA-MB-231^{shPIEZO1}) gene. The transduced cells were selected using the antibiotic selection marker, puromycin. The level of gene expression and the silencing of PIEZO1 was determined by real-time PCR and flow cytometry analysis and compared with the Control cells. A 10-fold decrease in the PIEZO1 mRNA levels was observed in MCF7^{shPIEZO1} cells compared to the control cells, and MDA-MB-231^{shPIEZO1} cells showed a 1.5 fold downregulation (**Fig.4.4.1a**). Flow cytometry analysis revealed that PIEZO1 expression was downregulated at the protein level in PIEZO1 silenced MCF7 and MDA-MB-231 cells (**Fig.4.4.1b**).

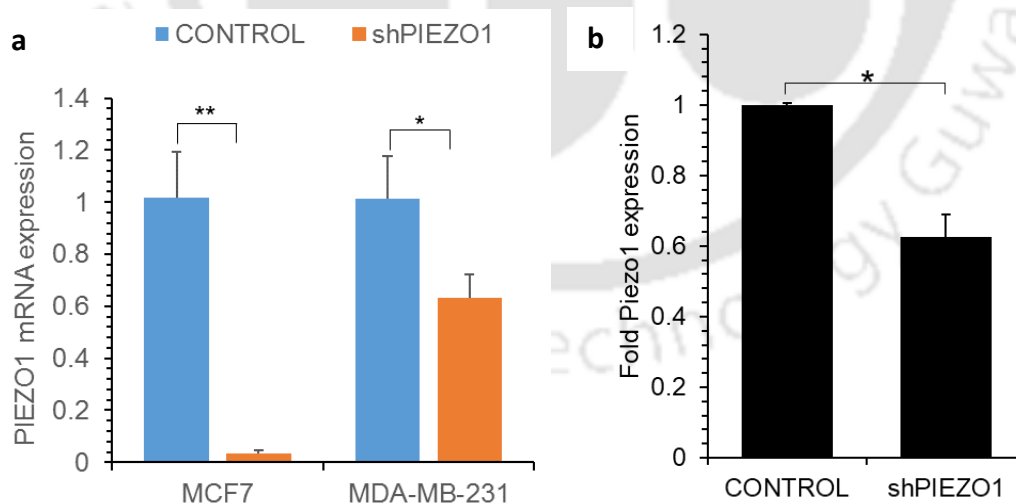


Fig.4.4.1. Lentiviral mediated gene silencing of PIEZO1 gene of breast cancer cells determined by real time PCR and flow cytometry. The expression of PIEZO1 m-RNA in PIEZO1 silenced MCF7 and MDA-MB-231 cells was determined with respect to control cells(a) by q-PCR. Fold expression of PIEZO1 protein in shPIEZO1 MCF7 cells was

determined by phospho-protein flow cytometry with respect to control cells**(b)**.

In order to understand whether the downregulation of PIEZO1 modified the activity of PIEZO1 channel in the breast cancer cells, a calcium flux assay was performed (**Fig.4.4.2**). The PIEZO1 channel agonist Yoda1 induced significant Ca^{2+} flux in control MCF7 cells; however, the Ca^{2+} flux was significantly downregulated in MCF7^{shPIEZO1} cells. Interestingly, uninduced MCF7^{shPIEZO1} cells showed higher Ca^{2+} flux compared to MCF7^{Control} cells which might be attributed to an increase in the expression of compensatory calcium ion channels, as reported earlier [116]. Thus, PIEZO1 silencing significantly downregulated PIEZO1 activity and its expression at mRNA and protein levels.

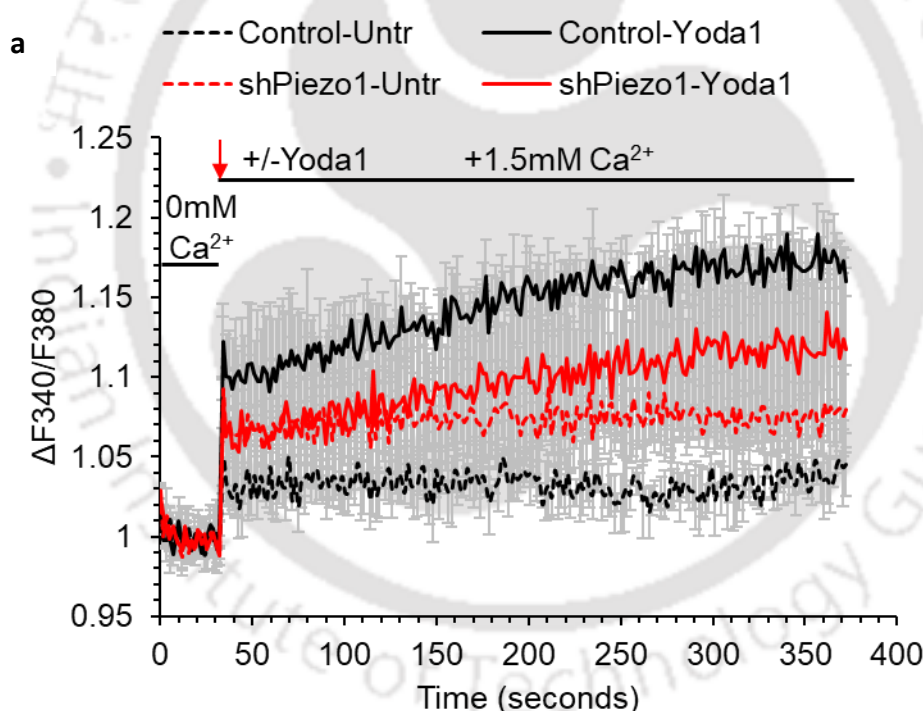


Fig.4.4.2. Effect of PIEZO1 silencing on intracellular Ca^{2+} influx of breast cancer cells. Calcium flux assay of shPIEZO1 and control MCF7 cells with and without Yoda1 treatment. **(a)**. The baseline signal was recorded by measuring the emission at 510nm after sequential excitations at 380nm and 340nm for 20 kinetic cycles with minimal time intervals using Tecan. The ratio of emission at 340nm (F_{340}) and 380nm (F_{380}) was calculated as indicator of intracellular Ca^{2+} concentration and the signal was recorded for another 200 cycles.

As a mechanosensitive protein, PIEZO1 can regulate the actin cytoskeleton to modify the cell structure [117], [118] and migration. For this, the morphology changes in PIEZO1 silenced MCF7 and MDA-MB-231 were analyzed microscopically (**Fig.4.4.3a**). No apparent changes in the morphology of breast cancer cells during PIEZO1 silencing were observed. To understand further, the arrangement of the actin cytoskeleton was determined in the MCF7^{shPIEZO1} and MDA-MB-231^{shPIEZO1} cells (**Fig.4.4.3b**). No significant changes were observed in the PIEZO1 silenced MCF7 cells; however, the F-actin arrangement was disrupted in MDA-MB-231^{shPIEZO1} cells. Whereas the control cells have actin-rich filopodia on the cell surface, the MDA-MB-231^{shPIEZO1} lack these filopodia-like structures in addition to the disruption of intracellular F-actin filaments.

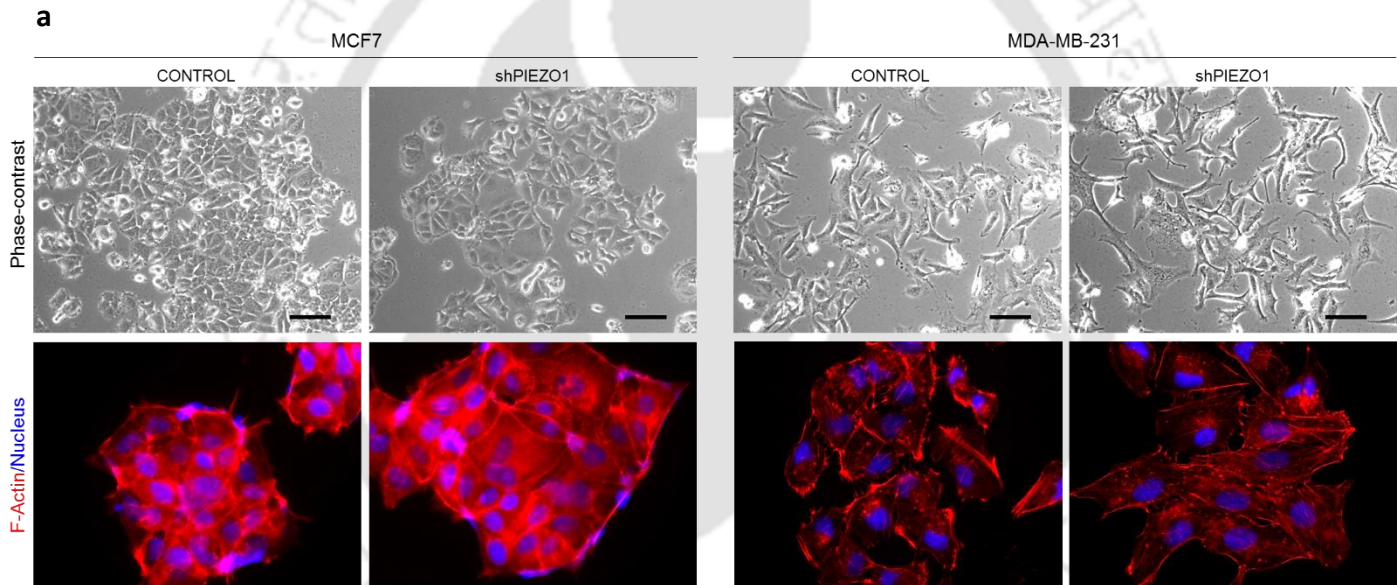
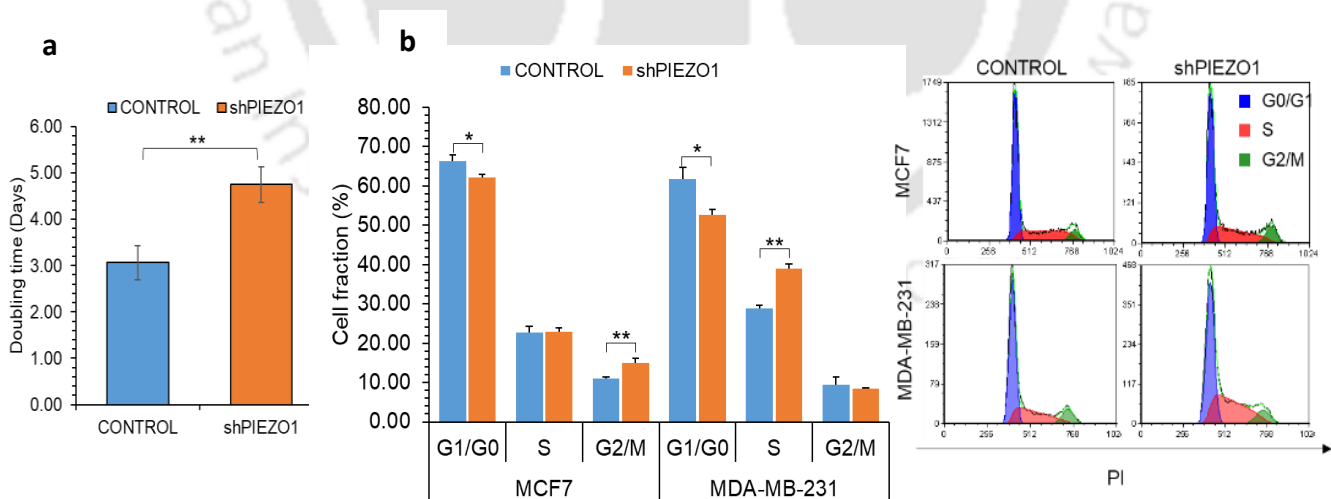


Fig.4.4.3. Effect of PIEZO1 silencing on cellular morphology and F-actin arrangement of breast cancer cells. Morphology changes in the silenced cells were analysed microscopically (**a**). Arrangement of actin cytoskeleton in MCF7^{shPIEZO1} and MDA-MB-231^{shPIEZO1} cells, was determined by immunocytochemistry (**b**).

In order to determine whether PIEZO1 plays a role in controlling the proliferation of breast cancer cells, the doubling time for the PIEZO1 silenced cells were analyzed. PIEZO1 significantly modified the cell proliferation where an increase in the doubling time was observed in MCF7^{shPIEZO1} cells compared to the control cells (**Fig.4.4.4a**). The increase in the doubling time was confirmed by cell cycle analysis, where the PIEZO1 silenced cells showed increased percentage of cells in G2/M stage suggesting a G2M arrest whereas an increase in proliferation accompanied by increased percentage of cells at the S phase was observed in MDA-MB-231^{shPIEZO1} compared to the control cells (**Fig.4.4.4b**). To confirm the changes in the proliferation and considering that the cancer cells grow as a tumor mass *in vivo*, the 3D growth of cells was analyzed in a spheroid assay. Control and PIEZO1 silenced cells were allowed to form 3D spheroids, and the proliferation of the cells as a spheroid was monitored periodically. As observed in the 2D growth, there was a significant reduction in the spheroid growth in MCF7^{shPIEZO1} cells compared to the control cells (**Fig.4.4.4c-d**). Yoda1 treatment significantly reduced the spheroid growth in control cells, whereas the spheroid size did not vary in MCF7^{shPIEZO1} cells, suggesting that when PIEZO1 was silenced, the effect of Yoda1 was no longer observed during the spheroid growth. In contrast, MDA-MB-231^{shPIEZO1} cells formed larger spheroids (**Fig.4.4.4c, e**) compared to the control cells.



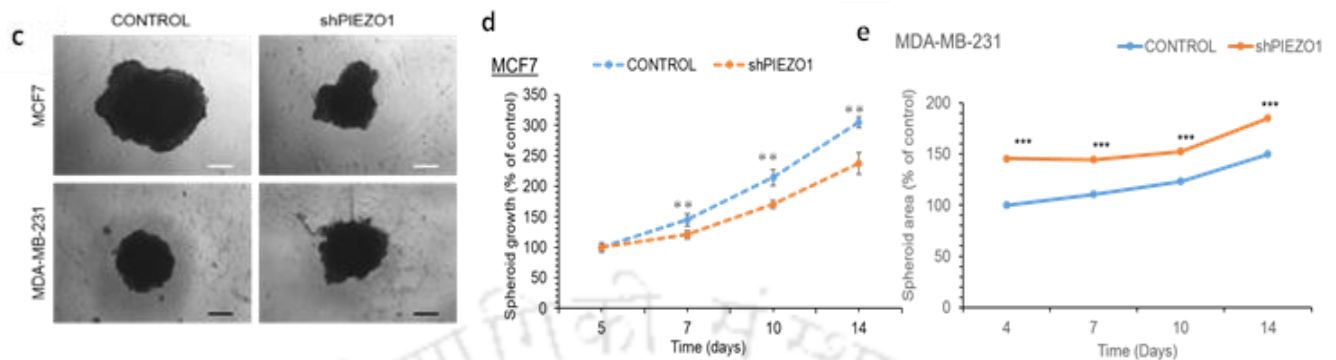
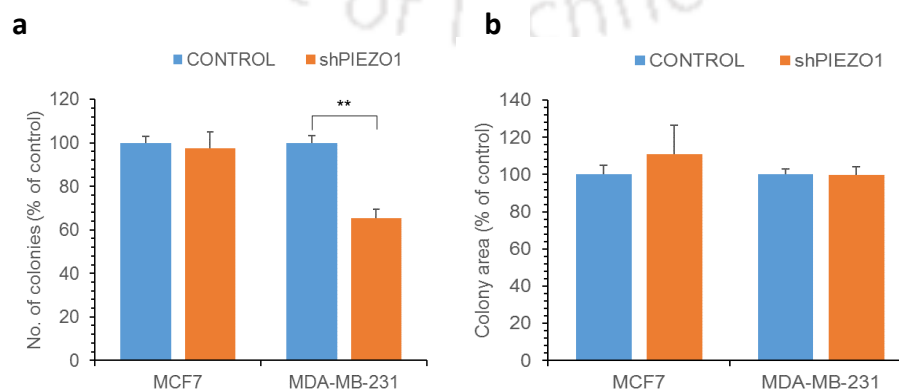


Fig.4.4.4. Effect of PIEZO1 silencing on the proliferation of breast cancer cells. The doubling time of MCF7 cells for control and shPIEZO1 conditions was determined (a). Cell cycle analysis was performed for both MCF7 and MDA-MB-231 cells (b). The proliferation of MCF7 (d) and MDA-MB-231(e) cells was further assayed by 3-dimensional spheroid growth over 14 days. Representative microscopic images of MCF7^{shPIEZO1} and MDA-MB-231^{shPIEZO1} cells, along with the control cells, are shown (c).

In order to understand the role of PIEZO1 in maintaining the self-renewal ability of breast cancer cells, a colony-formation assay was performed. Colony formation assay helps to determine the self-renewal ability of the cells and whether PIEZO1 modification leads to alteration in the self-renewal ability of these cells. Interestingly, PIEZO1 downregulation did not affect the self-renewal ability of MCF7 cells (Fig.4.4.5a, c); however, there was a significant reduction in the colony-forming ability of MDA-MB-231^{shPIEZO1} cells compared to the control cells (Fig.4.4.5a, d). This suggests that although PIEZO1 downregulation did not impact the proliferation greatly (Fig.4.4.5b), it plays a significant role in modulating the self-renewal ability of MDA-MB-231 cells.



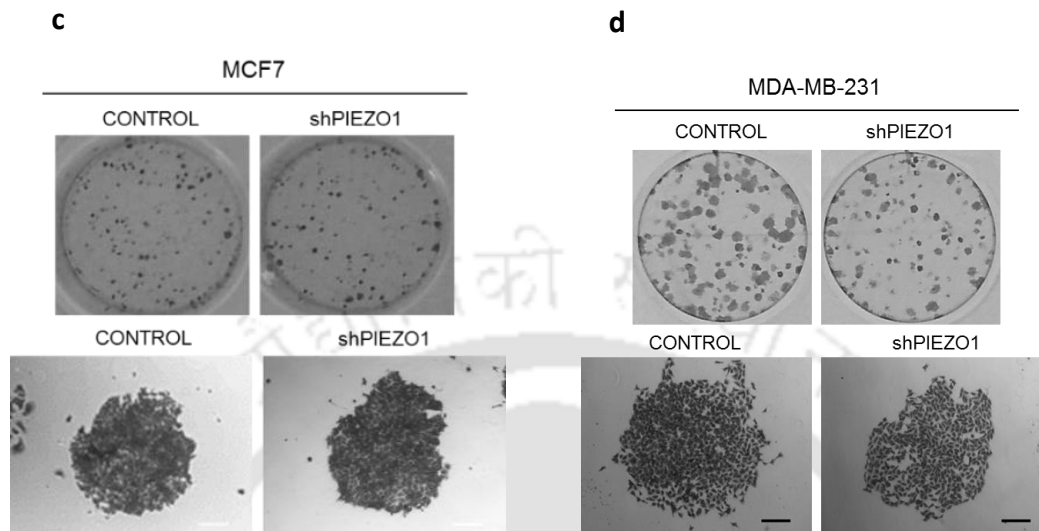


Fig.4.4.5. Effect of PIEZO1 silencing on self-renewal ability of breast cancer cells. Colony formation assay was performed to evaluate the effect of PIEZO1 silencing on (a) the number of colonies (self-renewal) and (b) the colony area (proliferation) of breast cancer cells. Representative well and microscopic images of MCF7 (c) and MDA-MB-231 (d) cells are shown.

Migration of cancer cells is an integral part of EMT (epithelial to mesenchymal transition) and 3D spheroid migration (Fig.4.4.6a), and wound healing migration assays (Fig.4.4.6b) were performed to understand the role of PIEZO1 in controlling the migration of breast cancer cells, thereby the EMT process. PIEZO1 silencing significantly inhibited the migration potential of both MCF7 and MDA-MB-231 cells. During 3D spheroid migration, the control cells migrated and invaded the collagen matrix, as reported earlier [119]; however, MCF7^{shPIEZO1} had significantly reduced migration potential (Fig.4.4.6a). Similarly, MDA-MB-231^{shPIEZO1} cells (Fig.4.4.6b) showed a 2-fold reduction in the migration speed compared to the control cells. Although PIEZO1 seem to modulate the proliferation of MCF7 and MDA-MB-231 cells differentially, migration potential was diminished in both MCF7 and MDA-MB-231 cells when PIEZO1 was downregulated. Gene expression analysis revealed that there was a significant downregulation in the mRNA expression levels of MMP9 in MCF7^{shPIEZO1} cells (Fig.4.4.6c), whereas the expression of VIM (Vimentin), CDH1(E-cadherin) and CDH2 (N-cadherin) did not change significantly. Similarly, no changes in the expression levels of VIM, CDH2 and SNAI2 were observed in MDA-MB-231^{shPIEZO1} cells

(Fig.4.4.6d). However, a significant downregulation in the expression levels of MMP14, RHOA and metastasis protein S100-A4 was observed. Thus, taken together, the data indicate that PIEZO1 silencing significantly downregulates the key EMT genes to inhibit migration.

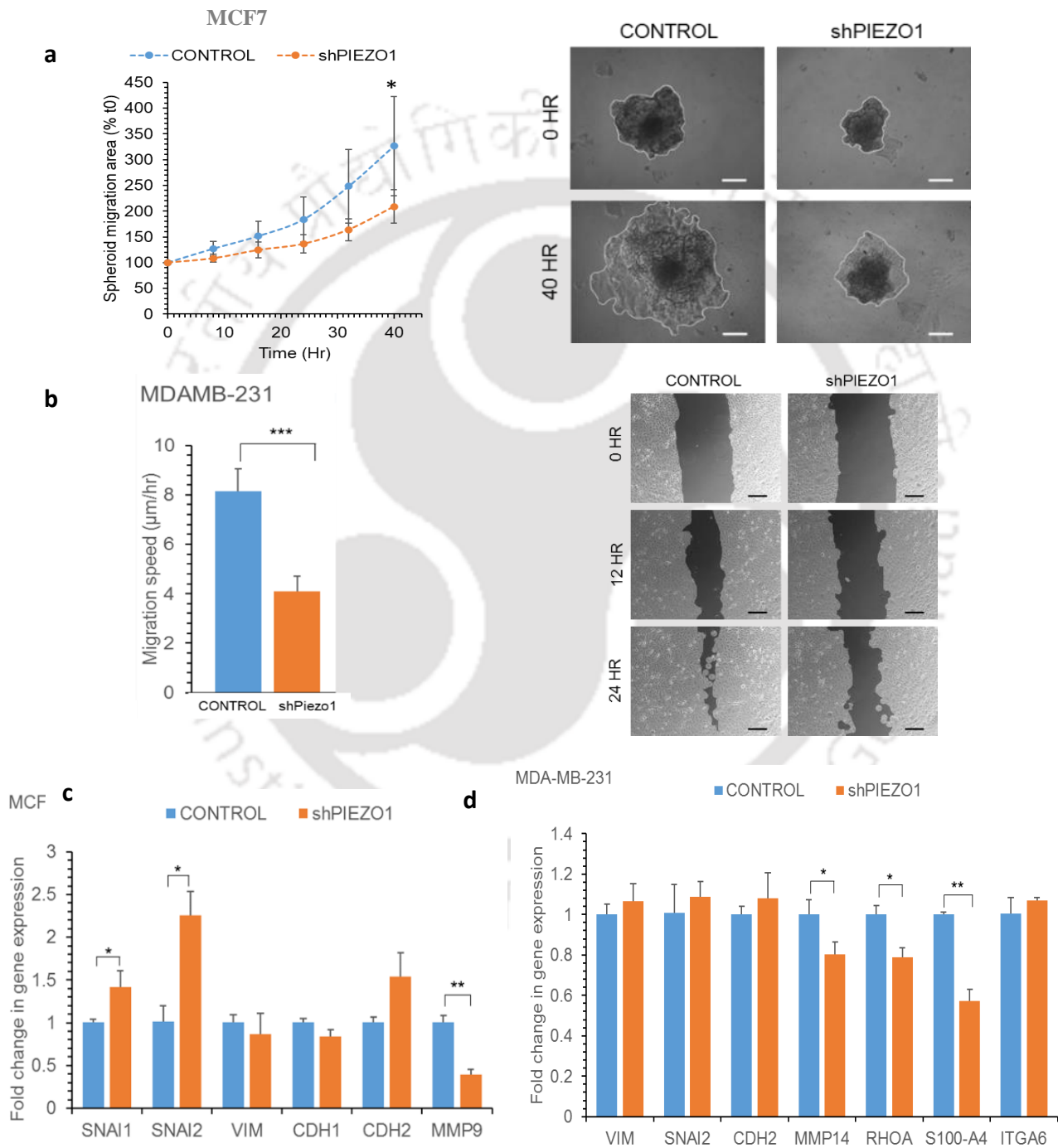


Fig.4.4.6. Effect of PIEZO1 silencing on the migration of breast cancer cells. Spheroid migration assay was performed on MCF7 cells to evaluate the effect of PIEZO1 silencing on the migration of transduced and control cells in 3-dimension spheroids **(a)** and **(b)** 2-dimension migration assay was performed in MDA-MB-231 cells. Gene expression analysis of MCF7 **(c)** and MDA-MB-231 cells **(d)** evaluated the fold change in the expression of genes related to cell migration and EMT.

Given that PIEZO1 silenced cells exhibited changes in their proliferation and migration ability, the changes in the gene expression that accompany these functional changes were determined. Immunoblotting analysis showed that in MCF7 cells **(Fig.4.4.7a)**, in line with the reduced proliferation, PIEZO1 silencing significantly downregulated the expression of proteins that regulate proliferation, such as β -CATENIN and AMPK, as well as there was a reduction in the levels of phosphoERK1/2 (pERK1/2). Furthermore, there was a reduction in the anti-apoptotic protein BCL2 and RHOA GTPase that controls the migration ability of the cells. Phospho flow cytometry analysis also showed that PIEZO1 silencing drastically downregulated pERK1/2 levels, whereas no changes were observed in the levels of phospho NF κ B (pNF κ B), phospho P38 MAPK (pP38MAPK) and phospho STAT3 (pSTAT3) between the control cells and MCF7^{shPIEZO1} cells **(Fig.4.4.7d)**. Similarly, immunoblotting analysis of MDA-MB-231^{shPIEZO1} cells **(Fig.4.4.7b)** exhibited reduced levels of β -CATENIN (β -CAT), BCL2 and RHOA whereas AMPK and pERK1/2 levels remained unchanged. These data suggest that PIEZO1 regulates the proliferation of breast cancer cells by modulating the levels of crucial cellular proteins such as β -CATENIN, BCL2 and pERK1/2. However, phospho flow cytometry analysis showed a reduction in pERK1/2 levels in MDA-MB-231^{shPIEZO1} cells, whereas pSMAD1/8 and pSTAT3 levels remained unchanged during PIEZO1 silencing **(Fig.4.4.7c)**.

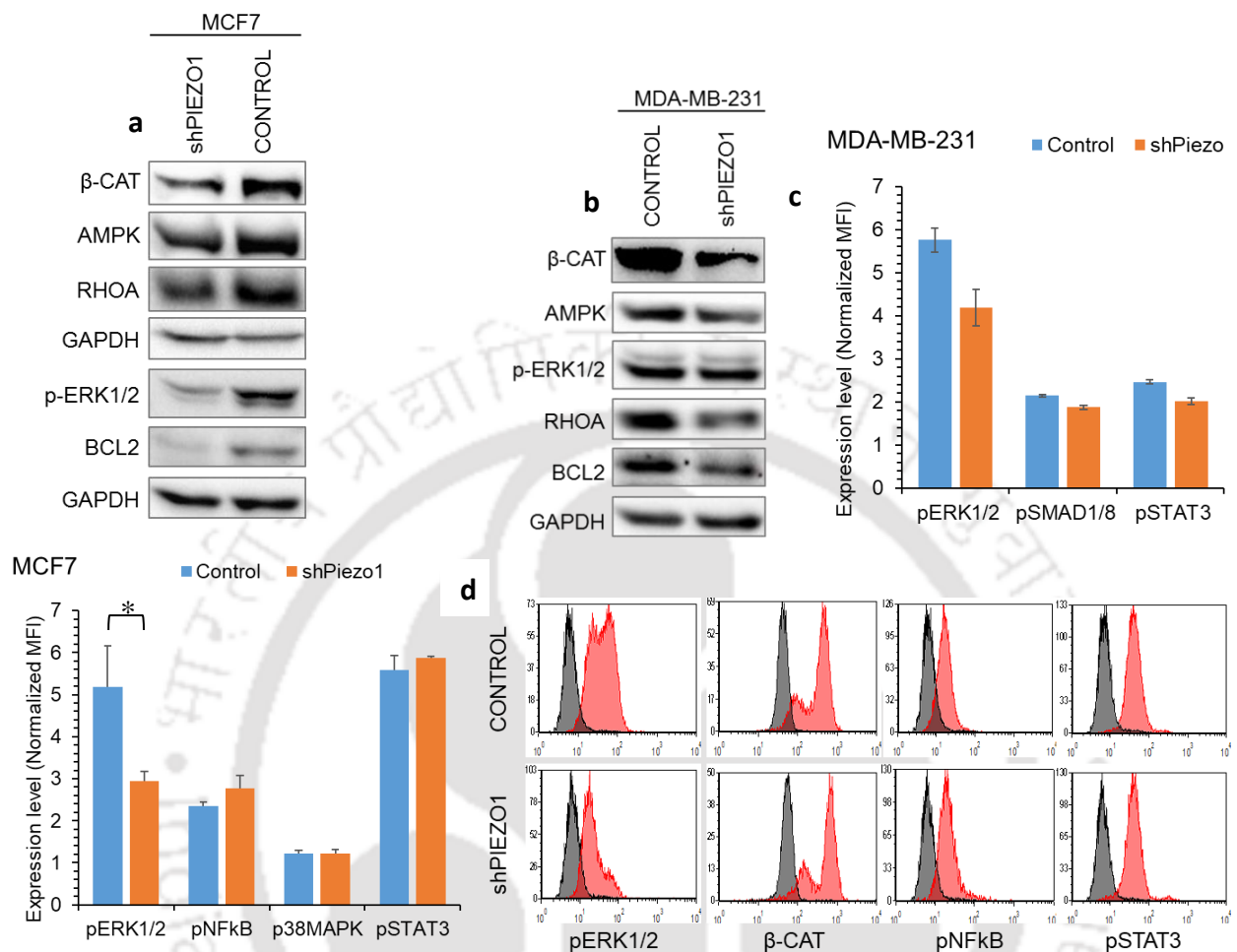
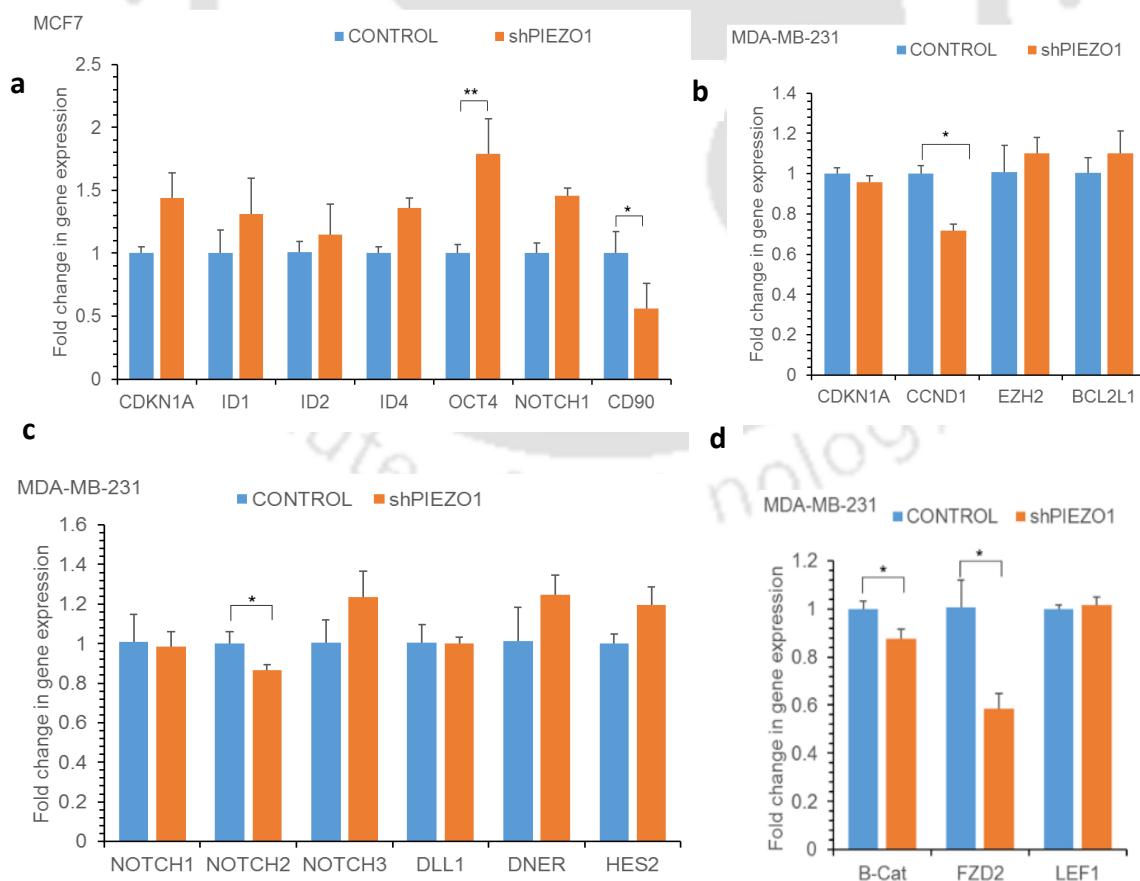


Fig.4.4.7. Effect of PIEZO1 silencing on gene expression changes in proliferation and migration related genes of breast cancer cells. Expression levels of key cellular proteins have been determined by immunoblotting in both MCF7 (**a**) and MDA-MB-231 (**b**) cells. Expression levels of other signaling pathway proteins – p-ERK1/2, p-SMAD1/8 and p-STAT3 in MDA-MB-231(**c**) and p-ERK1/2, p- NFκB, p38MAPK and p-STAT3 in MCF7 cells (**d**) have been assayed with the help of phospho protein flow cytometry. Representative flow cytometry histogram plots have been shown (**d**).

Quantitative real-time PCR analysis was performed to analyze how PIEZO1 modulation affects the expression of genes involved in key signaling pathways. A significant downregulation in the expression of CD90 was observed in MCF7^{shPIEZO1} cells (**Fig.4.4.8a**); however, several genes that represent proliferation were unaffected in these cells. Interestingly, PIEZO1 silencing significantly downregulated the cell cycle progression gene CCND1 without affecting the expression of EZH2 and BCL2L1(**Fig.4.4.8b**). In addition, PIEZO1 silencing modified the expression of genes involved in NOTCH and WNT signaling pathways and self-renewal. A significant downregulation was observed in NOTCH2, β -CATENIN (B-Cat) and FZD2 (Frizzled-2) genes in MDA-MB-231^{shPIEZO1} cells (**Fig.4.4.8c-d**), indicating suppression of Wnt signaling pathway. Further, genes that determine cancer stem cells and their self-renewal, such as OCT4, NANOG, SOX2, and ALDH1-A3 (**Fig.4.4.8e**), were significantly downregulated, which correlates with the reduced colony-forming ability observed in PIEZO1 silenced cells. However, the expression of drug efflux pump ABCG2 was upregulated by PIEZO1 silencing, which requires further investigation.



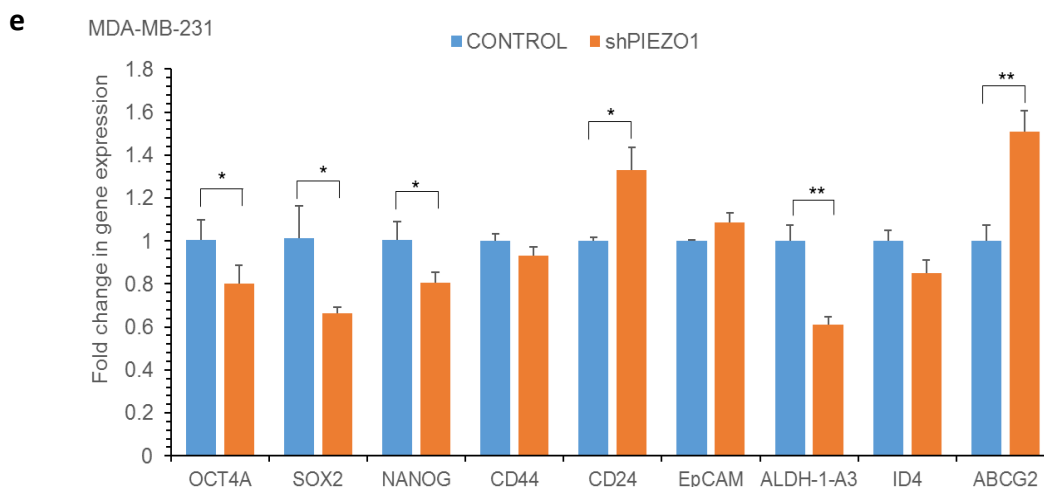
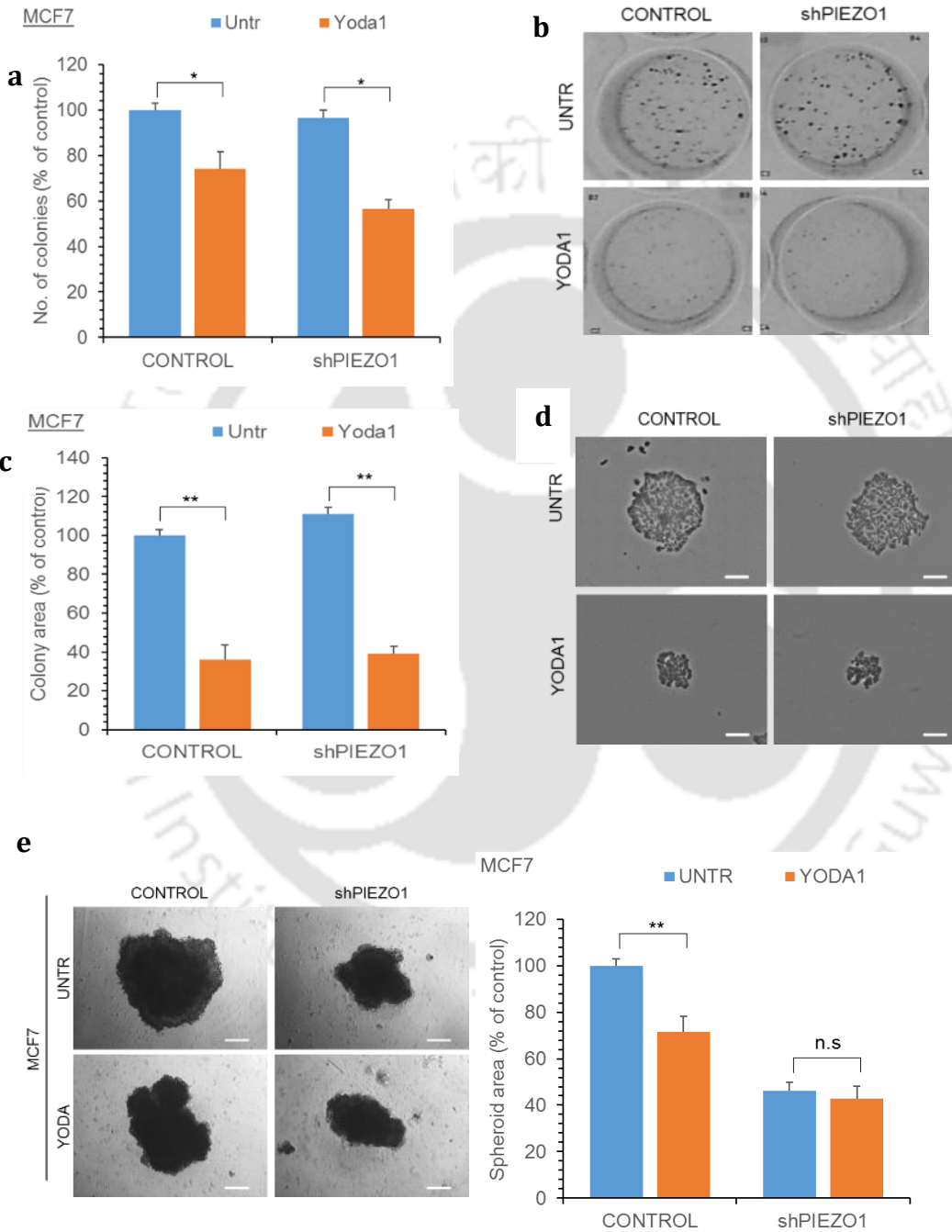


Fig.4.4.8. Effect of PIEZO1 silencing on modulation of genes involved in key signaling pathways MCF7^{shPIEZO1} cells (a) and MDA-MB-231^{shPIEZO1} cells (b-e) have shown modulation in genes related to stemness, self-renewal like OCT4A, SOX2, NANOG, CD44, CD24; ALDH1-A3; EMT marker genes like EpCAM, ID4 and other signaling pathways like β -catenin, Notch1,2,3, FZD2 and drug efflux pump like ABCG2.* $p < 0.05$, ** $p < 0.005$, *** $p < 0.0005$.

To understand the role of PIEZO1 further, PIEZO1 silenced MCF7 cells were treated with Yoda1, to check how the silenced cells respond to the PIEZO1 activation stimuli (Fig.4.4.9a-d). As described in the previous section, Yoda1 treatment significantly reduced the colony formation ability in both control and MCF7^{shPIEZO1} cells. The Yoda1 treated cells formed fewer colonies (Fig.4.4.9a-b) and were significantly smaller in size (Fig.4.4.9c-d) compared to the untreated cells. Similarly, the 3D growth of cells as spheroid was significantly reduced in the presence of Yoda1; however, the growth inhibitory effect of Yoda1 was less pronounced in MCF7^{shPIEZO1} cells compared to the control cells (Fig.4.4.9e). In contrast, no significant changes in the spheroid growth were observed in Yoda1 treated control and MDA-MB-231^{shPIEZO1} cells (Fig.4.4.9f).

As the ERK1/2 pathway is one of the key signaling pathways modulated by PIEZO1 modification, the effect of ERK1/2 inhibitor BVD523 on the growth of MCF7 (Fig.4.4.9g) and MDA-MB-231 (Fig.4.4.9h) as 3D spheroid was determined. BVD523 treatment significantly reduced the growth of MCF7 cells regardless of PIEZO1 expression levels; however, MCF7^{shPIEZO1} cells were less sensitive to BVD523 treatment and the growth inhibition was not as pronounced as seen in the control cells. MDAMB-231 cells, on the other hand, exhibited larger spheroid size on BVD523

treatment; however, PIEZO1 silencing significantly inhibited the spheroid growth, suggesting a context-dependent role of PIEZO1 in breast cancer cells belonging to different subtypes.



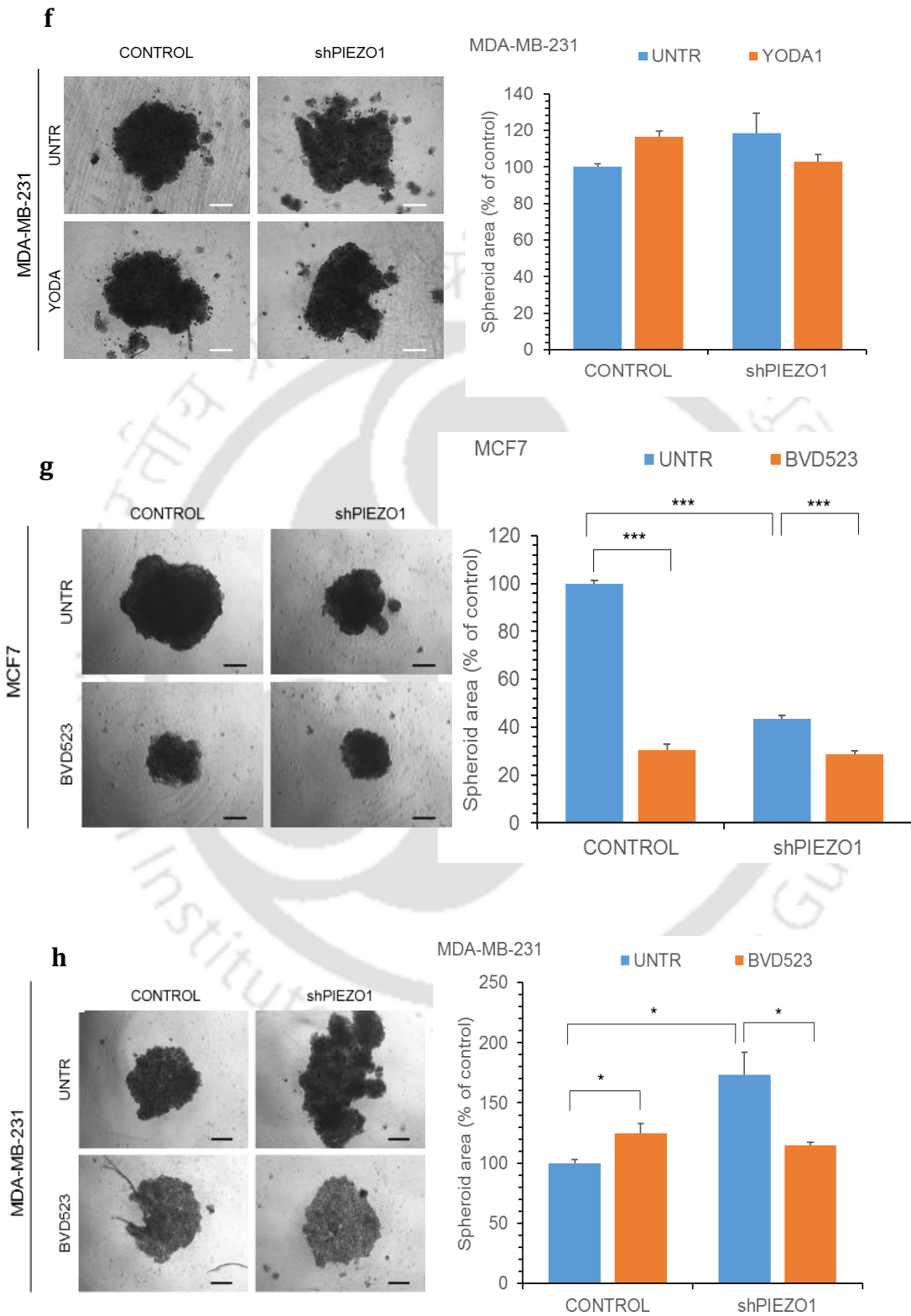
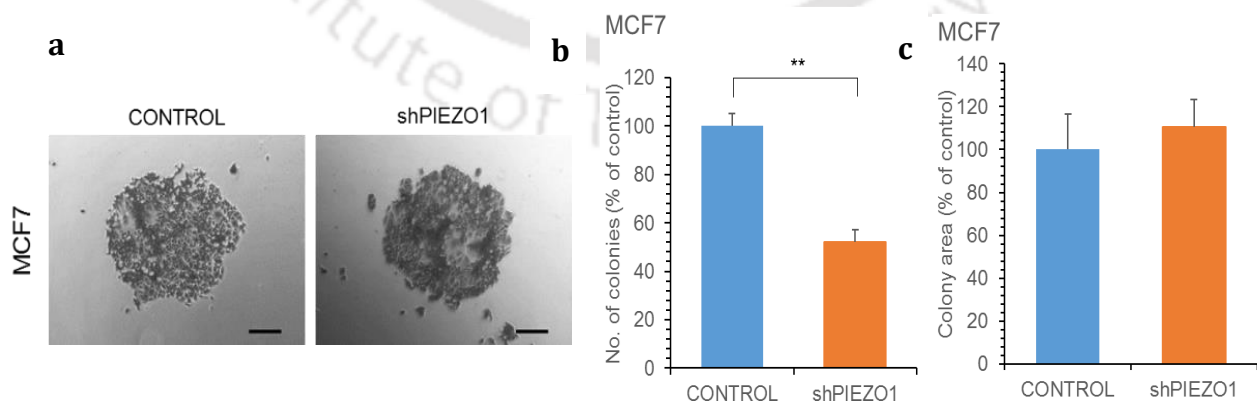


Fig.4.4.9 Effect of Yoda1 induced PIEZO1 activation on the self-renewal ability of breast cancer cells. Self-renewal ability of MCF7^{shPIEZO1} with Yoda1 treatment been assayed by colony formation assay (Fig a-d), both the number of colonies (**a-b**) as well as area of colonies (**c-d**) of the silenced cells were plotted with respect to the control cells with Yoda1 and without Yoda1(Untreated) conditions. Spheroid growth area of both MCF7^{shPIEZO1} and MDA-MB-231^{shPIEZO1} with their respective controls with Yoda1 (**e-f**) and BVD-523(**g-h**) and were calculated to determine the proliferation of cells in 3D mimicking *in-vivo* conditions. * $p < 0.05$, ** $p < 0.005$, *** $p < 0.0005$.

Cancer cells acquire anoikis resistance to help them survive during metastasis to distant organs. In addition, when the cancer cells disseminate to the distant organs through the circulatory system, they undergo shear stress and activate mechanosensing-related signaling pathways for survival and invasion into the tissue at the secondary site. To understand the role of PIEZO1 signaling in anoikis resistance, breast cancer cells were cultured in a non-adherent culture system, and its effect on self-renewal was determined by colony-formation assay. The cells cultured in the anoikis condition were also treated with doxorubicin (Dox) to determine how PIEZO1 signaling modulates chemoresistance and cell survival during anoikis resistance (**Fig.4.4.10a-f**). PIEZO1 silencing significantly inhibited the self-renewal and survival of MCF7^{shPIEZO1} cells (**Fig.4.4.10b**), and treatment with Dox completely abrogated the cell survival in both control and PIEZO1 silenced MCF7 cells. Interestingly, PIEZO1 silencing induced higher colony-forming/self-renewal ability in MDA-MB-231 cells compared to the control cells (**Fig.4.4.10e**). As expected, Dox treatment significantly inhibited the colony-forming ability of both control and MDA-MB-231^{shPIEZO1} cells. However, PIEZO1 silencing did not impact the colony-forming ability of MDA-MB-231 cells when Dox was added to the anoikis culture.



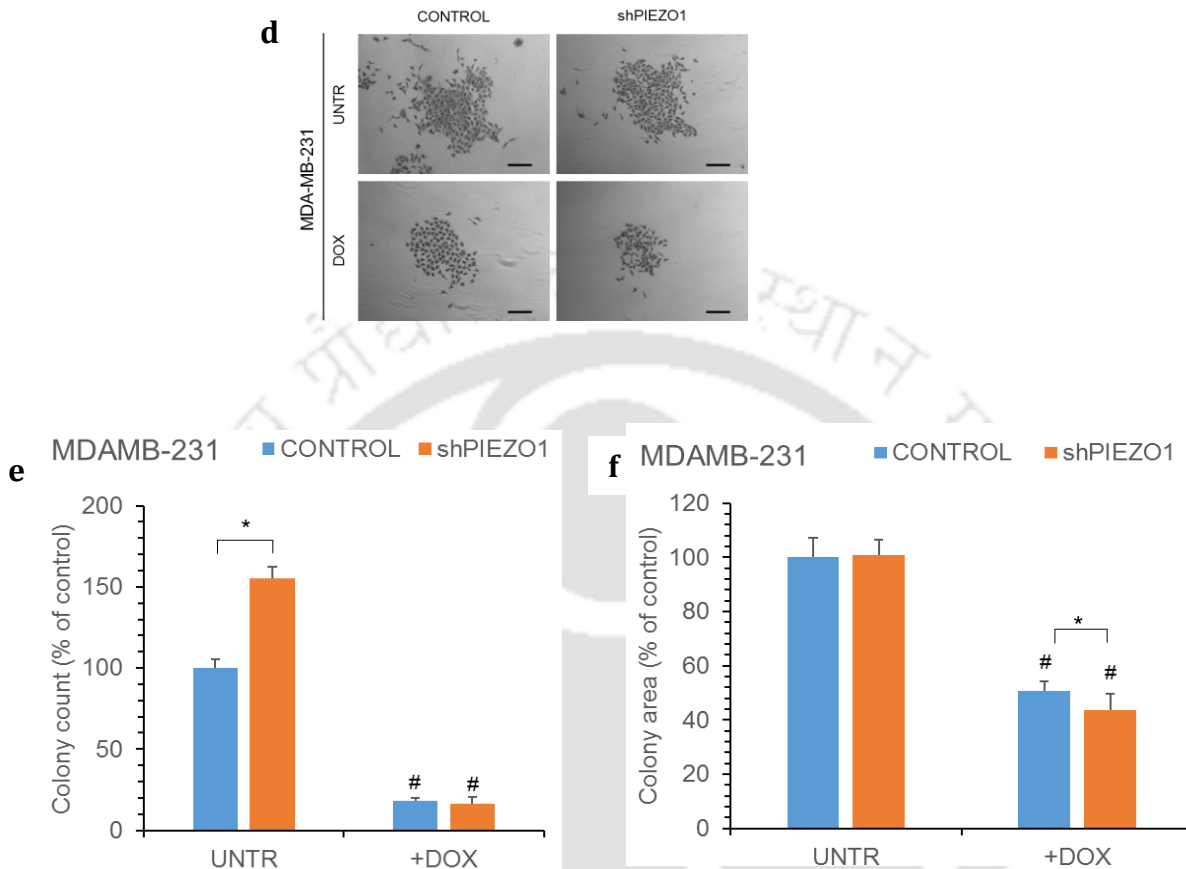
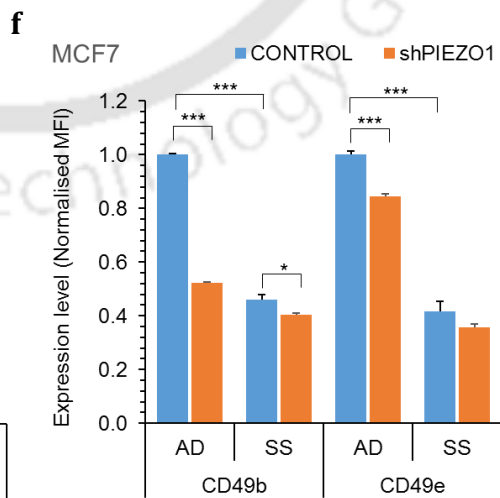
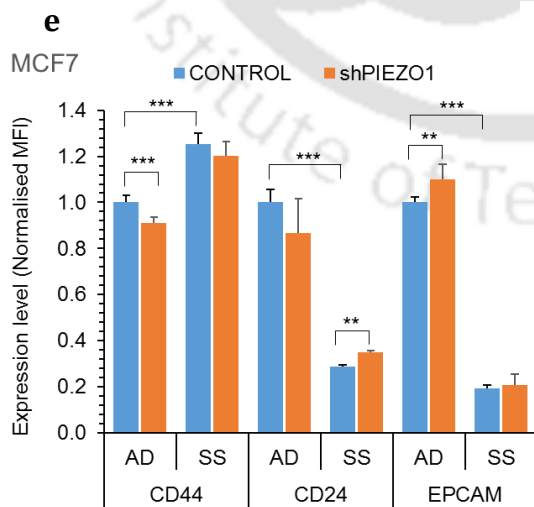
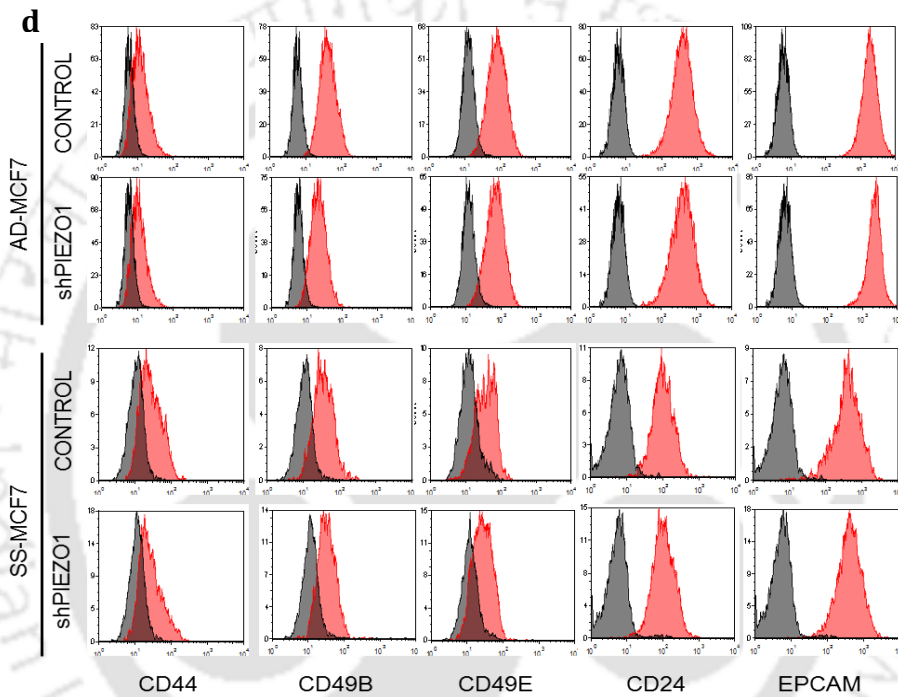
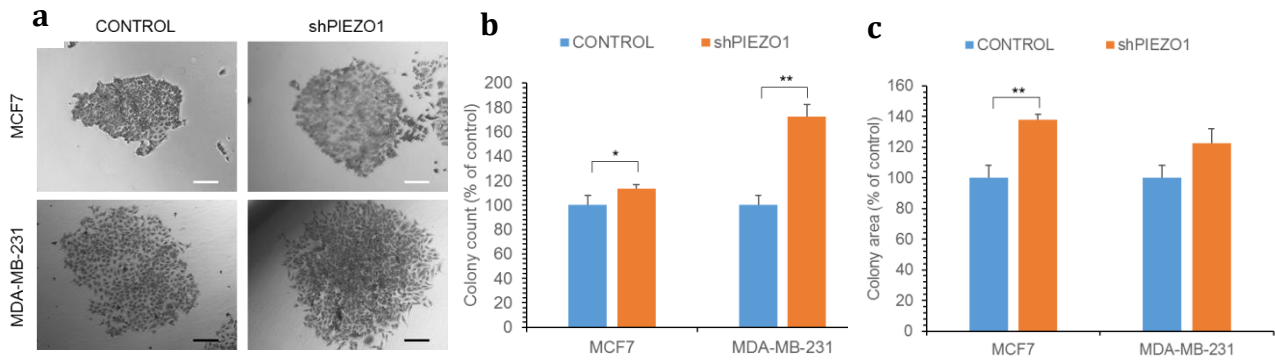


Fig.4.4.10 Effect of PIEZO1 silencing on the self-renewal ability and survival of breast cancer cells under anoikis condition. The self-renewal ability of MCF7^{shPIEZO1} (a-c) and MDA-MB-231^{shPIEZO1} under anoikis condition, with doxorubicin treatment (+DOX), was determined by colony formation assay (d-f). Both the number of colonies (b) as well as the area of colonies (c) of the silenced cells were plotted with respect to the control MCF7 cells. The number of colonies (e) and area of colonies (f) of control (CONTROL) and shPIEZO1 conditions in MDA-MB-231 with Dox treatment was determined. *p < 0.05, **p < 0.005, *** p < 0.0005.

To explore further how PIEZO1 regulates the survival of the breast cancer cells, MCF7^{shPIEZO1} and MDA-MB-231^{shPIEZO1} cells and the respective control cells were subject to shear stress in addition to anoikis culture condition. The survival and self-renewal ability of the cells were determined by colony formation assay. As observed with the anoikis condition, PIEZO1 silenced MDA-MB-231 cells showed better survival and formed higher number of colonies compared to the control cells. Under these culture conditions, the PIEZO1 silenced cells also formed a slightly higher number of colonies (Fig.4.4.11b) and larger colonies (Fig.4.4.11c). These data indicate that PIEZO1

silencing reduces the mechanosensing ability, thereby enhancing the survival of the cells under stress conditions specifically in the highly metastatic MDA-MB-231 breast cancer cells compared to MCF7 cells (**Fig.4.4.11b**). Further to understand the gene expression changes regulated by PIEZO1 during shear stress, MCF7 cells were subjected to shear stress conditions and the expression of cells surface proteins that represent cancer stem cell population was determined by flow cytometry. (**Fig.4.4.11d-f**). Subjecting the cells to shear stress significantly reduced the cell surface expression of CD24 and EPCAM, whereas there was a small yet significant increase in the expression of CD44 (**Fig.4.4.11e**). Further, the expression of integrins CD49B and CD49E were significantly downregulated under shear stress conditions. PIEZO1 silencing downregulated the expression of both CD49B and CD49E even in cells cultured under static, adherent conditions (**Fig.4.4.11f**). PIEZO1 silencing downregulated the expression of RHOA and β -CATENIN in MCF7 cells (**Fig.4.4.11g**). In agreement with the increased survival and colony forming ability observed in PIEZO1 silenced MDA-MB-231 cells, MDA-MB-231^{shPIEZO1} cells had significantly higher expression of survival factors BCL2, RHOA and pERK1/2 (**Fig.4.4.11h**). Thus, PIEZO1 silencing differentially modulates the breast cancer cells with reduced PIEZO1 favoring the survival and self-renewal of metastatic breast cancer cells MDA-MB-231 by enhancing the expression of survival genes BCL2 and pERK1/2.



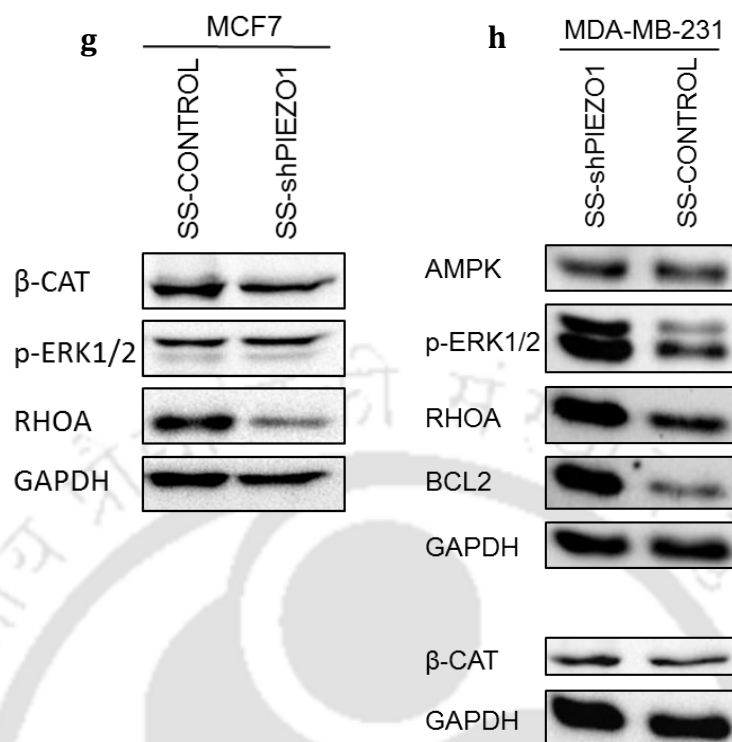


Fig.4.4.11 Effect of PIEZO1 regulation on the self-renewal ability and survival of breast cancer cells under shear stress/anoikis condition. Self-renewal ability of MCF7^{shPIEZO1} and MDA-MB-231^{shPIEZO1} under anoikis condition, has been assayed by colony formation assay (a-c), both the number of colonies (b) as well as area of colonies (c) of the silenced cells were plotted with respect to the control cells. Gene expression changes related to cell survival, stemness (e) and integrin expression (f) by PIEZO1 regulation under shear stress condition was further assessed by flow cytometry where the cell surface marker expression was quantified as normalized MFI (d-f). Expression of β-CATENIN, BCL2, RHOA and phosphoERK1/2 were determined by immunoblotting in MCF7 (g) and MDA-MB-231 (h) cells for both control and shPIEZO1 conditions under shear stress. *p < 0.05, **p < 0.005, *** p < 0.0005.

Thus PIEZO1 is required for mechanosensing of cancer cells during metastasis and migration, and downregulation, although inhibited the migration of cells in 2D and 3D environments, it enhanced the survival of cancer cells under anoikis and shear stress conditions.

Discussion:**5.1 ERK pathway inhibition diminishes breast cancer proliferation and metastatic properties**

The first section of the study elucidates the role of ERK signaling pathway in breast cancer. The effect of multi-kinase inhibitor sorafenib on proliferation, migration, cell cycle, invasion and gene expression of breast cancer cells has been studied. Breast cancer cell line MCF7 is estrogen and progesterone receptor positive, non-invasive and weakly aggressive. MDA-MB-231 on the other hand, is highly aggressive, metastatic and receptor negative breast cancer cell line. Both the cell lines represent the different kinds of cancer that breast cancer patients are diagnosed with and thus serve as excellent models for *in-vitro* studies. As reported in other cancers, like hepatocellular carcinoma, sorafenib treatment resulted in diminished proliferation in both metastatic MDA-MB-231 and non-metastatic MCF7 cells. MCF7 cells exhibited higher sensitivity to sorafenib compared to MDA-MB-231 cells. In breast cancer patients, studies have shown that high ERK levels correspond to poor prognosis. The signaling pathway is instrumental in regulating metastasis in cancer cells[33, 35]. In this study, sorafenib treatment in breast cancer cells drastically reduced phospho ERK1/2 levels. Sorafenib induced cell cycle arrest in both MCF7 and MDA-MB-231 cells, with a significant increase of cells in the G0/G1 stage of the cell cycle. This was further observed by an accumulation of cells in the G1 phase of cell cycle, accompanied by an increase in cell death like in other cancers [45] [120]. Treatment with sorafenib further increased the level of mitochondrial superoxide in the MDA-MB-231 cells suggesting that ROS production is one of the mechanisms through which sorafenib inhibits breast cancer cell proliferation and survival. In breast cancer, the initiation, progression, recurrence of cancer and chemoresistance are controlled by the cancer stem cells, which are characterised by the presence of CD44+/CD24-/lo along with other markers such ALDH and CD49F[62, 110], [121] [122]. In basal like breast cancer cells as in MDA-MB-231, majority of cell populations have CD44+/CD24-/lo phenotype. As reported by Schabath et al [123] CD24 expression, which inhibits stemness in breast cancer cells was upregulated, upon addition of sorafenib treatment. CD49F, another well-known breast cancer stem cell marker, was downregulated upon treatment with sorafenib. This implied reduction in metastatic effect since CD49F has also been reported to be a marker for metastasis. [62]

One of the hallmarks of cancer cells is metastasis, the ability of the cells to migrate and invade distant tissues and organs, and it is a major bottleneck for complete eradication of the cancer cells

in breast cancer patients. [124]. Metastasis is initiated by epithelial-mesenchymal transition (EMT) which induces changes in the morphology and gene expression profile of the migrating cells. The actin cytoskeleton plays an important role in regulating the migration of cells and EMT is accompanied by changes in the cell morphology and the rearrangement of F-actin in the cells. Interestingly, sorafenib treatment increased the cell-cell contact and reduced actin projections in MCF7 and MDA-MB-231 cells, suggesting its anti-migratory effect. In MCF7 cells, filopodia formation and loss of E-cadherin expression induced by EGF treatment were reversed when sorafenib was added along with EGF. Sorafenib interferes with the migration and invasion ability of breast cancer cells and showed significant inhibition in migration of cells in monolayer adherent culture of cells. EGF treatment on the other hand significantly increased the migration of MCF7 and MDA-MB-231 cells. Further evaluation of sorafenib on the migration of breast cancer cells, in a 3D spheroid invasion assay, closely mimicking the migration of cancer cells in *in-vivo* showed similar results like 2D conditions. Reduced migration was coupled with upregulated EPCAM expression. Downregulation of EPCAM led to metastatic phenotype and poor clinical outcome in breast cancer as reported by Ye F et al [67]. Reduction in invasive phenotype was characterised by high Ep-CAM expression in MDA-MB-231 cells [125]. In this study the reduction in migration and invasion of breast cancer cells was associated with significant upregulation of E-cadherin (CDH1) and TIMPs [126], [127] and a simultaneous downregulation of MMPs and EREG (associated with EMT and migration) transcript levels. In contrast, EGF induced the expression of matrix metalloproteinases.

Earlier reports state that sorafenib downregulated phosphorylated levels of p38MAPK [120], [128] and STAT5 [129] in other cancers. p-38 MAPK activation promoted metastatic signaling and proliferation [34] and STAT5 signaling promoted growth and metastasis of breast cancer cells. [130] [131]. In this study, sorafenib treatment impacted other cancer-related signaling pathways, the expression levels of phospho P38MAPK (pP38MAPK) and phospho STAT5 (pSTAT5) were significantly downregulated in sorafenib treated breast cancer cells. This further confirms its anti-tumorigenic effects. In conclusion it can be said that sorafenib effectively reduced proliferation, migration, invasion of breast cancer cells as well as modified gene expression of signaling pathway molecules. Mechanism of action of sorafenib can be further studied in combination therapies with other drugs to inhibit metastasis in breast cancer.

Certain types of breast cancer acquire aggressive properties and exhibit poor prognoses in patients. Reports suggest hyperactivation of RAS-RAF-MEK-ERK signaling pathways in a wide range of cancers, including breast cancer [132] [133]. Although RAF / MEK inhibitors serve to be a

desirable target to treat majority of the cancers, but in clinical trials they did not succeed. Due to RAF dimerization and reactivation of ERK signaling along with limitations of MEK inhibitors, the development of ERK1/2 specific inhibitors is required as promising anti-cancer therapeutics. Ulixertinib or BVD-523 is a known first-in-class ERK-specific inhibitor, showing promising antitumor activity in a phase I clinical trial for advanced solid tumours having BRAF and NRAS mutations [47].

The role of BVD-523 in regulating proliferation, migration, self-renewal ability and metastasis of breast cancer cells has been assessed in this study. Similar to the effect observed with sorafenib, both the MCF7 and MDA-MB-231 cell lines showed a significant dose-dependent decrease in cell number. In line with the reduced proliferation potential of the breast cancer cells in monolayer 2D culture, the cells showed marked inhibition of spheroid growth upon BVD treatment. The cell cycle profile of BVD-treated MCF7 and MDA-MB-231 cells was analyzed to understand the mechanism of growth arrest [134], and BVD treatment showed a G₀/G₁ cell cycle arrest confirming that ERK1/2 inhibition affects proliferation in breast cancer cells.

Self-renewal is a known hallmark feature of cancer cells, enabling continued proliferation at the primary tumor site and secondary metastatic growth from the dispersed cells [135]. Therefore, the effect of BVD on the clonogenicity of MCF7 and MDA-MB-231 cells was evaluated. BVD treatment of MCF7 and MDA-MB-231 cells showed a significant reduction in the number and area of the colonies compared to the control cells. Together these results indicate that ERK1/2 is an instrumental regulator of cell proliferation and self-renewal in breast cancer cells.

In order to study the role of ERK1/2 in regulation of breast cancer cell migration [136] [126], MCF7 and MDA-MB-231 cells were subjected to wound healing assay in the presence of BVD. BVD treatment of both MCF7 and MDA-MB-231 cells resulted in a significant reduction of their migration speed. Therefore, specific inhibition of ERK1/2 can be a potential strategy to target breast cancer cell migration.

The effect of BVD treatment on various stemness, proliferation, and migration related genes was further established to understand the molecular mechanism of ERK-mediated proliferation and migration of breast cancer cells. The self-renewal characteristic is often attributed to cancer stem cells, which are defined by CD44^{high}/CD24^{low} and CD49F^{high} expression in the case of breast cancer [110] [67]. BVD treated MDA-MB-231 cells showed significant and prominent downregulation of stemness, compared to MCF7 cells. These differences substantiate a differential role of ERK signaling in different subtypes of breast cancer.

EMT (epithelial to mesenchymal transition), the primary feature of metastatic cancer cells, is regulated by the presence of integrins, which also regulates stemness and cell migration. as they cross talk with the intracellular proteins mediated by actin [137] [138]. The increase in expression levels of CD24 along with decrease in CD44 in MDA-MB-231 cells upon BVD treatment, indicated reduction in stemness, similar to that observed with sorafenib treatment in breast cancer cells. This was accompanied by reduction in CD49F expression indicating inhibition of stemness and migration potential in breast cancer cells, which corresponds to the inhibition of MEK pathway with the help of RAF/RAS inhibitors [139] [140].

From the first section of the study which focuses on understanding the role of ERK signaling in breast cancer, it can be said that both Sorafenib and BVD-523 treatment showed promising effect in reducing proliferation, migration and stemness of breast cancer cells *in vitro*. It also indicates that breast cancer treatment can be made effective in targeting the ERK pathway kinases and better therapeutic strategies need to be applied on developing these inhibitors and checking their efficacy in clinical trials. The new insight gained upon studying the results of Sorafenib versus BVD might put forward the fact that Raf inhibitors, upstream to ERK1/2 might be effective but not specific in their mode of action. The need for the development of target specific small molecule inhibitors might provide valuable therapeutic index which will be high on efficacy and low on toxicity as ERK pathway is ubiquitously present across all cell types

5.2 Role of PIEZO1 in breast cancer cells

The next section of the study focuses on understanding the role of mechanotransduction in breast cancer cells. Mechanotransduction is defined as the process by which a cell senses extracellular mechanical forces arising due to the interaction between the cell and extracellular matrix, and converts these mechanical forces to biochemical signals [105]. The mechanosensitive ion channels for example PIEZO1 and PIEZO2 have been identified to be expressed in many cell types [94] [68]. Breast cancer, notably, has shown the presence of PIEZO1 as a key regulator in the progression and development of breast cancer tissue. PIEZO1 has recently gained attention as a regulator of tumour progression due to its aberrant expression in various cancers [71], [141]. Yu et.al. demonstrated the widespread expression of PIEZO1 in both normal and malignant breast cancer cells. However cancerous cells showed higher expression of PIEZO1 as compared to control and studies indicate the role of PIEZO1 in regulating cancer cell behaviour [71].

PIEZO1 is activated by various types of mechanical stimuli as well as by some chemically

synthesized small molecules. One such compound named Yoda1 has been identified as an agonist for both mice and human PIEZO1. PIEZO1 has been found to be activated by Yoda1 even in absence of other cellular components. This paved way for the fact that Yoda1 can provide detailed insight to study PIEZO1 regulation and function. [2] [72]

As tumors progress in a confined tissue space, the growing tumour mass experiences alterations in the mechanical cues in form of increased tissue stiffness. The effect of PIEZO1 activation on the proliferation and growth of breast cancer cells MCF7 and MDA-MB-231, *in vitro*, was assessed by treating cells with Yoda1 [142] and Dooku1, an allosteric antagonist of Yoda1 [90]. Both the cell lines exhibited significant dose dependent inhibition in proliferation upon treatment with Yoda, whereas treatment with Dooku did not show any significant effect on the proliferation of MCF7 cells while in MDA-MB treatment with Dooku alone showed a significant dose-dependent increase in cell number.

It is to be noted that cancer cells undergo changes in conformation and alter the neighbouring microenvironment before progressing into the metastatic series of events. [143]. Effect on breast cancer cell morphology by Yoda1 induced PIEZO1 activation, showed that Yoda-treated MDA-MB-231 cells assumed an elongated morphology. The combination of Yoda and Dooku induced a similar spindle-shaped morphology in some cells and also induced cell detachment, due to the presence of high number of round cells. MCF7 cells retained their typical polygonal morphology upon treatment with Yoda/Dooku or their combination.

The growth inhibitory effect of Yoda was evident on MCF7 cells grown as 3D-spheroids where Yoda treatment formed significantly smaller spheroids and Dooku could not antagonize the effect of Yoda on the proliferation of breast cancer cells. In order to understand the mechanism of growth arrest induced by Yoda1 [142], cell cycle profile of breast cancer cells was analyzed which showed Yoda+Dooku treated MDA-MB-231 cells exhibiting a growth arrest in G0/G1 phase. The growth inhibitory effect of Yoda on MCF7 was established by the presence of higher proportion of cells in S-phase indicating S-phase arrest. The molecular basis of the growth inhibition and cell cycle arrest was further confirmed by q-PCR analysis which showed a significant reduction in CCND1 and cell cyclin inhibitor CDKN1A in Yoda treated MCF7 cells.

Studies have shown that enhanced intraosseous pressure supports successful colonization of the bone by prostate cancer cells [144] and PIEZO1 gets activated by increased mechanical loading of bones [145] indicating a connection between metastatic colonization and PIEZO1. Evidences suggest correlation between PIEZO1 expression and activation of proteins associated with higher proliferation and colonization such as ERK, Akt/m-TOR [146] [89]. In this study, the effect of

Yoda-induced PIEZO1 activation on the self-renewal of breast cancer cells showed that Yoda-treatment formed fewer and smaller colonies than the non-treated conditions. In line with the proliferation data, Dooku-treated cells showed similar colony size and number as the control cells. Thus, it can be said that Dooku could not antagonize the effect of Yoda on self-renewal ability of breast cancer cells.

The effect of Yoda on stemness of breast cancer cells was evaluated in correlation with the proliferation and self-renewal ability. Yoda-treated MCF7 cells showed a significant upregulation of the stemness genes NANOG and OCT4 m-RNA expression. On the other hand, Yoda + Dooku combination treatment led to a significant increase in ID4 expression, indicating that Yoda and Dooku can act synergistically to affect expression of some genes. Mitosox assay performed with Yoda treated breast cancer cells showed significant increase in percentage of MitoSOX positive cells indicating that Yoda might be inducing mitochondrial stress response. Therefore, upregulation of Nanog and Oct4 in the Yoda treated cells can be explained in the context of the cells maintaining the state of quiescence. This may be supported by the study where SOX2 is regulated differentially than NANOG and OCT4 in Human embryonic stem cells [147]. Yoda/Dooku-treated MCF7 and MDA-MB-231 showed a significant downregulation of stemness markers by flowcytometry which may further explain that the cells could be experiencing a stress response upon addition of Yoda or Dooku. Down regulation of CD44 can explain the decreased self-renewal associated with reduction in colony forming ability upon Yoda treatment. Hence, PIEZO1 might be involved in regulating stemness transcription factors in different types of breast cancer cells.

Activation of PIEZO1 promotes migration in several cancers like breast, gastric, colorectal, pancreatic, and prostate cancer cells [148]. PIEZO1 is also known to promote EMT and invasive potential of cancer cells coupled with anti-apoptotic behaviour and enhanced metastasis [149] [150]. In order to elucidate the role of PIEZO1 in mediating the metastatic potential of breast cancer cells, the effect of Yoda-induced PIEZO1 activation on the migration capacity of MCF7 and MDA-MB-231 cells was studied. Treatment with Yoda significantly impeded the migration of both cell lines both in 2D and 3D culture *invitro*. Furthermore, MDA-MB-231 cells also showed a drastic reduction in expression of CD49F when treated with either Yoda, Dooku or their combination. qPCR analysis of migration related genes further confirmed the migration inhibitory effect of Yoda, where Yoda treated MCF7 cells showed a significant downregulation of EMT associated gene SNAI2.

PIEZO1 activation is known to modulate ERK phosphorylation in several cell types. In canine

epithelial cells, downstream of calcium influx, ERK1/2 was shown to be a phosphorylation target by PIEZO1 activation and phosphorylated ERK1/2 caused a significant increase in cellular mitosis. Deformation of cell membrane due to substrate stretching lead to the activation of PIEZO1 and this promoted enhanced proliferation [91]. To understand the effect of Yoda-induced PIEZO1 activation on the phosphorylation of ERK1/2 in MCF7 and MDA-MB-231 cells, assessment by immunoblotting revealed that Yoda treated cells showed a significant upregulation of p-ERK1/2 levels. Yoda-treatment significantly reduced the expression of RHOA in both MCF7 and MDA-MB-231 cells, which could not be reversed by Dooku, which is in line with the anti-migratory effect of Yoda. Treatment of MDA-MB-231 cells with Yoda or Dooku showed a significant reduction in the expression of β -catenin, and their combination showed a marginal additive effect. This indicates that Yoda induced PIEZO1 activation can cause alterations in the expression of proteins involved in proliferation and migration of breast cancer cells.

Raf kinase inhibitor, sorafenib showed reduced efficacy on stiffer microenvironments, rich in collagen [1]. Considering the effect of Yoda-induced PIEZO1 activation on the ERK-phosphorylation in breast cancer cells, the role of PIEZO1 activation in mediating sensitivity to sorafenib was assessed. Addition of Yoda did not affect the response to sorafenib treatment in MDA-MB-231 cells in-vitro, since there was a similar reduction in colony forming ability by both sorafenib treated and combination treated conditions. MCF7 cells treated with combination of sorafenib and Yoda produced significantly larger colonies than sorafenib alone. Cell cycle analysis of MCF7 cells treated with Yoda/sorafenib or their combination revealed that Yoda addition rescued the G2/M population, inhibited by sorafenib treatment. This implies that activation of PIEZO1 may impart resistance against anti-cancer agents in some subtypes of breast cancer.

Overall, PIEZO1 activation by Yoda1 led to the reduction in proliferation and migration of breast cancer cells. Dooku1, which is a reported PIEZO1 inhibitor could not reverse the effect of Yoda in regulating breast cancer cell behaviour. Therefore, lentiviral mediated gene silencing was performed to downregulate PIEZO1 gene and to understand the effect of PIEZO1 inhibition in breast cancer cells.

PIEZO1 knockdown studies suggest differential behaviour of cancer cells with respect to proliferation, survival and metastasis. [151] [152]. As mentioned previously, the inhibition of PIEZO1 was done through lentiviral mediated PIEZO1 silencing and the reduction in expression of PIEZO1 was confirmed by real-time PCR and flow cytometry.

Activation of PIEZO1 results in calcium influx that help transduce mechanical forces into biochemical response. Since calcium is a ubiquitous second messenger instrumental in regulating

multiple cellular functions like cell survival, proliferation, migration, cytoskeletal remodelling [153], it is responsible for cancer metastasis and progression.

Calcium flux assay was performed to understand the effect of PIEZO1 downregulation on the activity of PIEZO1 channel. As expected, the Ca^{2+} flux was significantly downregulated in MCF7^{shPIEZO1} cells whereas Yoda1 induced significant Ca^{2+} flux in control MCF7 cells. Interestingly, uninduced MCF7^{shPIEZO1} cells showed higher Ca^{2+} flux compared to MCF7^{Control} cells which may signify the expression of compensatory calcium ion channels as reported earlier [116]. Thus, PIEZO1 silencing significantly downregulated PIEZO1 activity and its expression at mRNA and protein level in breast cancer cells.

PIEZO1 modifies the cell structure by regulating actin filament and migration [117], [118]. The effect of PIEZO1 silencing on the arrangement of actin cytoskeleton showed prominent disruption of F-actin arrangement and loss of filopodia on cell surface in MDA-MB-231^{shPIEZO1} cells but not in MCF7^{shPIEZO1} cells. However, no significant change in the morphology of PIEZO1 silenced breast cancer cells was observed.

PIEZO1 has been reported to regulate opposite cellular processes in epithelial cells; cell division and cell death [97], [154]. PIEZO1 activation at lower cell density promotes proliferation [91], but its activation during cell crowding induces extrusion in epithelial cells leading to cell death [154]. The effect of PIEZO1 silencing on the proliferation of breast cancer cells in-vitro was assessed by calculating doubling time which was higher in MCF7^{shPIEZO1} cells. This was further confirmed by G2/M arrest of MCF7^{shPIEZO1} cell cycle along with significant reduction in 3D spheroid growth which is in line with lesser proliferation of MCF7^{shPIEZO1} culture in 2D. Cell cycle profile of MDA-MB-231^{shPIEZO1} on the contrary, showed increased percentage population of cells in S-phase, which is in line with the formation of larger MDA-MB-231^{shPIEZO1} spheroids compared to control cells. This suggests that downregulation of PIEZO1 did not affect the proliferation of the metastatic MDA-MB-231 cells. Moreover, there was a significant reduction in 3D growth of Yoda treated MCF7 control spheroids. The spheroid size however, did not vary in MCF7^{shPIEZO1} cells, indicating the inability of Yoda1 to exert its effect when PIEZO1 is silenced. This supports the fact that PIEZO1 has a wide spread and diverse response in mediating cell proliferation and survival responsible for cancer progression [143].

Self-renewal ability of breast cancer cells with silenced PIEZO1 showed yet another differential effect in two different types of breast cancer cells where MDA-MB-231^{shPIEZO1} exhibited reduced colony forming ability but MCF7^{shPIEZO1} did not show any effect. This suggests that PIEZO1 downregulation helped in modulating self-renewal ability of MDA-MB-231^{shPIEZO1} cells.

PIEZO1 knockdown studies demonstrated inhibition of fibroblast formation and expression of matrix metalloproteinases. PIEZO1 has a regulatory role in migration of various cancers [150, 155, 156]. Studies have indicated that PIEZO1 regulates migration and metastasis, suggesting complex behaviour of cancer progression [151] [152]. In order to elucidate the role of PIEZO1 in mediating the metastatic potential of breast cancer cells, the effect of PIEZO1 silencing on the migration capacity of MCF7 3D spheroids and MDA-MB-231 cells in 2D monolayer was studied. Both MCF7^{shPIEZO1} and MDA-MB-231^{shPIEZO1} cells showed reduced migration potential, although there was a differential role of PIEZO1 in modulating proliferation of breast cancer cells upon PIEZO1 downregulation. MMP9 m-RNA expression got significantly downregulated in MCF7^{shPIEZO1} cells and similarly the expression of EMT genes like MMP14, RHOA and S100-A4 was inhibited in MDA-MB-231^{shPIEZO1} cells, which corresponds to the reduced migration ability of the silenced cells.

PIEZO1 silenced breast cancer cells revealed downregulation of proteins related to proliferation like p-ERK, β -CATENIN and AMPK; anti-apoptotic protein BCL2; migration related RHOA GTPase in MCF7^{shPIEZO1}. Both the cells with silenced PIEZO1 showed downregulation in p-ERK. A similar reduction in β -CATENIN (β -CAT), BCL2 and RHOA was observed in MDA-MB-231^{shPIEZO1} cells. This suggests that under adherent condition, PIEZO1 is imperative for the expression of p-ERK1/2. ERK1/2 signaling pathway is central to proliferation, migration, self-renewal ability and progression of cancer cells. The crosstalk between ERK and other signaling pathways like Wnt signaling has been well established. The role of PIEZO1 as a mediator of mechanotransduction regulating ERK in particular, has been identified [157-159].

ERK1/2 pathway is one of the major signaling pathways affected by PIEZO1 modification [157-159]. Hence, the effect of ERK1/2 inhibitor BVD523 on the growth of PIEZO silenced MCF7 and MDA-MB-231 as 3D spheroid was determined. BVD treatment significantly reduced the growth of MCF7 cells regardless of PIEZO1 expression levels, and MCF7^{shPIEZO1} cells were less sensitive to BVD523 treatment. MDAMB-231 cells formed larger spheroids on BVD523 treatment, but PIEZO1 silencing significantly inhibited the spheroid growth. Thus, PIEZO1 silencing in breast cancer, suggests a context dependent differential role in proliferation mimicking *in-vivo* conditions. Cancer cells survive during metastasis by acquiring a mechanism known as anoikis resistance [160]. While dissemination to the distant sites through the circulatory system, they experience shear stress and activate mechanosensing-related signaling pathways for survival and invasion into the tissue at the secondary site. [161, 162] To understand the role of PIEZO1 signaling in anoikis resistance, breast cancer cells, cultured in a non-adherent culture system was subjected to colony-

formation assay. PIEZO1 silencing significantly inhibited the self-renewal and survival of MCF7 but promoted self-renewal ability in MDA-MB-231 cells. It has been reported that PIEZO1 inhibition through knockdown inhibited the growth of cancer cell and increased the sensitivity of the cells to chemotherapy in gastric and prostate cancer *in vitro* [163] [164]. However, *in vivo* PIEZO1 knockdown caused a more prominent effect on tumor growth [89]. To understand how PIEZO1 signaling modulates chemoresistance and cell survival during anoikis resistance, the breast cancer cells in non-adherent condition was also treated with doxorubicin where dox treatment completely inhibited cell survival in both control and PIEZO1 silenced MCF7 and MDA-MB-231 cells. However, PIEZO1 silencing did not alter the colony forming ability of MDA-MB-231 cells when Dox was added to the anoikis culture. This suggests that PIEZO1 silencing reduces the mechanosensing ability in breast cancer cells, as evident by the enhanced survival and self-renewal behaviour of the metastatic MDA-MB-231 cells. This was further confirmed by a significantly higher expression of survival factors BCL2, RHOA and phosphoERK1/2 in MDA-MB-231^{shPIEZO1} cells. Whereas, downregulation of RHOA and β -CATENIN in MCF7^{shPIEZO1} cells correlates with the reduced self-renewal ability and proliferation of MCF7^{shPIEZO1}.

Overall knowledge gained by evaluating all the results gives a detailed idea about how ERK signaling pathway regulates the breast cancer cell behaviour with respect to the inhibitory activities of different types of small molecule inhibitors either upstream to or specific to the ERK1/2. Matrix stiffness plays a critical role in determining cancer progression. Changes in the extracellular matrix are known to modulate the mechanosensing ability of a cancer cell, which in turn transduces the mechanical stimuli to biochemical signals. Moreover, the mechanosensitive ion channel PIEZO1 is known to modulate ERK phosphorylation in several cell types. In one of the studies, ERK1/2 was shown to be a phosphorylation target by PIEZO1 activation and phosphorylated ERK1/2 caused a significant increase in cellular mitosis. Thus, targeting mechanotransducers seem to have a context dependent role in regulating breast cancer cell behaviour.

Hence, this study implies that Piezo1 activation and silencing do not yield exactly opposite results even across different subtypes of similar kind of cancer. Optimal Piezo1 activation can be a possible way to study its multidirectional effects on breast cancer cell behavior across different cell lines.

The potential limitations for each objective and research finding could be the inability to conduct *in-vivo* studies. The results obtained from the *in-vitro* conditions can be correlated in a better way with the findings which may further improve the therapeutic clinical trials. However, the corresponding advantages of the study would be the cheaper alternative way of using cell lines

which are reliable, simple to procure and have infinite lifespan that eases the drug discovery studies against a specific target.

Therefore, this study suggests that both activating and inhibiting PIEZO1 may have a potential role in regulating breast cancer cell behaviour. Previous studies have also highlighted the fact that the role of PIEZO1 may be dual in nature where in one context, it can be an ideal target to inhibit metastasis but in another its activation may help inhibit metastasis. Therefore, detailed research into the arena of mechanotransduction in breast cancer is required to ascertain the role of PIEZO1 as a crucial therapeutic target.



6. Conclusion

Breast cancer is currently the most prevalent cancer affecting a large number of people and their lives, worldwide. One of the major signaling pathways crucially regulating breast cancer cell proliferation, migration, metastasis, stemness and angiogenesis is the ERK signaling pathway. Aberrant activity of its downstream signaling kinases are the forerunners of malignancy. Thus, targeting the ERK signaling pathway at different levels can provide insights into the mechanism by which oncogenic properties like stem-ness, chemoresistance, anoikis resistance, epithelial to mesenchymal transitions or EMT, are inhibited by and large.

In this study two cell lines MCF7 and MDA-MB-231 have been used as a model for human breast cancer. MCF7 is estrogen and progesterone receptor positive, non-invasive and weakly aggressive cell line. MDA-MB-231 on the other hand, is highly aggressive, metastatic and receptor negative cell line. Both the cell lines represent the different kinds of cancer that breast cancer patients are diagnosed with and thus serve as excellent models for *in-vitro* studies.

The first aspect of the study focuses on the treatment of breast cancer cells with Raf inhibitor Sorafenib and ERK1/2 specific inhibitor BVD-523. *In vitro* treatment of breast cancer cells MCF7 and MDA-MB-231 with Sorafenib showed effective inhibition of proliferation, migration, stemness and downregulation of other tumorigenic pathways. Treatment with BVD-523 similarly inhibited proliferation, migration and self-renewal ability in breast cancer cells, thereby suggesting potential role of ERK signaling pathway in regulating breast cancer cell behaviour. As compared to other cancers, breast cancer shows lesser frequency of mutation in MAP-K pathway but its dysregulation causes poor prognosis in patients. Therefore, further studies need to be executed to develop better therapeutic targets specific to ERK signaling pathway.

The second aspect of the study focuses on the progressive behaviour of tumour with alterations in the mechanochemical changes in the extracellular matrix of breast cancer. Matrix stiffness has been identified as a critical factor in the progression of cancer. PIEZO1, a mechanosensitive ion channel is a key regulator in the progression and development of breast cancer tissue. Yoda1 mediated activation of PIEZO1 downregulated proliferation and migration of breast cancer cells and its antagonist Dooku1 failed to reverse the effect of Yoda1. Re-evaluation of Dooku1 as an allosteric inhibitor of PIEZO1 is required.

In order to downregulate PIEZO1 gene, lentiviral mediated shRNA construct against PIEZO1 gene was used to silence PIEZO1 in breast cancer cells. As ERK1/2 pathway is one of the key

signaling pathways modulated by PIEZO1 modification, the effect of ERK1/2 inhibitor BVD523 on the growth of MCF7 and MDA-MB-231 as 3D spheroid was determined. BVD523 treatment significantly reduced the growth of MCF7 cells regardless of PIEZO1 expression levels, however, MCF7^{shPIEZO1} cells were less sensitive to BVD523 treatment and the growth inhibition was not as pronounced as seen in the control cells. MDA-MB-231 cells on the other hand, exhibited higher spheroid size on BVD523 treatment, however, PIEZO1 silencing significantly inhibited the spheroid growth, suggesting a context dependent role of PIEZO1 in breast cancer cells of different subtypes.

A differential role in proliferation was observed in breast cancer cells upon PIEZO1 silencing. PIEZO1 downregulation, although did not impact the proliferation, it plays a role in modulating the self-renewal ability of MDA-MB-231 cells. PIEZO1 silencing significantly inhibited the migration potential of both MCF7 and MDA-MB-231 cells. A significant downregulation was observed in NOTCH2, β -CATENIN (B-Cat) and FZD2 (Frizzled-2) genes in MDA-MB-231^{shPIEZO1} cells indicating suppression of Wnt signaling pathway. Further, genes that determine cancer stem cells and their self-renewal such as OCT4, NANOG, SOX2, ALDH1-A3 were significantly downregulated, which correlates with the reduced colony forming ability observed in PIEZO1 silenced cells. PIEZO1 silencing reduces the mechanosensing ability, enhancing the survival of the cells under stress conditions specifically, the highly metastatic MDA-MB-231 breast cancer cells compared to MCF7 cells. Under shear stress conditions, PIEZO1 silencing downregulated the expression of both CD49B and CD49E in cells cultured under shear stress and adherent conditions. PIEZO1 silencing downregulated the expression of RHOA and β -CATENIN in MCF7 cells. In agreement with the increased survival and colony forming ability observed in PIEZO1 silenced MDA-MB-231 cells, MDA-MB-231^{shPIEZO1} cells had significantly higher expression of survival factors BCL2, RHOA and phosphoERK1/2. Thus, PIEZO1 silencing differentially modulates the breast cancer cells with reduced PIEZO1 favoring the survival and self-renewal of metastatic breast cancer cells MDA-MB-231 by enhancing the expression of survival genes BCL2 and pERK1/2. In conclusion it can be said that PIEZO1 expression can serve as a prognostic marker and should be assessed while considering the use of ERK pathway inhibitors in breast cancer patients.

References

1. Nguyen, T.V., et al. *Extracellular matrix stiffness protects carcinoma cells from sorafenib via JNK signaling*. in *2014 40th Annual Northeast Bioengineering Conference (NEBEC)*. 2014.
2. Syeda, R., et al., *Chemical activation of the mechanotransduction channel Piezo1*. *Elife*, 2015. **4**.
3. Paul, D., *The systemic hallmarks of cancer*. *Journal of Cancer Metastasis and Treatment*, 2020. **6**: p. 29.
4. Siegel, R.L., K.D. Miller, and A. Jemal, *Cancer Statistics, 2017*. *CA Cancer J Clin*, 2017. **67**(1): p. 7-30.
5. Tysnes, B.B. and R. Bjerkvig, *Cancer initiation and progression: Involvement of stem cells and the microenvironment*. *Biochimica et Biophysica Acta (BBA) - Reviews on Cancer*, 2007. **1775**(2): p. 283-297.
6. DeVita, V.T., Jr. and E. Chu, *A history of cancer chemotherapy*. *Cancer Res*, 2008. **68**(21): p. 8643-53.
7. Wang, H. and X. Mao, *Evaluation of the Efficacy of Neoadjuvant Chemotherapy for Breast Cancer*. *Drug Des Devel Ther*, 2020. **14**: p. 2423-2433.
8. Anand, U., et al., *Cancer chemotherapy and beyond: Current status, drug candidates, associated risks and progress in targeted therapeutics*. *Genes & Diseases*, 2022.
9. Hanahan, D. and R.A.J.c. Weinberg, *Hallmarks of cancer: the next generation*. 2011. **144**(5): p. 646-674.
10. Holderfield, M., et al., *Targeting RAF kinases for cancer therapy: BRAF-mutated melanoma and beyond*. *Nature Reviews Cancer*, 2014. **14**(7): p. 455-467.
11. Siegel, R.L., et al., *Cancer statistics, 2022*. 2022. **72**(1): p. 7-33.
12. Harbeck, N., et al., *Breast cancer*. *Nature Reviews Disease Primers*, 2019. **5**(1): p. 66.
13. Ataollahi, M.R., et al., *Breast cancer and associated factors: a review*. *J Med Life*, 2015. **8**(Spec Iss 4): p. 6-11.
14. Derakhshan, F. and J.S. Reis-Filho, *Pathogenesis of Triple-Negative Breast Cancer*. *Annu Rev Pathol*, 2022. **17**: p. 181-204.
15. Economopoulou, P., V.G. Kaklamani, and K. Siziopikou, *The role of cancer stem cells in breast cancer initiation and progression: potential cancer stem cell-directed therapies*. *Oncologist*, 2012. **17**(11): p. 1394-401.
16. Allan, A.L., et al., *Tumor dormancy and cancer stem cells: implications for the biology and treatment of breast cancer metastasis*. *Breast Dis*, 2006. **26**: p. 87-98.

17. Klein, C.A., *Framework models of tumor dormancy from patient-derived observations*. *Curr Opin Genet Dev*, 2011. **21**(1): p. 42-9.
18. Steeg, P.S. and D. Theodorescu, *Metastasis: a therapeutic target for cancer*. *Nat Clin Pract Oncol*, 2008. **5**(4): p. 206-19.
19. Al-Mahmood, S., et al., *Metastatic and triple-negative breast cancer: challenges and treatment options*. *Drug Deliv Transl Res*, 2018. **8**(5): p. 1483-1507.
20. Becker, S., *A historic and scientific review of breast cancer: The next global healthcare challenge*. *Int J Gynaecol Obstet*, 2015. **131 Suppl 1**: p. S36-9.
21. Redig, A.J. and S.S. McAllister, *Breast cancer as a systemic disease: a view of metastasis*. *J Intern Med*, 2013. **274**(2): p. 113-26.
22. Peinado, H., S. Lavotshkin, and D. Lyden, *The secreted factors responsible for pre-metastatic niche formation: old sayings and new thoughts*. *Semin Cancer Biol*, 2011. **21**(2): p. 139-46.
23. Coghlin, C. and G.I. Murray, *Current and emerging concepts in tumour metastasis*. *J Pathol*, 2010. **222**(1): p. 1-15.
24. Talmadge, J.E. and I.J. Fidler, *AACR centennial series: the biology of cancer metastasis: historical perspective*. *Cancer Res*, 2010. **70**(14): p. 5649-69.
25. Adjei, A.A. and M. Hidalgo, *Intracellular signal transduction pathway proteins as targets for cancer therapy*. *J Clin Oncol*, 2005. **23**(23): p. 5386-403.
26. Faivre, S., S. Djelloul, and E. Raymond, *New paradigms in anticancer therapy: targeting multiple signaling pathways with kinase inhibitors*. *Semin Oncol*, 2006. **33**(4): p. 407-20.
27. Bertoni, E. and M. Salvadori, *Antineoplastic effect of proliferation signal inhibitors: from biology to clinical application*. *J Nephrol*, 2009. **22**(4): p. 457-62.
28. Keshet, Y. and R. Seger, *The MAP kinase signaling cascades: a system of hundreds of components regulates a diverse array of physiological functions*. *Methods Mol Biol*, 2010. **661**: p. 3-38.
29. Eblen, S.T., *Extracellular-Regulated Kinases: Signaling From Ras to ERK Substrates to Control Biological Outcomes*. *Adv Cancer Res*, 2018. **138**: p. 99-142.
30. Yao, Z. and R. Seger, *The Molecular Mechanism of MAPK / ERK Inactivation*. *Current Genomics*, 2004. **5**(4): p. 385-393.
31. Kotb, A.M., A. Hierholzer, and R. Kemler, *Replacement of E-cadherin by N-cadherin in the mammary gland leads to fibrocystic changes and tumor formation*. *Breast Cancer Res*, 2011. **13**(5): p. R104.
32. Merdad, A., et al., *Expression of matrix metalloproteinases (MMPs) in primary human breast cancer: MMP-9 as a potential biomarker for cancer invasion and metastasis*. *Anticancer Res*, 2014. **34**(3): p. 1355-66.

33. Bartholomeusz, C., et al., *High ERK protein expression levels correlate with shorter survival in triple-negative breast cancer patients*. *Oncologist*, 2012. **17**(6): p. 766-74.
34. Limoge, M., et al., *Tumor p38MAPK signaling enhances breast carcinoma vascularization and growth by promoting expression and deposition of pro-tumorigenic factors*. *Oncotarget*, 2017. **8**(37): p. 61969-61981.
35. Seddighzadeh, M., et al., *ERK signalling in metastatic human MDA-MB-231 breast carcinoma cells is adapted to obtain high urokinase expression and rapid cell proliferation*. *Clinical & Experimental Metastasis*, 1999. **17**(8): p. 649-654.
36. Khokhlatchev, A.V., et al., *Phosphorylation of the MAP kinase ERK2 promotes its homodimerization and nuclear translocation*. *Cell*, 1998. **93**(4): p. 605-15.
37. Chang, L. and M. Karin, *Mammalian MAP kinase signalling cascades*. *Nature*, 2001. **410**(6824): p. 37-40.
38. Avruch, J., et al., *Ras activation of the Raf kinase: tyrosine kinase recruitment of the MAP kinase cascade*. *Recent Prog Horm Res*, 2001. **56**: p. 127-55.
39. Roskoski, R., Jr., *RAF protein-serine/threonine kinases: structure and regulation*. *Biochem Biophys Res Commun*, 2010. **399**(3): p. 313-7.
40. Lawrence, M.C., et al., *The roles of MAPKs in disease*. *Cell Res*, 2008. **18**(4): p. 436-42.
41. Kolch, W., *Meaningful relationships: the regulation of the Ras/Raf/MEK/ERK pathway by protein interactions*. *Biochem J*, 2000. **351 Pt 2**(Pt 2): p. 289-305.
42. Keating, G.M. and A. Santoro, *Sorafenib: a review of its use in advanced hepatocellular carcinoma*. *Drugs*, 2009. **69**(2): p. 223-40.
43. Iyer, R., et al., *Sorafenib: a clinical and pharmacologic review*. *Expert Opin Pharmacother*, 2010. **11**(11): p. 1943-55.
44. Cervello, M., et al., *Molecular mechanisms of sorafenib action in liver cancer cells*. *Cell Cycle*, 2012. **11**(15): p. 2843-55.
45. Liu, L., et al., *Sorafenib blocks the RAF/MEK/ERK pathway, inhibits tumor angiogenesis, and induces tumor cell apoptosis in hepatocellular carcinoma model PLC/PRF/5*. *Cancer Res*, 2006. **66**(24): p. 11851-8.
46. Zafrakas, M., P. Pappasozomenou, and C. Emmanouilides, *Sorafenib in breast cancer treatment: A systematic review and overview of clinical trials*. *World J Clin Oncol*, 2016. **7**(4): p. 331-6.
47. Jiang, H., et al., *Concurrent HER or PI3K Inhibition Potentiates the Antitumor Effect of the ERK Inhibitor Ulixertinib in Preclinical Pancreatic Cancer Models*. *Mol Cancer Ther*, 2018. **17**(10): p. 2144-2155.
48. Giménez, N., et al., *Mutations in the RAS-BRAF-MAPK-ERK pathway define a specific subgroup of*

- patients with adverse clinical features and provide new therapeutic options in chronic lymphocytic leukemia. *Haematologica*, 2019. **104**(3): p. 576-586.
49. Lebedev, T.D., et al., *Identification of cell type-specific correlations between ERK activity and cell viability upon treatment with ERK1/2 inhibitors*. *J Biol Chem*, 2022. **298**(8): p. 102226.
50. Zhang, L., et al., *Discovery of Novel Dual Extracellular Regulated Protein Kinases (ERK) and Phosphoinositide 3-Kinase (PI3K) Inhibitors as a Promising Strategy for Cancer Therapy*. *Molecules*, 2020. **25**(23).
51. Germann, U.A., et al., *Targeting the MAPK Signaling Pathway in Cancer: Promising Preclinical Activity with the Novel Selective ERK1/2 Inhibitor BVD-523 (Ulixertinib)*. *Mol Cancer Ther*, 2017. **16**(11): p. 2351-2363.
52. Shin, M., C.E. Franks, and K.L. Hsu, *Isoform-selective activity-based profiling of ERK signaling*. *Chem Sci*, 2018. **9**(9): p. 2419-2431.
53. Hayes, T.K., et al., *Long-Term ERK Inhibition in KRAS-Mutant Pancreatic Cancer Is Associated with MYC Degradation and Senescence-like Growth Suppression*. *Cancer Cell*, 2016. **29**(1): p. 75-89.
54. Da Cruz Paula, A., et al., *Molecular characterization of CD44(+)/CD24(-)/Ck(+)/CD45(-) cells in benign and malignant breast lesions*. *Virchows Arch*, 2017. **470**(3): p. 311-322.
55. Nam, K., et al., *CD44 regulates cell proliferation, migration, and invasion via modulation of c-Src transcription in human breast cancer cells*. *Cell Signal*, 2015. **27**(9): p. 1882-94.
56. Babina, I.S., et al., *A novel mechanism of regulating breast cancer cell migration via palmitoylation-dependent alterations in the lipid raft affiliation of CD44*. *Breast Cancer Res*, 2014. **16**(1): p. R19.
57. Uchino, M., et al., *Nuclear beta-catenin and CD44 upregulation characterize invasive cell populations in non-aggressive MCF-7 breast cancer cells*. *BMC Cancer*, 2010. **10**: p. 414.
58. Hiraga, T., S. Ito, and H. Nakamura, *EpCAM expression in breast cancer cells is associated with enhanced bone metastasis formation*. *Int J Cancer*, 2016. **138**(7): p. 1698-708.
59. Ouhtit, A., et al., *Novel CD44-downstream signaling pathways mediating breast tumor invasion*. *Int J Biol Sci*, 2018. **14**(13): p. 1782-1790.
60. Pećina-Šlaus, N., *Tumor suppressor gene E-cadherin and its role in normal and malignant cells*. *Cancer Cell International*, 2003. **3**(1): p. 17.
61. Riehl, B.D., et al., *The Role of Microenvironmental Cues and Mechanical Loading Milieus in Breast Cancer Cell Progression and Metastasis*. *Front Bioeng Biotechnol*, 2020. **8**: p. 608526.
62. Ye, F., et al., *CD49f Can Act as a Biomarker for Local or Distant Recurrence in Breast Cancer*. *J Breast Cancer*, 2017. **20**(2): p. 142-149.
63. Hwang, R. and J. Varner, *The role of integrins in tumor angiogenesis*. *Hematol Oncol Clin North Am*, 2004. **18**(5): p. 991-1006, vii.

64. Avraamides, C.J., B. Garmy-Susini, and J.A. Varner, *Integrins in angiogenesis and lymphangiogenesis*. Nat Rev Cancer, 2008. **8**(8): p. 604-17.
65. Vassilopoulos, A., et al., *A critical role of CD29 and CD49f in mediating metastasis for cancer-initiating cells isolated from a Brca1-associated mouse model of breast cancer*. Oncogene, 2014. **33**(47): p. 5477-82.
66. Lim, E., et al., *Aberrant luminal progenitors as the candidate target population for basal tumor development in BRCA1 mutation carriers*. Nat Med, 2009. **15**(8): p. 907-13.
67. Ye, F., et al., *The Presence of EpCAM(-)/CD49f(+) Cells in Breast Cancer Is Associated with a Poor Clinical Outcome*. J Breast Cancer, 2015. **18**(3): p. 242-8.
68. Ranade, S.S., et al., *Piezo1, a mechanically activated ion channel, is required for vascular development in mice*. Proc Natl Acad Sci U S A, 2014. **111**(28): p. 10347-52.
69. Aglialoro, F., et al., *A Novel Role for PIEZO1 in Calcium Homeostasis during Erythropoiesis*. Blood, 2018. **132**(Supplement 1): p. 2321-2321.
70. Xiao, B., *Levering Mechanically Activated Piezo Channels for Potential Pharmacological Intervention*. Annu Rev Pharmacol Toxicol, 2020. **60**: p. 195-218.
71. Yu, Y., et al., *Piezo1 regulates migration and invasion of breast cancer cells via modulating cell mechanobiological properties*. Acta Biochim Biophys Sin (Shanghai), 2021. **53**(1): p. 10-18.
72. Yu, J.L. and H.Y. Liao, *Piezo-type mechanosensitive ion channel component 1 (Piezo1) in human cancer*. Biomed Pharmacother, 2021. **140**: p. 111692.
73. Humphrey, J.D., E.R. Dufresne, and M.A. Schwartz, *Mechanotransduction and extracellular matrix homeostasis*. Nat Rev Mol Cell Biol, 2014. **15**(12): p. 802-12.
74. Keely, P.J., *Mechanisms by which the extracellular matrix and integrin signaling act to regulate the switch between tumor suppression and tumor promotion*. J Mammary Gland Biol Neoplasia, 2011. **16**(3): p. 205-19.
75. Naylor, M.J., et al., *Ablation of beta1 integrin in mammary epithelium reveals a key role for integrin in glandular morphogenesis and differentiation*. J Cell Biol, 2005. **171**(4): p. 717-28.
76. Provenzano, P.P., et al., *Mammary epithelial-specific disruption of focal adhesion kinase retards tumor formation and metastasis in a transgenic mouse model of human breast cancer*. Am J Pathol, 2008. **173**(5): p. 1551-65.
77. Luo, M., et al., *Mammary epithelial-specific ablation of the focal adhesion kinase suppresses mammary tumorigenesis by affecting mammary cancer stem/progenitor cells*. Cancer Res, 2009. **69**(2): p. 466-74.
78. Choquet, D., D.P. Felsenfeld, and M.P. Sheetz, *Extracellular matrix rigidity causes strengthening of integrin-cytoskeleton linkages*. Cell, 1997. **88**(1): p. 39-48.

79. Lu, P., V.M. Weaver, and Z. Werb, *The extracellular matrix: a dynamic niche in cancer progression*. J Cell Biol, 2012. **196**(4): p. 395-406.
80. Butcher, D.T., T. Alliston, and V.M. Weaver, *A tense situation: forcing tumour progression*. Nat Rev Cancer, 2009. **9**(2): p. 108-22.
81. Zanutelli, M.R. and C.A. Reinhart-King, *Mechanical Forces in Tumor Angiogenesis*. Adv Exp Med Biol, 2018. **1092**: p. 91-112.
82. Jain, R.K., *Normalization of tumor vasculature: an emerging concept in antiangiogenic therapy*. Science, 2005. **307**(5706): p. 58-62.
83. Nagy, J.A., et al., *Why are tumour blood vessels abnormal and why is it important to know?* Br J Cancer, 2009. **100**(6): p. 865-9.
84. Jain, R.K., *Antiangiogenesis strategies revisited: from starving tumors to alleviating hypoxia*. Cancer Cell, 2014. **26**(5): p. 605-22.
85. Morgan, R., et al., *Wnt Signaling as a Therapeutic Target in Cancer and Metastasis*. 2017.
86. Li, C., et al., *Piezo1 forms mechanosensitive ion channels in the human MCF-7 breast cancer cell line*. Sci Rep, 2015. **5**: p. 8364.
87. Xu, H., Z. Chen, and C. Li, *The prognostic value of Piezo1 in breast cancer patients with various clinicopathological features*. Anticancer Drugs, 2021. **32**(4): p. 448-455.
88. Gao, L., et al., *Suppression of Esophageal Squamous Cell Carcinoma Development by Mechanosensitive Protein Piezo1 Downregulation*. ACS Omega, 2021. **6**(15): p. 10196-10206.
89. Han, Y., et al., *Mechanosensitive ion channel Piezo1 promotes prostate cancer development through the activation of the Akt/mTOR pathway and acceleration of cell cycle*. Int J Oncol, 2019. **55**(3): p. 629-644.
90. Evans, E.L., et al., *Yoda1 analogue (Dooku1) which antagonizes Yoda1-evoked activation of Piezo1 and aortic relaxation*. Br J Pharmacol, 2018. **175**(10): p. 1744-1759.
91. Gudipaty, S.A., et al., *Mechanical stretch triggers rapid epithelial cell division through Piezo1*. Nature, 2017. **543**(7643): p. 118-121.
92. O'Callaghan, P., et al., *Piezo1 activation attenuates thrombin-induced blebbing in breast cancer cells*. J Cell Sci, 2022. **135**(7).
93. Luo, M., et al., *Compression enhances invasive phenotype and matrix degradation of breast Cancer cells via Piezo1 activation*. BMC Mol Cell Biol, 2022. **23**(1): p. 1.
94. De Felice, D. and A. Alaimo, *Mechanosensitive Piezo Channels in Cancer: Focus on altered Calcium Signaling in Cancer Cells and in Tumor Progression*. Cancers (Basel), 2020. **12**(7).
95. Seo, B.R., et al., *Obesity-dependent changes in interstitial ECM mechanics promote breast tumorigenesis*. Sci Transl Med, 2015. **7**(301): p. 301ra130.

96. Pavel, M., et al., *Contact inhibition controls cell survival and proliferation via YAP/TAZ-autophagy axis*. Nature Communications, 2018. **9**(1): p. 2961.
97. Gudipaty, S.A. and J. Rosenblatt, *Epithelial cell extrusion: Pathways and pathologies*. Semin Cell Dev Biol, 2017. **67**: p. 132-140.
98. Nosyreva, E.D., D. Thompson, and R. Syeda, *Identification and functional characterization of the Piezo1 channel pore domain*. J Biol Chem, 2021. **296**: p. 100225.
99. Vero Li, J., D.C. C, and B. Martinac, *The anchor domain is critical for Piezo1 channel mechanosensitivity*. Channels (Austin), 2021. **15**(1): p. 438-446.
100. Carrillo-Garcia, J., et al., *The mechanosensitive Piezo1 channel controls endosome trafficking for an efficient cytokinetic abscission*. Sci Adv, 2021. **7**(44): p. eabi7785.
101. Yang, S., et al., *Membrane curvature governs the distribution of Piezo1 in cellulo*. 2022: p. 2022.06.22.497259.
102. Atcha, H., et al., *Mechanically activated ion channel Piezo1 modulates macrophage polarization and stiffness sensing*. Nature Communications, 2021. **12**(1): p. 3256.
103. Jiang, Y., et al., *Targeting extracellular matrix stiffness and mechanotransducers to improve cancer therapy*. Journal of Hematology & Oncology, 2022. **15**(1): p. 34.
104. Wang, N., J.D. Tytell, and D.E. Ingber, *Mechanotransduction at a distance: mechanically coupling the extracellular matrix with the nucleus*. Nat Rev Mol Cell Biol, 2009. **10**(1): p. 75-82.
105. Chin, L., et al., *Mechanotransduction in cancer*. Curr Opin Chem Eng, 2016. **11**: p. 77-84.
106. Levental, K.R., et al., *Matrix crosslinking forces tumor progression by enhancing integrin signaling*. Cell, 2009. **139**(5): p. 891-906.
107. Conklin, M.W., et al., *Aligned collagen is a prognostic signature for survival in human breast carcinoma*. Am J Pathol, 2011. **178**(3): p. 1221-32.
108. Provenzano, P.P., et al., *Collagen reorganization at the tumor-stromal interface facilitates local invasion*. BMC Medicine, 2006. **4**(1): p. 38.
109. Somasiri, A., et al., *Overexpression of the integrin-linked kinase mesenchymally transforms mammary epithelial cells*. J Cell Sci, 2001. **114**(Pt 6): p. 1125-36.
110. Rabinovich, I., et al., *Cancer stem cell markers ALDH1 and CD44⁺/CD24⁻ phenotype and their prognosis impact in invasive ductal carcinoma*. Eur J Histochem, 2018. **62**(3).
111. Pratt, S.J.P., R.M. Lee, and S.S. Martin, *The Mechanical Microenvironment in Breast Cancer*. Cancers (Basel), 2020. **12**(6).
112. Jiang, F., et al., *The mechanosensitive Piezo1 channel mediates heart mechano-chemo transduction*. Nature Communications, 2021. **12**(1): p. 869.
113. Ren, X., et al., *High expression of Piezo1 induces senescence in chondrocytes through calcium ions*

- accumulation*. Biochemical and Biophysical Research Communications, 2022. **607**: p. 138-145.
114. Wang, B., et al., *Mechanosensitive Ion Channel Piezo1 Activated by Matrix Stiffness Regulates Oxidative Stress-Induced Senescence and Apoptosis in Human Intervertebral Disc Degeneration*. Oxidative Medicine and Cellular Longevity, 2021. **2021**: p. 8884922.
115. Brand, M.D., et al., *Mitochondrial superoxide: production, biological effects, and activation of uncoupling proteins*. Free Radical Biology and Medicine, 2004. **37**(6): p. 755-767.
116. Peng, Y., et al., *Mechano-signaling via Piezo1 prevents activation and p53-mediated senescence of muscle stem cells*. Redox Biology, 2022. **52**: p. 102309.
117. Morachevskaya, E.A. and A.V. Sudarikova, *Actin dynamics as critical ion channel regulator: ENaC and Piezo in focus*. 2021. **320**(5): p. C696-C702.
118. Nourse, J.L. and M.M. Pathak, *How cells channel their stress: Interplay between Piezo1 and the cytoskeleton*. Semin Cell Dev Biol, 2017. **71**: p. 3-12.
119. Li, A., et al., *Mesenchymal-endothelial nexus in breast cancer spheroids induces vasculogenesis and local invasion in a CAM model*. Communications Biology, 2022. **5**(1): p. 1303.
120. Broecker-Preuss, M., et al., *Sorafenib inhibits intracellular signaling pathways and induces cell cycle arrest and cell death in thyroid carcinoma cells irrespective of histological origin or BRAF mutational status*. BMC Cancer, 2015. **15**: p. 184.
121. Gómez-Miragaya, J., et al., *Resistance to Taxanes in Triple-Negative Breast Cancer Associates with the Dynamics of a CD49^f Tumor-Initiating Population*. Stem Cell Reports, 2017. **8**(5): p. 1392-1407.
122. Ricardo, S., et al., *Breast cancer stem cell markers CD44, CD24 and ALDH1: expression distribution within intrinsic molecular subtype*. J Clin Pathol, 2011. **64**(11): p. 937-46.
123. Schabath, H., et al., *CD24 affects CXCR4 function in pre-B lymphocytes and breast carcinoma cells*. J Cell Sci, 2006. **119**(Pt 2): p. 314-25.
124. Sun, B., et al., *Identification of metastasis-related proteins and their clinical relevance to triple-negative human breast cancer*. Clin Cancer Res, 2008. **14**(21): p. 7050-9.
125. Martowicz, A., et al., *Phenotype-dependent effects of EpCAM expression on growth and invasion of human breast cancer cell lines*. BMC Cancer, 2012. **12**: p. 501.
126. Ha, T.Y., et al., *Sorafenib inhibits migration and invasion of hepatocellular carcinoma cells through suppression of matrix metalloproteinase expression*. Anticancer Res, 2015. **35**(4): p. 1967-76.
127. Yoshida, M., et al., *Sorafenib suppresses extrahepatic metastasis de novo in hepatocellular carcinoma through inhibition of mesenchymal cancer stem cells characterized by the expression of CD90*. Sci Rep, 2017. **7**(1): p. 11292.
128. Wilhelm, S., et al., *Discovery and development of sorafenib: a multikinase inhibitor for treating*

- cancer*. Nat Rev Drug Discov, 2006. **5**(10): p. 835-44.
129. Martin del Campo, S.E., et al., *The Raf Kinase Inhibitor Sorafenib Inhibits JAK-STAT Signal Transduction in Human Immune Cells*. J Immunol, 2015. **195**(5): p. 1995-2005.
130. Koppikar, P., et al., *Constitutive activation of signal transducer and activator of transcription 5 contributes to tumor growth, epithelial-mesenchymal transition, and resistance to epidermal growth factor receptor targeting*. Clin Cancer Res, 2008. **14**(23): p. 7682-90.
131. Wang, J., et al., *ABL kinases promote breast cancer osteolytic metastasis by modulating tumor-bone interactions through TAZ and STAT5 signaling*. Sci Signal, 2016. **9**(413): p. ra12.
132. Samatar, A.A. and P.I. Poulidakos, *Targeting RAS-ERK signalling in cancer: promises and challenges*. Nature Reviews Drug Discovery, 2014. **13**(12): p. 928-942.
133. Li, P., et al., *A novel chemical inhibitor suppresses breast cancer cell growth and metastasis through inhibiting HPIP oncoprotein*. Cell Death Discovery, 2021. **7**(1): p. 198.
134. Zhang, W. and H.T. Liu, *MAPK signal pathways in the regulation of cell proliferation in mammalian cells*. Cell Research, 2002. **12**(1): p. 9-18.
135. Franken, N.A.P., et al., *Clonogenic assay of cells in vitro*. Nature Protocols, 2006. **1**(5): p. 2315-2319.
136. Dattachoudhury, S., et al., *Sorafenib Inhibits Proliferation, Migration and Invasion of Breast Cancer Cells*. Oncology, 2020. **98**(7): p. 478-486.
137. Desgrosellier, J.S. and D.A. Cheresh, *Integrins in cancer: biological implications and therapeutic opportunities*. Nat Rev Cancer, 2010. **10**(1): p. 9-22.
138. Felding-Habermann, B., et al., *Integrin activation controls metastasis in human breast cancer*. 2001. **98**(4): p. 1853-1858.
139. Durrant, D.E. and D.K. Morrison, *Targeting the Raf kinases in human cancer: the Raf dimer dilemma*. Br J Cancer, 2018. **118**(1): p. 3-8.
140. Galiè, M., *RAS as Supporting Actor in Breast Cancer*. Front Oncol, 2019. **9**: p. 1199.
141. Chen, X., et al., *A Feedforward Mechanism Mediated by Mechanosensitive Ion Channel PIEZO1 and Tissue Mechanics Promotes Glioma Aggression*. Neuron, 2018. **100**(4): p. 799-815.e7.
142. Botello-Smith, W.M., et al., *A mechanism for the activation of the mechanosensitive Piezo1 channel by the small molecule Yoda1*. Nat Commun, 2019. **10**(1): p. 4503.
143. Dombroski, J.A., et al., *Channeling the Force: Piezo1 Mechanotransduction in Cancer Metastasis*. Cells, 2021. **10**(11).
144. Sottnik, J.L., et al., *Tumor-Induced Pressure in the Bone Microenvironment Causes Osteocytes to Promote the Growth of Prostate Cancer Bone Metastases*. Cancer Research, 2015. **75**(11): p. 2151-2158.
145. Sun, W., et al., *The mechanosensitive Piezo1 channel is required for bone formation*. eLife, 2019. **8**:

- p. e47454.
146. Alexis, C., et al., *PIEZO1 activation delays erythroid differentiation of normal and hereditary xerocytosis-derived human progenitor cells*. Haematologica, 2020. **105**(3): p. 610-622.
 147. Kallas, A., et al., *SOX2 Is Regulated Differently from NANOG and OCT4 in Human Embryonic Stem Cells during Early Differentiation Initiated with Sodium Butyrate*. Stem Cells Int, 2014. **2014**: p. 298163.
 148. Li, C., et al., *Piezol forms mechanosensitive ion channels in the human MCF-7 breast cancer cell line*. Scientific Reports, 2015. **5**(1): p. 8364.
 149. Kalluri, R. and R.A. Weinberg, *The basics of epithelial-mesenchymal transition*. The Journal of Clinical Investigation, 2009. **119**(6): p. 1420-1428.
 150. Sun, Y., et al., *The function of Piezo1 in colon cancer metastasis and its potential regulatory mechanism*. J Cancer Res Clin Oncol, 2020. **146**(5): p. 1139-1152.
 151. Yang, X.-N., et al., *Piezol Is as a Novel Trefoil Factor Family 1 Binding Protein that Promotes Gastric Cancer Cell Mobility In Vitro*. Digestive Diseases and Sciences, 2014. **59**(7): p. 1428-1435.
 152. Zhu, B., et al., *Piezo 1 activation facilitates cholangiocarcinoma metastasis via Hippo/YAP signaling axis*. Molecular Therapy - Nucleic Acids, 2021. **24**: p. 241-252.
 153. Friedrich, E.E., et al., *Endothelial cell Piezo1 mediates pressure-induced lung vascular hyperpermeability via disruption of adherens junctions*. 2019. **116**(26): p. 12980-12985.
 154. Eisenhoffer, G.T., et al., *Crowding induces live cell extrusion to maintain homeostatic cell numbers in epithelia*. Nature, 2012. **484**(7395): p. 546-9.
 155. Huang, Z., et al., *Loss of stretch-activated channels, PIEZO1s, accelerates non-small cell lung cancer progression and cell migration*. Biosci Rep, 2019. **39**(3).
 156. McHugh, B.J., et al., *Loss of the integrin-activating transmembrane protein Fam38A (Piezo1) promotes a switch to a reduced integrin-dependent mode of cell migration*. PLoS One, 2012. **7**(7): p. e40346.
 157. Gagliardi, M., et al., *Differential functions of ERK1 and ERK2 in lung metastasis processes in triple-negative breast cancer*. Scientific Reports, 2020. **10**(1): p. 8537.
 158. Huang, C., et al., *ERK1/2-Nanog signaling pathway enhances CD44(+) cancer stem-like cell phenotypes and epithelial-to-mesenchymal transition in head and neck squamous cell carcinomas*. Cell Death & Disease, 2020. **11**(4): p. 266.
 159. McHugh, B.J., et al., *Integrin activation by Fam38A uses a novel mechanism of R-Ras targeting to the endoplasmic reticulum*. J Cell Sci, 2010. **123**(Pt 1): p. 51-61.
 160. Paoli, P., E. Giannoni, and P. Chiarugi, *Anoikis molecular pathways and its role in cancer progression*. Biochimica et Biophysica Acta (BBA) - Molecular Cell Research, 2013. **1833**(12): p.

- 3481-3498.
161. Lai, A., et al., *Piezol Response to Shear Stress Is Controlled by the Components of the Extracellular Matrix*. ACS Applied Materials & Interfaces, 2022. **14**(36): p. 40559-40568.
162. Hyman, A.J., S. Tumova, and D.J. Beech, *Chapter Two - Piezo1 Channels in Vascular Development and the Sensing of Shear Stress*, in *Current Topics in Membranes*, P.A. Gottlieb, Editor. 2017, Academic Press. p. 37-57.
163. Wang, X., et al., *Piezo type mechanosensitive ion channel component 1 facilitates gastric cancer omentum metastasis*. 2021. **25**(4): p. 2238-2253.
164. Zhang, J., et al., *PIEZO1 functions as a potential oncogene by promoting cell proliferation and migration in gastric carcinogenesis*. 2018. **57**(9): p. 1144-1155.



ACKNOWLEDGEMENT

I would like to take this opportunity to express my heartfelt gratitude to people without whose help and support this thesis would not have been possible.

I express my sincere gratitude to my thesis supervisor Prof. Bithiah Grace Jaganathan for giving me an opportunity to work in the field of cancer, teaching me every day and motivating me to explore my knowledge in research. Her immense support and hard work have helped me a lot in performing the experiments and analyzing the data.

I am thankful to my doctoral committee members Dr. Sanjukta Patra, Dr. Manish Kumar and Dr. Krishnapada Bhabak for their constructive suggestions, constant support and motivation during my research experience.

I would like to express my utmost gratitude to my PhD **Viva-Voce** board members, **Prof. Vivekanandan Perumal (external examiner of PhD thesis), Prof. Sanjukta Patra(chairperson), Dr. Abhishek Kumar and Dr. Kusum K Singh.**

I would like to extend my sincere gratitude towards Dr. Rakhi Chaturvedi, Head of the Department, Department of Biosciences and Bioengineering, IITG Guwahati.

I would like to acknowledge MHRD for my fellowship.

I would like to thank the Department of Biosciences and Bioengineering, IIT Guwahati for providing the necessary infrastructure and facilities for carrying out my thesis work.

I would like to thank all the non-teaching staff of Department of Biosciences and Bioengineering, IITG Guwahati.

I would like to thank all my lab members.

I would like to extend my appreciation for my friends at IIT Guwahati and outside. I thank all the people whom I met throughout my journey.

Lastly, and most importantly I thank my parents Mr. Manas Dattachoudhury and Mrs. Sharmistha Dattachoudhury for their endless and unconditional love, support, patience and affection.

List of Publications:

1. **Sreeja Dattachoudhury**, Renu Sharma, Atul Kumar, Bithiah Grace Jaganathan*. Sorafenib Inhibits Proliferation, Migration and Invasion of Breast Cancer Cells. *Oncology*. 2020;98(7):478-486. doi: 10.1159/000505521. Epub 2020 May 20.
2. Atul Kumar, Renu Sharma, **Sreeja Dattachoudhury**, Amit Sharma, Trishna Anand, Jina Bhattacharyya, Kasturi Bhattacharjee, Bithiah Grace Jaganathan*. OCT4A transcript level correlates with proliferation potential of human mesenchymal stem cells. *Gene reports* (2019) <https://doi.org/10.1016/j.genrep.2019.100459>.

Conferences and workshops attended:

1. Haematocon 2017 – workshop, 2017, IIT Guwahati
2. ZE5 and digital droplet PCR-QX200-Bio-Rad lab- workshop-2017, IIT Guwahati
3. 20th INDO-US Flow Cytometry workshop and symposium-2019, IIT Guwahati
4. Research conclave-2019, IIT Guwahati
5. Online Workshop on Flow Cytometry Techniques and Applications, 2020, NECBH
6. 5th World Cancer Congress - 2021 Arjyopa Healthcare, New Delhi
7. Research and Industrial Conclave, 2022, IIT Guwahati
8. North East Research Conclave, 2022, IIT Guwahati